University of Alberta

BIOCHEMICAL CONVERSION OF CARBAZOLE: ISOLATION AND CHARACTERIZATION OF *SPHINGOMONAS* SP. CP19

By

Leah A. Kirkpatrick ©

A thesis submitted to the Faculty of Graduate Studies and Research in partial fulfillment of the requirements for the degree of Masters of Science in Chemical Engineering

Department of Chemical and Materials Engineering

Edmonton, Alberta

Spring 2003

National Library
of Canada

Acquisitions and
Bibliographic Services

395 Wellington Street
Ottawa ON K1A 0N4
Canada

Bibliothèque nationale
du Canada

Acquisitions et
services bibliographiques

395, rue Wellington
Ottawa ON K1A 0N4
Canada

Your file Votre référence

Our file Notre référence

The author has granted a non-exclusive licence allowing the National Library of Canada to reproduce, loan, distribute or sell copies of this thesis in microform, paper or electronic formats.

L'auteur a accordé une licence non exclusive permettant à la Bibliothèque nationale du Canada de reproduire, prêter, distribuer ou vendre des copies de cette thèse sous la forme de microfiche/film, de reproduction sur papier ou sur format électronique.

The author retains ownership of the copyright in this thesis. Neither the thesis nor substantial extracts from it may be printed or otherwise reproduced without the author's permission.

L'auteur conserve la propriété du droit d'auteur qui protège cette thèse. Ni la thèse ni des extraits substantiels de celle-ci ne doivent être imprimés ou autrement reproduits sans son autorisation.

0-612-82297-4

Canada

University of Alberta

Library Release Form

Name of Author: Leah Anne Kirkpatrick

Title of Thesis: Biochemical Conversion of Carbazole: Isolation and Characterization of *Sphingomonas* sp. CP19

Degree: Masters of Science in Chemical Engineering

Year this Degree Granted: 2003

Permission is hereby granted to the University of Alberta Library to reproduce single copies of this thesis and to lend or sell such copies for private, scholarly or scientific research purposes only.

The author reserves all other publication and other rights in association with the copyright in the thesis, and except as herein before provided, neither the thesis nor any substantial portion thereof may be printed or otherwise reproduced in any material form whatever without the author's prior written permission.

L A Kirkpatrick

271 Regency Drive
Sherwood Park, Alberta
T8A 5P4

March 28, 2003

University of Alberta

Faculty of Graduate Studies and Research

The undersigned certify that they have read, and recommend to the Faculty of Graduate Studies and Research for acceptance, a thesis entitled **Biochemical Conversion of Carbazole: Isolation and Characterization of *Sphingomonas* sp. CP19** submitted by **Leah Anne Kirkpatrick** in partial fulfillment of the requirements for the degree of Masters of Science in Chemical Engineering.

Dr. Murray R. Gray

P. Fedorak

Dr. Phil M. Fedorak

Dr. Julia M. Foght

March 25, 2003

ABSTRACT

This project investigated the feasibility of improving efficiencies of carbazole removal in hydrotreating with a biocatalytic pre-treatment step. The ideal biocatalyst was defined as one able to denitrogenate carbazole with minimal carbon mineralization and with activity selective for carbazole. Such biological activity had not previously been identified. Bacteria were isolated from creosote-contaminated soil and screened for this activity. One isolate, *Sphingomonas* sp. CP19, was investigated in detail. Its specific activity for carbazole transformation was 1.8μmol carbazole (mg dry cell weight-d)$^{-1}$. Further characterization showed that this activity did not meet the specifications of the ideal biocatalyst. The coloured product that distinguished CP19 from other isolates was identified as an abiotic condensation product of 2-aminophenol. The accumulation of the condensation product from a biological oxidation product re-enforced the need for a suitable biocatalyst to completely denitrogenate carbazole. The formation of 2-aminophenol represents a newly identified step in the carbazole degradation pathway.

ACKNOWLEDGEMENTS

In the course of my time at the University of Alberta I have met many phenomenal people and with some have been fortunate to develop friendships. I have received a tremendous amount of support and motivation with each one and am extremely grateful.

For the opportunity to work on such a fascinating project within a very strong, diverse, and dedicated group of researchers, I would like to first thank my supervisor Dr. Murray Gray. His patience, guidance, encouragement and kindness have supported me throughout this project and my career as a graduate student. I am pleased to have had the opportunity to learn from him.

The funding of this project was supplied by the Syncrude/NSERC Industrial Research Chair in Advanced Upgrading of Bitumen. In addition, I would like to acknowledge NSERC for supporting me financially throughout the course of this program and to the University of Alberta for granting me the Walter H. Johns Graduate Fellowship each year of my study.

I would like to thank Marilee Barry and Dr. William McCaffry whose commitment to the graduate program in the Department of Chemical and Materials Engineering made coming to U of A a very welcoming experience. From the Department of Biological Sciences, I am grateful to Dr. Julia Foght for her efforts in teaching me the art of microbiology and to Dr. Phil Fedorak for his generous advice and use of resources.

For their energy, their willingness to teach and share ideas and for their laughter I would like to thank: Kathlyn Kirkwood, Seena Farea, Beth Hearn, Dr. Jon van Hamme, Dr. Inseon Kim from the biochemical upgrading research group; Ruth Eckford, Joyce Clemente, Melissa Haveroen, Roz McInnis, Sara Ebert, Cathy Secord and Debbie Coy from the Foght/Fedorak laboratories; Anna, Tom and Maria from the prep laboratory; Randy, Jack and Rakesh from the microscopy laboratory; and Andrée Koenig from chemical and materials engineering .

The results of this research was strengthened and solidified by the technical expertise of Dr. David Bressler. I am thankful to have had Dave as my counterpart and mentor on this project. Not only was he willing to answer my endless supply of questions he managed to meet my stubborness with patience and thought-provoking debate.

Finally I would like to express my gratitude to my family. Jacque, Jen, Chris, Tracy and Angela my “adopted” family in the west; my parents and my brother, your belief in me is my motivation.

TO MY FAMILY AND FRIENDS,

Your constant support and encouragement are the foundation of my learning.

1.0 INTRODUCTION 1
2.0 LITERATURE REVIEW 3
  2.1 CHARACTERISTICS AND PROCESSING OF SYNTHETIC CRUDE OIL 3
    2.1.1 Oil supplies in Alberta: Athabasca Bitumen 3
    2.1.2 Processing synthetic crude oil 3
    2.1.3 Characteristics and treatments of nitrogen compounds 5
  2.2 BIOCATALYSIS OF COMPOUNDS WITH LOW AQUEOUS SOLUBILITY 8
    2.2.1 Mass transfer 8
    2.2.2 Applications of biocatalysis 11
    2.2.3 Enzymatic control 13
      2.2.3.1 Control of enzymatic activity 14
      2.2.3.2 Cellular control of enzyme production 16
  2.3 BIOCHEMICAL TRANSFORMATION OF POLYCYCLIC AROMATIC COMPOUNDS 22
    2.3.1 Biotransformation of naphthalene 24
    2.3.2 Dibenzothiophene biotransformation 26
    2.3.3 Carbazole biotransformation 31
      2.3.3.1 Carbazole degradation pathways 32
      2.3.3.2 Genetic analysis of carbazole genes 38
    2.3.4 Abiotic transformation of biological oxidation products 40
    2.3.5 Hydrotreating biological oxidation products of carbazole 43
3.0 MATERIALS AND METHODS 45
  3.1 MATERIALS 45
    3.1.1 Growth medium and buffers 45
    3.1.2 Chemicals and solvents 46
    3.1.3 Microorganisms 47
  3.2 METHODS 47
    3.2.1 Glassware preparation 47
    3.2.2 Preparation, inoculation and incubation of cultures. 48
      3.2.2.1 Test Tube Cultures 48
      3.2.2.2 Erlenmeyer Shake Flask Cultures (500 mL) 49
      3.2.2.3 Enrichment Cultures 49
      3.2.2.4 Isolate CP19 49
      3.2.2.5 Biometers (250 mL) 50
      3.2.2.6 Screw-Cap Shake Flasks (500 mL) 51
    3.2.3 Isolation methods 52
    3.2.4 Evaluation of screening results 52
      3.2.4.1 Isolate Screening 52
      3.2.4.2 Profile of Suitable Candidates 56
    3.2.5 Chemical analysis 58
      3.2.5.1 Carbazole loss 58
      3.2.5.2 Liquid-Liquid Extraction 58
      3.2.5.3 Aqueous solubilization of carbazole using ethanol 60

3.2.5.4 Acetate consumption ... 61
3.2.5.5 Conversion of polycyclic aromatic compounds (PACs) ... 62
3.2.5.6 Radiolabelled carbazole ... 64
3.2.5.7 Mass spectrometry and derivatization methods ... 65
3.2.6 Biomass measurement ... 66
3.2.6.1 Optical density (OD_{600}) ... 66
3.2.6.2 Dry cell weight ... 66
3.2.6.3 Protein content ... 67
3.2.6.4 Elemental carbon, hydrogen and nitrogen analysis ... 68
3.3 CHARACTERIZATION OF *SPHINGOMONAS* SP. CP19 ... 68
3.3.1 Identification ... 68
3.3.2 Solubilization mechanisms ... 69
3.3.3 Recovery of metabolites ... 69

4.0 RESULTS ... 71

4.1 VALIDATION OF EXPERIMENTAL PROCEDURES ... 71
4.1.1 Error analysis and experimental controls ... 71
4.1.2 Analysis of carbazole concentrations ... 72
4.1.2.1 Ratio of internal standard to substrate ... 72
4.1.2.2 Sensitivity of gas chromatography ... 75
4.1.2.3 Effectiveness of liquid-liquid extraction in test-tube cultures ... 77
4.1.2.4 Effectiveness of carbazole solubilization technique. ... 77
4.1.3 Biocataylst measurements ... 79
4.1.3.1 Biomass measurements ... 79
4.1.3.2 Validation of protein content determinations ... 81
4.1.3.3 Ratio of dry cell weight to protein content ... 84
4.2 ISOLATION AND SCREENING OF CARBAZOLE DEGRADERS ... 87
4.3 CHARACTERIZATION OF ISOLATE CP19 ... 96
4.3.1 Growth characteristics ... 96
4.3.2 Species identification and characterization ... 98
4.3.2.1 Capsule Staining ... 101
4.3.2.2 Microstructures of CP19 ... 103
4.3.2.3 Growth of CP19 on Carbazole Crystals ... 106
4.3.3 Mechanisms for carbazole solubilization ... 108
4.4 REGULATION OF CARBAZOLE TRANSFORMATION BY CP19 WITH ADDITIONAL CARBON AND NITROGEN SOURCES ... 110
4.4.1 Overall conversion of carbazole and conversion rates ... 111
4.4.2 Relationship of acetate consumption to carbazole transformation. ... 118
4.4.3 Elemental composition of biomass ... 120
4.4.4 Aqueous concentration of carbazole in live cultures. ... 122
4.5 REGULATION BY ACETATE OF CARBAZOLE MINERALIZATION ... 124
4.6 SELECTIVITY OF STRAIN CP19 FOR CARBAZOLE RELATIVE TO OTHER PACS. .. 131
4.7 FORMATION OF CARBAZOLE METABOLITES BY CP19 ... 135

5.0 DISCUSSION ... 138

5.1 ISOLATION OF BACTERIA GROWING ON CARBAZOLE AS A NITROGEN SOURCE. . 138
5.2 CONVERSION OF CARBAZOLE BY *SPHINGOMONAS SP.* CP19 ... 140

5.2.1 Reasons for slow growth ... 141
5.2.1.1 Induction ... 141
5.2.1.2 Solid substrate mass transfer limitations ... 143
5.2.1.3 Formation of condensation product ... 146
5.2.2 Regulation of carbazole degradation ... 146
5.2.2.1 Reconciliation of dry cell weight measurement ... 148
5.2.2.2 Validation of assumptions ... 155
5.2.2.3 Inconsistencies between mineralization and transformation experiments: sources of discrepancies ... 160
5.3 METABOLITE FORMATION FROM CARBAZOLE DEGRADATION ... 162
5.4 SUBSTRATE SPECIFICITY ... 164
5.4.1 Conversion of carbazole within substrate mixture ... 164
5.4.2 Selectivity of strain CP19 for carbazole. ... 165

6.0 CONCLUSIONS ... 168

7.0 REFERENCES ... 172

8.0 APPENDIX A ... 179
8.1 HYDROCARBONS ... 181
8.2 MISCELLANEOUS PRODUCTS ... 181
8.3 SOLVENTS AND ACIDS ... 182

9.0 APPENDIX B ... 183

10.0 APPENDIX C ... 184
10.1 SAMPLE CALCULATION FOR ERROR ANALYSIS ... 184
10.1.1 Error analysis for numbers undergoing addition or subtraction. ... 184
10.1.2 Error analysis for numbers undergoing multiplication or division. ... 184
10.2 SAMPLE CALCULATION FOR CARBAZOLE CONVERSION RATE ... 185
10.3 SAMPLE CALCULATION FOR $^{14}CO_2$ RELEASE ... 186
10.4 SAMPLE CALCULATION FOR ^{14}C IN BIOMASS ... 187
10.5 SAMPLE CALCULATION FOR PROTEIN CONTENT ... 187

11.0 APPENDIX D ... 188

12.0 APPENDIX E ... 189
12.1 VALIDATION EXPERIMENT FOR HPLC VERSUS GC ... 189
12.2 RAW DATA FOR VALIDATING THE RECOVERY OF ETHANOL-TREATED CELLS. ... 193
12.3 DATA FOR CALCULATING THE RATIO OF DRY CELL WEIGHT TO PROTEIN CONTENT 196
12.4 DATA FROM MEASURMENTS OF THE AQUEOUS SOLUBILITY OF CARBAZOLE INCUBATED WITH CP19 FILTRATE ... 200
12.5 DATA FROM EXPERIMENTS MEASURING CARBON REGULATION OF CARBAZOLE TRANSFORMATION. ... 203

LIST OF FIGURES

Figure 2-1 Structures of various nitrogen compounds found in crude oil. 7

Figure 2-2 Induction of a positively controlled system (after Madigan *et al.*, 1997). 19

Figure 2-3 Induction of a negatively controlled system (after Madigan et al., 1997). 20

Figure 2-4 The process of gene repression (after Madigan *et al.*, 1997). 21

Figure 2-5 Microbial metabolism of catechol (after Atlas and Bartha, 1998). 23

Figure 2-6 Microbial metabolism of naphthalene, an example of a PAH (after Denome *et al.*, 1993; Eaton and Chapman, 1992). 25

Figure 2-7 Numbering convention of atoms that make up the oxygen, sulphur and nitrogen analogues of fluorene. 27

Figure 2-8 Biotransformation pathways of dibenzothiophene following Kodama et al. (1973), van Afferden et al. (1993) and Omori et al. (1992). 30

Figure 2-9 Carbazole degradation pathway proposed by Ouchiyama *et al.* (1992). 34

Figure 2-10 Carbazole degradation pathway proposed by Gieg (1996) using *Pseudomonas* sp. LD2. 37

Figure 2-11 Selective removal of nitrogen from quinoline using isolate *Pseudomonas ayucida* IGTN9m (Kilbane *et al.*, 2000). 38

Figure 2-12 Abiotic oxidation of a biological product of dibenzothiophene degradation (after Bressler and Fedorak, 2001). 42

Figure 2-13 Condensation products of catechol. A. catechol, B. catechol product formed from C-C condensation, C. catechol product from C-O-C condensation (Sáchez-Cortés *et al.*, 2001) 42

Figure 2-14 Hydrotreatment of a carbazole biological oxidation product (after Bressler and Gray, 2002). 44

Figure 3-1 Strategy for evaluating isolates from enrichment cultures. The combined results of growth and substrate loss measurements in the four testing conditions in Table 3-1 along with the release of $^{14}CO_2$ were used. 55

Figure 3-2 Hypothetical growth characteristics of an ideal carbazole degrader under the testing conditions. 57

Figure 3-3 Structures of PACs used in the selectivity experiments with CP19 63

Figure 4-1 Calibration curve of carbazole and thianthrene in ethyl acetate on the GC-FID. 74

Figure 4-2 Calibration curve of carbazole determined by GC-FID. 76

Figure 4-3 Time course evaluating the length of sonication time required to lyse CP19 and release cellular protein. 83

Figure 4-4 Ratio between DCW and protein content of CP19 cells. HKC refers to heat-killed controls 85

Figure 4-5 Growth yield from isolates in test conditions. 89

Figure 4-6 Growth of isolates with acetate supplemented conditions and only carbazole. 90

Figure 4-7 Removal of carbazole by isolates incubated with various sources of nitrogen and carbon. 92

Figure 4-8 Degradation of the carbon backbone of carbazole by isolates, determined by the production of $^{14}CO_2$ from ^{14}C-carbazole. 94

Figure 4-9 Distribution of radiolabel from ^{14}C-carbazole in ethyl acetate: extract, aqueous phase and carbon dioxide release. 95

Figure 4-10 Growth curve of CP19 grown on TSB. 97

Figure 4-11 Illustration of Neighbour Joining Tree resulting from 1500 bp concise alignment report. Reproduced from the data supplied by MIDI labs on the 16S rDNA sequencing of CP19. 100

Figure 4-12 Capsule stain of *Sphingomonas* sp. CP19 using India ink and methylene blue 102

Figure 4-13 Transmission electron micrograph (TEM) of *Sphingomonas* sp. CP19 grown on TSB medium. 104

Figure 4-14 TEM micrograph of *Sphingomonas* sp. CP19 grown on carbazole as sole nitrogen source. 105

Figure 4-16 Solubilization effects on carbazole by *Sphingomonas* sp. CP19 cells. 109

Figure 4-17 Removal of carbazole by CP19 in the presence of various carbon and nitrogen sources. 112

Figure 4-18 Increase in dry cell weight by CP19 with incubation. 113

Figure 4-19 Transformation of carbazole by CP19 in the presence of various combinations of carbon and nitrogen sources. 114

Figure 4-20 Change of culture pH during growth of CP19 under test conditions. 116

Figure 4-21 Time course of acetate and carbazole transformation by strain CP19. 119

Figure 4-22 Elemental carbon and nitrogen concentrations in dry CP19 cells 121

Figure 4-23 Aqueous concentration of carbazole in the presence of *Sphingomonas* sp. CP19 123

Figure 4-24 Time course of $^{14}CO_2$ released by CP19 from radiolabelled carbazole...... 126

Figure 4-25 Distribution of radiolabel from CP19 cultures grown under two growth conditions. 127

Figure 4-26 Removal of PACs by strain CP19. 133

Figure 4-27 Structures of identified carbazole metabolites produced by strain CP19 ... 137

Figure 5-1 Consistency check on formation of biomass using the yield coefficients calculated from all the measured data of the transformation experiment. 154

Figure 5-2 Consistency check on dry cell weight data, using the carbazole yield coefficients as calculated from the mineralization experiment (Table 5-1). 159

Figure 12-1 Calibration curve for HPLC used in quantifying carbazole loss in the validation experiment. 191

Figure 12-4 HPLC calibration curve for measuring the aqueous solubility of carbazole and for quantifying the effects of the presence of cells. 200

Figure 12-5 Data from monitoring acetate concentrations over incubation time of CP19 with carbazole. 4

LIST OF TABLES

Table 2-1 Properties of crude oil (Hyndman, 1991). 4

Table 2-2 Removal of nitrogen compounds from Syncrude coker gas oil (after Gray 1990). 7

Table 2-3 Intermediates in dibenzothiophene metabolism as outlined in Figure 2-8. 31

Table 3-1 Summary of conditions for screening isolates and the hypotheses tested. 53

Table 3-2 Retention times of the PACs tested as substrates with strain CP19. 63

Table 4-1 Comparison of procedures to quantify carbazole concentration. 78

Table 4-2 Summary of biomass measurements from filtering untreated TSB cells and ethanol treated TSB grown cells. 80

Table 4-3 Evaluation of filtering method whereby efficiency is measured using OD_{600} readings before and after filtering. 81

Table 4-4 Results from protein and DCW measurements of CP19 and heat-killed controls (HKC). 86

Table 4-5 Summary of biochemical test performed on CP19. 98

Table 4-6 Mean rate of carbazole removal from testing conditions. 117

Table 4-7 Composition of each fraction after liquid-liquid extraction of radiolabelled carbazole in CP19 liquid cultures. 124

Table 4-8 Summary of measurements taken in the flasks containing un-radiolabelled carbazole that were incubated in parallel to those containing radiolabelled carbazole. 128

Table 4-9 Summary of normalized data collected by extracting and counting the amount of radiolabel in each fraction. 130

Table 4-10 Aqueous solubilities of polycyclic aromatic compounds used in selectivity experiment. 134

Table 4-11 Mass spectrum of CP19 metabolites 136

Table 5-1 Summary of yield coefficients calculated for carbazole and acetate using the data from ^{14}C- carbazole. 158

Table 12-1 Raw data from ethyl acetate extraction of carbazole flasks. 189

Table 12-3 Raw data for determining effectiveness of dry cell weight collection with vacuum filtering. 193

Table 12-4 Statistical analysis of dry cell weight data where one sample set contained untreated cells and the other contained cells treated with ethanol prior to filtering. 194

Table 12-5 Raw data of optical density readings completed on samples before and after filtering. 195

Table 12-6 Descriptive statistics on biomass collection of carbazole grown cultures. 195

Table 12-7 Dry cell weight of biomass collection for the experiment to correlate dry cell weight to protein content. 196

Table 12-8 Raw data for protein analysis. All OD_{600} readings were taken without the need for any dilution. 198

Table 12-10 Statistical analysis of the correlation relating dry weight to protein content and how it behaves over time in CP19 cells. 199

Table 12-11 HPLC data for HKC samples of solubilization experiment. 201

Table 12-12 HPLC data of CP19 culture filtrate exposed to carbazole. 202

Table 12-13 Dry cell weight data from regulation experiment. 203

Table 12-14 HPLC data for measuring residual carbazole remaining after exposure to CP19 growing in the presence of various carbon and nitrogen sources. 206

Table 12-15 Normalized carbazole conversions for CP19 exposed to carbazole in the presence of various combinations of carbon and nitrogen sources. 207

Table 12-16 Statistical analysis of the normalized carbazole conversion for each growing condition. 207

Table 12-17 Data and calculations of the mean rate of carbazole conversion within all growing conditions. 2

Table 12-18 Final composition of biomass from CN analysis. 3

Table 12-19 Data collected by measuring $^{14}CO_2$ release from CP19 cultures with ^{14}C-carbazole. 6

Table 12-20 ^{14}Carbon dioxide release data corrected for background ^{14}C. 7

Table 12-21 Calculated data for the amount of radiolabel removed from each culture from daily sampling of KOH. 8

Table 12-22 Calculated values of cumulative $^{14}CO_2$ release from CP19 cultures with ^{14}C-carbazole. 9

Table 12-23 Distribution of radiolabel throughout culture fractions. 10

Table 12-24 Distribution of radiolabel throughout culture fractions, continued from Table 12-23. 11

LIST OF DEFINITIONS

Abiotic: physical and chemical changes in the absence of biological activity.

Anabolism: the biochemical process of combining building molecules required for cell functions, usually requiring energy.

Biodegradation: the biochemical process in which microorganisms break down molecules into small molecules.

Biotransformation: the process in which microorganisms change the structure of a compound, not necessarily to carbon dioxide.

Catabolism: the biochemical process of breaking a molecule into smaller parts for the production of energy.

Catalyst: a substance that promotes a chemical reaction without reacting itself.

Induction: the process of control of synthesis of an enzyme in response to an external factor.

Inhibition: the mechanism of control of enzyme activity by interfering with the enzyme's ability to bind with the active site.

Inoculum: the material used to initiate a microbial culture.

Metabolism: all biochemical reactions within a cell including anabolic and catabolic.

Mineralization: the process of converting organic compounds into carbon dioxide and water.

Polycylic aromatic compounds (PAC): similar in structure to PAH but contains an additional type of atom such as nitrogen or sulphur.

Polycylic aromatic hydrocarbons (PAH): aromatic compounds with multiple rings which consist of only carbon and hydrogen atoms.

Repression: the process by which the synthesis of an enzyme is stopped as a result of an external factor.

Substrate: the molecule undergoing a reaction with an enzyme.

Supernatant: the liquid portion of a culture, remaining after the removal of cells.

Turnover Number: the number of substrate molecules converted to product per enzyme molecule per unit of time.

LIST OF ABBREVIATIONS AND NOMENCLATURE

A: contact surface area, m^2

AOSTRA: Alberta oil sands technology and research authority

b_{ACT}: moles of CO_2 from acetate carbon

b_{CAR}: moles of CO_2 from carbazole carbon

B+8P: buffered, mineral salts medium

B+N8P: buffered, mineral salts medium with a nitrogen source

ACT: acetate

CAR: carbazole

CAR+ACT: mineral salts medium with carbazole and acetate as carbon sources

CAR+ACT+N: mineral salts medium with carbazole and acetate as carbon sources and ammonium and nitrate as nitrogen source.

CARDO: carbazole 1,9a-dioxygenase enzymes

C_{eq}: equilibrium concentration of the substrate in solution, kg m^{-3}

$C_{t:}$ concentration of substrate in solution, kg m^{-3}

DCM: dichloromethane

DCW: dry cell weight

DPM: disintegrations per minutes

f_{ACT}: composition of biomass from acetate, moles of acetate carbon in biomass per mg of biomass formed from acetate carbon

f_{CAR}: composition of biomass from carbazole, moles of carbazole carbon per mg of biomass formed from carbazole carbon

GC: gas chromatography

GC-MS: gas chromatography with mass spectrometry.

HPLC: high performance liquid chromatography

IBP: initial boiling point

K_l: the mass transfer constant, m h^{-1}

LHSV: liquid hourly space velocity, mL h^{-1} g $catalyst^{-1}$

MW: molecular weight

OD_{600}: optical density measured at a wavelength of 600 nm

PCA: Plate count agar

Q_t: amount of adsorbed substrate, kg

R_{ACT}: fraction of acetate carbon mineralized, moles of acetate carbon mineralized to CO_2 per mole of acetate carbon in biomass

R_{CAR}: fraction of carbazole carbon mineralized, moles of carbazole carbon mineralized to CO_2 per mole of carbazole carbon in biomass

RPM: revolutions per min

S_t: the total amount of substrate per unit volume (kg m^{-3})

StCntl: sterile control, used to monitor abiotic activity

T: time, h

TSB: trypic soy broth, complex medium

V: volume, m^3

X_{ACT}: biomass formed from acetate carbon, mg

X_{CAR}: biomass formed from carbazole carbon, mg

X_t : biomass concentration kg m^{-3}

X_{TOTAL}: total biomass formed, mg

Y: yield constant, kg biomass kg^{-1} substrate consumed

$Y_{CO2/ACT}$: yield coefficient of acetate mineralization, mg CO_2 mg^{-1} acetate consumed

$Y_{CO2/CAR}$: yield coefficient of carbazole mineralization, mg CO_2 mg^{-1} carbazole consumed

$Y_{X/ACT}$: yield coefficient for biomass accumulation from acetate, mg biomass formed mg^{-1} acetate consumed

$Y_{X/CAR}$: yield coefficient for biomass accumulation from carbazole, mg biomass formed mg^{-1} carbazole consumed

ΔACT: conversion of acetate, moles

ΔCAR: conversion of carbazole, moles

1.0 INTRODUCTION

Athabasca bitumen and heavy oil, from which synthetic crude is processed, must undergo various thermal and chemical treatments to be an economical alternative to conventional crude oil. This treatment consists of two steps: primary and secondary upgrading. Primary upgrading consists of a series of thermal treatments that break large molecules into molecules more suitable for marketable petroleum products. Secondary upgrading treatments remove undesirable compounds such as sulphur, nitrogen and oxygen. One specific objective is to remove nitrogen compounds to concentrations acceptable to conventional oil refineries. Concentrations must be low because nitrogen tends to poison reactor catalysts, resulting in more frequent and costly regeneration or replacement. The majority of nitrogen in Athabasca bitumen is located in complex aromatic structures. After undergoing the thermal treatments of primary upgrading, the nitrogen concentrates in the non-basic indole and carbazole derivatives. Removal of nitrogen is completed in secondary upgrading by breaking open the aromatic structures in a process called hydrotreating. Despite the severe temperatures and pressures used in hydrotreating, the non-basic alkyl carbazoles persist in the product stream.

Biochemical treatments offer a potential supplement to hydrotreating because bacteria have the ability to accomplish the same chemical reactions as those completed in the process of hydrotreating. Biocatalysis is an attractive addition to secondary upgrading because the enzyme systems responsible for catalyzing chemical reactions can be selective for the compounds they attack, and they can be selective for the reaction pathway they follow in that attack. This approach is more sophisticated, as compared to the chemistry of thermal treatments that is somewhat random. Bacteria can be active at ambient temperatures and pressures with basic nutrient requirements, all representing low operating costs when compared to those of high pressure and high temperature chemical reactors.

By removing the nitrogen compound, carbazole, before hydrotreating, improvements in efficiency and effectiveness are possible. The severe operating conditions used in order to remove the carbazoles could be reduced. Bacteria have the ability to break the same carbon-nitrogen bonds as those targeted in hydrotreating. A bacterium useful for improving the removal efficiency of nitrogen compounds from gas oil must be specific in its transformation of carbazole without affecting the structure of other polyaromatic compounds or hydrocarbons in the feed. Also, its biodegradation of carbazole must be specific to the nitrogen atom with minimal degradation to the carbon skeleton, because the fuel value of oil is found in the carbon. Suitability also depends on the products of biological oxidation: the products must be more susceptible to hydrotreatment than the original compound. To meet this objective, the bacterium must completely remove the nitrogen atom from the carbon backbone (Bressler and Gray, 2002). Free amine groups and the oxygen functional groups that typically characterize biological oxidation reactions tend to react together, under hydrotreating conditions, to form closed ring structures. These products can be as stable as the original compound.

Currently known carbazole degraders do not show such specific activity. The metabolites that characterize carbazole degradation by these bacteria are nitrogen-free only after significant carbon degradation. The products with minimal carbon degradation contain nitrogen and tend to give ring closure reactions.

In the absence of an identified, biochemical pathway suitable for pretreating hydrotreater feed, this research involved isolation and screening of a more suitable isolate. Aged creosote-contaminated soil was enriched on carbazole as sole nitrogen source. Additional soluble carbon in the form of sodium acetate was supplied to promote activity specific to the nitrogen atom of carbazole. The most interesting isolate from this work was identified by its metabolic characteristics and its formation of a unique metabolite. Detailed investigations were completed to characterize its metabolic abilities, physical properties, selectivity toward carbazole in the presence of various hydrocarbons and polyaromatic compounds typical of hydrotreater feed streams, and to define the possible metabolic pathways involved.

2.0 LITERATURE REVIEW

2.1 Characteristics and processing of synthetic crude oil

2.1.1 Oil supplies in Alberta: Athabasca Bitumen

Due to the depleting reserves of light and medium conventional crude oil, the petroleum industry has been required to focus on processing the more difficult heavy oils and bitumen. According to a 1991 report from AOSTRA (Hyndman, 1991), there is an estimated 635 billion m^3 of oil in the world. Conventional crude makes up only 25 % of that total, and a mere 1.1 % of that total is located in Canada. The remaining petroleum reserves are found in such materials as heavy oils and oil sands where Canada, more specifically Alberta, holds over 40 % of the world's supply. This abundant reserve of natural resources supplies Canada with 1/3 of its oil requirements and supplies the US with 13 % of its imported oil and oil products (Hyndman, 1991).

Canada's oil sands are largely concentrated in Athabasca, a northern region of Alberta. There are two major processing companies, Syncrude and Suncor, and one under construction, Albian, in that region. These facilities mine the oil sands, extract the tar-like bitumen from the sand and upgrade the bitumen to synthetic crude oil.

2.1.2 Processing synthetic crude oil

Most oil refineries are designed and operated to process conventional crude oil. Heavy oil and bitumen-derived oil are chemically different from conventional crude oils and consequently must undergo various degrees of upgrading to be an economical option for refineries.

Table 2-1 summarizes the main characteristics of bitumen, synthetic crude oil and conventional crude oil. A direct comparison of bitumen to conventional crude illustrates the differences in composition between the two types of oil. The concentrations of both nitrogen and sulphur are over 10 times greater in bitumen than in conventional oil. Also, there is a higher concentration of the heavier oil fractions in the bitumen extracted oil than in conventional oil. These differences are lessened once the bitumen undergoes upgrading to become synthetic crude.

Limits are placed on the concentrations of nitrogen and sulphur compounds in refinery feedstocks because of the problems they cause in the refining process. Compounds containing either of these elements react with oxygen to form air pollutants (NO_X and SO_X, respectively). Nitrogen compounds also contribute to processing problems. Their tendency to adsorb to reactor catalysts leads to catalyst poisoning that requires more frequent, costly regeneration cycles or complete replacement of catalyst.

Table 2-1 Properties of crude oil (after Hyndman, 1991).

	Bitumen	Synthetic Crude	Conventional Crude
°API	8	32	41
Sulphur, wt%	4.8	0.08	0.2
Nitrogen, wt%	0.45	0.03	0.04
Viscosity, cSt, 40°C	3000	3	2.9
Pour Point, °C	18	-4.5	-6
Metals, ppm	450	<1	**INS**[1]

Upgrading is composed of two main parts namely primary and secondary upgrading. Primary upgrading consists of thermal treatments such as coking or hydrocracking that break or 'crack' large molecules. This cracking helps redistribute the boiling fractions, bringing more of the heavy residues into the lighter fractions. Despite these harsh thermal treatments, the aromatic compounds which characterize the carbon structures of bitumen and heavy oil remain intact. They tend to concentrate in the product stream known as gas oil. This fraction has a boiling point range of 343-525 °C. The ring structures are often the location of the sulphur and nitrogen atoms which make up approximately 1.05-2.07 wt% and 0.38-0.45 wt%, respectively, of typical gas oil produced from Alberta bitumen and heavy oil (Gray, 1990). In order decrease the concentrations of nitrogen and sulfur, the ring structures must be opened and the heteroatom removed. This is done in secondary upgrading or hydrotreating.

---

[1] Information not supplied.

Hydrotreating employs conditions of high pressure (4-13.9 MPa) and high temperature (380-420 °C) over a Ni-Mo sulfided catalyst to remove undesirable components such as nitrogen and sulphur compounds. The severity of the reaction conditions is largely dependent on the nitrogen compounds, as they are the most resistant to hydrotreating. In order to satisfy the thermodynamic requirements of the denitrogenation reactions for all types of compounds, both temperature and pressure must be high. For example, high temperature is required to remove the alkyl carbazoles and high hydrogen pressure is required to remove the benzocarbazoles (Dorbon *et al.*, 1984).

2.1.3 Characteristics and treatments of nitrogen compounds

Nitrogen compounds are found in both heterocyclic structures and non-heterocyclic structures. Amine compounds, an example of non-heterocyclic nitrogen, release ammonia very quickly under hydrotreating conditions (Furimsky, 1977) and are thus more readily removed by thermochemical treatment. Heterocyclic compounds must undergo a series of more intensive reaction steps to remove the amine group and thus are more resistant. Unfortunately, only a negligible portion of the nitrogen compounds fed to hydrotreaters is non-heterocyclic in structure. The thermal treatments of the upgrading process that precede hydrotreating tend to produce heterocyclic nitrogen compounds. These types of structures can be classified into two groups: basic and non-basic. Compounds such as pyridine and quinoline belong to the basic group whereas pyrrole and carbazole belong to the non-basic group. Analysis of light crude oil by Dorbon and Bernasconi (1989) showed the nitrogen content to be predominantly non-basic structures: only 75-100 ppm was basic compounds and the total nitrogen content was 440-670 ppm.

The total nitrogen content of Athabasca bitumen averages 0.53 wt %, of which basic nitrogen compounds make up 0.09 mol kg^{-1} and non-basic compounds make up 0.12 mol kg^{-1} (Gray, 1990). Frakman *et al.* (1987) showed that the total nitrogen concentration of Athabasca asphaltenes was approximately 2.7 wt %, where carbazole nitrogen amounted to approximately 50 wt% of this total. It is important to distinguish between the two classes of nitrogen compounds, because the rate of denitrogenation is dependent on the basicity of the compounds (Furimsky, 1977). Also, non-basic compounds have a lesser tendency to adsorb to catalyst, and therefore, they are more resistant to denitrogenation. This high stability of non-basic nitrogen compounds is illustrated in Table 2-2 (Gray, 1990). Hydrotreatment of Syncrude coker gas oil shows an overall removal of total nitrogen ranging from 40-50 % whereas a mere 4-28 % of that is removal of non-basic, pyrrole compounds. Dorbon *et al.* (1984) showed that this group of pyrroles in gas oil was largely composed of alkyl carbazoles followed by benzocarbazoles where the unsubstituted form was the more dominant species. Comparisons between gas chromatographs before and after hydrotreating showed that carbazoles were more resistant to treatment than benzocarbazoles and unsubstituted carbazole was more persistent than substituted carbazole. Because of its high resistance to hydrotreating and its concentrations in gas oil, carbazole was chosen as the model compound in this study.

Table 2-2 Removal of nitrogen compounds from Syncrude coker gas oil (after Gray 1990). This coker gas oil is a product stream from primary upgrading. The column headings "MG" designate product resulting from treating the feed under various operating conditions.

		Products		
	Feed	MG-2	MG-7	MG-3
LHSV, mL h^{-1} g^{-1} cat		12.5	16	23.5
N, mol kg^{-1}	0.217			
% Removal		50	43	40
Pyrroles, mol kg^{-1}	0.053			
% Removal		28	19	4

Figure 2-1 Structures of various nitrogen compounds found in crude oil. The compounds are also found with alkyl and benzo-substituted groups.

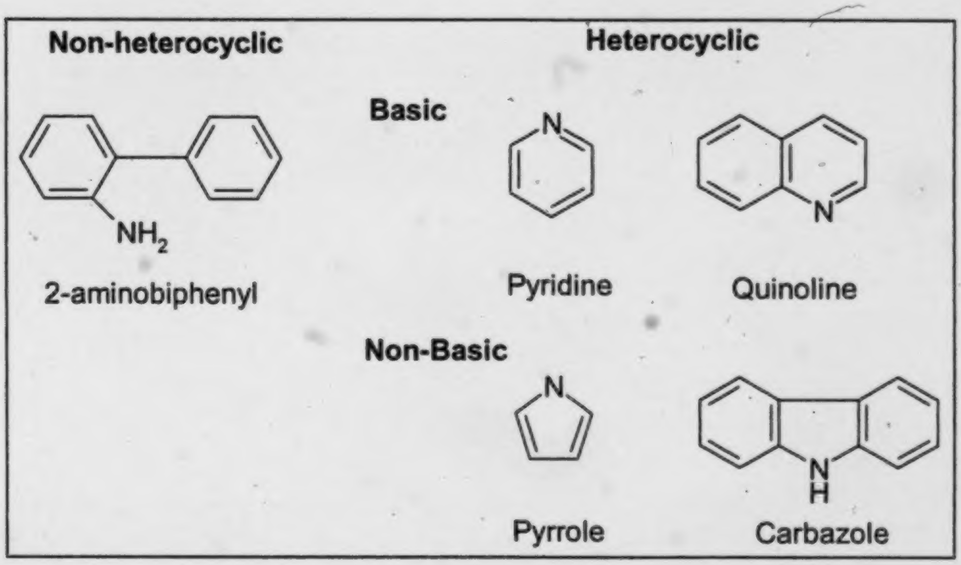
Non-heterocyclic
Heterocyclic
Basic
NH2
2-aminobiphenyl
N
Pyridine
N
Quinoline
Non-Basic
N
Pyrrole
N
H
Carbazole

2.2 Biocatalysis of compounds with low aqueous solubility

2.2.1 Mass transfer

One of the main variables affecting the efficiency and rates of hydrocarbon transformation and degradation is the bioavailability of the substrate. Bioavailability refers to the rate of mass transfer to microbial cells relative to the cells' ability to use the substrate (Wick *et al.*, 2002). The concentration of substrate in the bulk phase of a liquid culture limited by bioavailability is much lower than the aqueous saturation of that compound because the compound is actively removed from the aqueous phase faster than it is replenished.

The uptake of poorly soluble compounds is believed to occur through one or a combination of three mechanisms. These mechanisms focus on how the chemical is transferred from the environment to the cell surface where it is transported through the membrane. One mechanism is passive uptake of the compound, once it is transferred to the aqueous phase via dissolution, or via desorption, in the case of compounds attached to soil particles (Volkering *et al.*, 1992; Wodzinski and Coyle, 1974). Another mechanism is the active secretion of biosurfactants or other extracellular surface active agents that facilitate partitioning of the chemical to the water phase by micellar solubilization or by emulsification in the case of liquid chemicals (Rosenberg and Rosenberg, 1985; Stucki *et al.*, 1987). Finally, direct uptake mechanisms are possible whereby extracellular structures such as thin fimbriae or capsule layers are responsible for improved substrate uptake. The dominant mechanism of transport depends on the compound involved, the specific bacterium and the environmental conditions (Mukherji and Weber, 1998).

Volkering *et al.* (1992) studied the effect of substrate availability on bacterial growth kinetics. Using the following derivations, they confirmed that the rate of substrate dissolution or desorption restricts bacterial growth. The rates of biomass formation from substrate uptake are described with the following equation where X_t is biomass concentration, S_t is the total amount of substrate per until volume, Y is the yield constant of biomass from substrate, and t is time.

$$\frac{dX_t}{dt} = -Y\frac{dS_t}{dt} \tag{2-1}$$

In the case of a solid substrate present in both the liquid and solid phase, the dissolution rate can be represented with Equation 2-2 where V is the volume of the culture, Q_t is the mass of adsorbed substrate, and C_{aq} is the concentration of substrate in solution.

$$\frac{dS_t}{dt} = \frac{1}{V} * \frac{dQ_t}{dt} + \frac{dC_{aq}}{dt} \tag{2-2}$$

Equation 2-3 describes the mass transfer of a solid from the solid phase to the aqueous phase where K_1 is a rate constant; A is the contact surface area and C_{eq} concentration of the substrate in solution at equilibrium.

$$-\frac{dQ_t}{dt} = K_1 * A * (C_{eq} - C_{aq}) \tag{2-3}$$

At high cell densities the C_{aq} can be assumed to be much smaller than C_{eq} and dC_{aq}/dt is essentially zero. The change in substrate concentration takes on the form of a zero-order reaction. The resulting biomass formation equation then takes the zero-order form:

$$\frac{dX_t}{dt} = -\frac{Y}{V}(K_1 * A * C_{eq}) \tag{2-4}$$

The rate of growth is independent of biomass concentration. This derivation suggests that the maximum specific growth rates in batch cultures growing on poorly soluble substrates cannot be obtained. The growth rate of bacteria employing passive uptake is limited by the compound's rate of dissolution. For the case of dissolution-limited growth, the change of biomass with time is linear with constant yield (Y) and surface area of the substrate.

As shown in the final equation (Equation 2-4), growth rate in this situation is dependent only on the surface area (A) of exposed substrate.

In some cases, the biodegradation rate may be lower than the dissolution rate such as in the case of the *Pseudomonas* sp. growing on biphenyl (Stucki and Alexander, 1987). The amount of substrate in the aqueous phase is greater than the amount that the culture requires for growth thus growth rates in this scenario are not dependent on the dissolution rate of substrate. Growth tends to follow the typical growth pattern, beginning with a lag phase, followed by an exponential growth phase and then a stationary phase.

One physical method to increase the contact surface area is to provide glass beads in the culture. The cells can adhere to the bead surface, increasing the surface area of cells exposed to the substrate. Also, the surface area of the crystalline substrate increases by mechanical fragmentation. Adam *et al.* (1992) used this method to increase the biodegradation rates of 3-chlorobiphenyl by *Pseudomonas* sp. CB15. The beads improved removal from 12.6- 97 %.

Surfactants also enhance the dissolution of poorly soluble substrates. When added in non-toxic concentrations to microbial cultures, surfactants can improve the mass transfer properties of poorly soluble compounds via three main mechanisms. They increase the dispersion of organic liquids and solids by reducing the surface and interfacial tension at the aqueous/hydrocarbon interface. They can also increase the solubility of a liquid substrate by forming micro-emulsions, whereby hydrocarbons can become soluble in water (Desai and Banat, 1997). Finally, surfactants can provide facilitated transport of substrate from the solid to aqueous phase (Volkering *et al.*, 1995). The presence of surfactants or biosurfactants can be determined by measuring changes in surface or interfacial tensions. For example, Desai and Banat (1997) reported distilled water to have a surface tension of 72 mN m^{-1}, which was reduced to 30 mN m^{-1} with the addition of surfactant. Commercial surfactants can be added to bacterial systems to improve mass transfer, or the bacteria may synthesize their own surfactants called biosurfactants.

Acinetobacter calcoaceticus RAG-1 is an example of a bacterium that produces its own bioemulsifier. This bacterium was isolated by Reisfeld *et al.* (1972) for its growth on crude oil. These cells form emulsions with the alkane, *n*-hexadecane, during growth. Further studies on the mechanisms of uptake by RAG-1 were completed by Rosenberg and Rosenberg (1985). They attributed the cells' ability to adhere to the hydrocarbon to the production of a surface-active component, emulsan. During the early growth stage, emulsan covered the cell; however, later in the growth cycle it sloughed off into the supernatant where it functioned as a surfactant. Negligible affinity to the hydrocarbon layer was evident for cells in the exponential phase of growth; however, as many as 87 % of stationary cells were bound to hexadecane. The formation of emulsan was concluded to be responsible for this change.

Direct uptake mechanisms can also improve mass transfer of organic compounds. The formation of hair-like structures on the surface of hydrocarbon-grown cells were determined to be functionally related to the transport of hexadecane in the yeast *Candida tropicalis* (Kappeli *et al.*, 1984). Using microscopy, this group was able to detect the presence of the hair-like structures on the hydrocarbon-grown cells that were not evident on glucose-grown cells. *Mycobacterium* sp. LB501T was found to form a biofilm when grown on anthracene as a carbon source, whereas the same characteristic was not present when glucose was added as additional carbon source (Wick *et al.*, 2002).

All or one of these mechanisms may be employed by bacteria to degrade poorly water soluble substrates. The contribution of one mechanism as compared to another is dependent on the culture, stage of growth and environment.

2.2.2 Applications of biocatalysis

Over the course of evolution, microorganisms have developed the ability to metabolize and transform a wide range of substrates. Survival in environments characterized by various potential substrates for growth, with various levels of toxicity, has led to the development of enzyme systems that can transform many unrelated natural organic compounds (Dua *et al.* 2002). The resulting microbial enzymes serves as a resource of biological information available for use by organisms when new organic material is introduced to the environment.

The ability of a microorganism to transform chemicals into products of various structures comes from the activity of its enzymes. These enzymes catalyze chemical reactions. The effects of biocatalysts are similar to that of traditional chemical catalysts in that they decrease activation energy of a reaction, increasing the rate of reaction and allowing it to occur at less severe operating conditions such as temperature and pressure. Biocatalysts offer several advantages over traditional chemical catalysts, including higher reaction rates or higher turnover number in terms of the rate of an enzyme system, milder reaction conditions, reaction specificity and the capacity to be regulated (Voet and Voet, 1995).

The enzymatic capabilities of microorganisms can be employed industrially in the form of a whole-cell catalyst or a purified enzyme. Purified enzymes have the advantage of being immediately available in active form: enzymes can remain stable during storage and do not require time lags to start activity (Alexander, 1994). Reactions with purified enzymes are expensive to operate, but their activity is very specific to substrates for which they were isolated. For example, a purified enzyme was obtained from *Pseudomonas putida* strain BS202-P1 that catalysed the oxidation of 1-hydroxy-2-naphthoate to 1,2-dihydroxynaphthalene (Balashova *et al.* 2001). 1-Hydroxy-2-naphthoate is an intermediate product in the degradation of phenanthrene and BS202-P1 was isolated for its ability to degrade phenanthrene and naphthalene. For enzymatic activity, the cofactors NAP(P)H and FAD were required.

Whole cell systems can be less expensive than purified enzyme systems. Because the entire cell structure is present, the addition of cofactors and coenzymes required by the enzymes is not necessary (Voet and Voet 1995). Use of whole cells also means that other enzyme systems are present in the reactor, leaving the possibility of side reactions to interfere with the targeted reaction. For example, Held *et al.* (1999) used whole-cell biocatalysis to convert 2-phenylphenol to 3-phenylcatechol. The parent strain of

Pseudomonas azelaica HBP1 contained multiple catechol degrading systems and thus was not efficient in the production of the target product 3-phenylcatechol. They addressed this difficulty by using a recombinant strain, *Escherichia coli* JM101 (pHBP461), containing only the enzymes required for the desired pathway.

The types of biochemical reactions being studied in this research may involve multiple enzyme systems; therefore, whole cell biocatalysis is most appropriate for these applications.

2.2.3 Enzymatic control

A chemical reaction catalysed by an enzyme can be described with the following equation:

$$E+S \rightleftharpoons ES \longrightarrow P+E \qquad (2\text{-}5)$$

Where E represents an enzyme, S is the substrate, ES is the enzyme-substrate complex and P is the final product.

Excluding zero order reactions, the rate of reaction for most chemical reactions is proportional to the concentration of the reactants. In this case, the rate is proportional to the concentration of the enzyme-substrate complex, which in turn is dependent on the concentration of both the enzyme and the substrate. In addition, the ability of the substrate to actually bind with the enzyme is a factor. In response to environmental changes, a cell is able to direct this reaction by either controlling the amount of enzyme produced or controlling the ability of the enzyme to bind to the substrate. Control employed at the activity level is more refined than that at the production level in that the response time to environmental changes is much faster with a shorter lag period (Madigan *et al.*, 1997).

Although not all enzyme systems are controlled, it is beneficial for the cell to control some enzymatic activity, as it is a method of energy conservation. If a particular enzyme function is not needed, it is more efficient for the cell not to produce that enzyme. Enzymes that are not affected by the presence of a particular substrate are called constitutive enzymes and they are synthesised at a rate sufficient to maintain constant concentration in the cell (Voet and Voet, 1995). Typically the enzymes responsible for routine cell functions are constitutive.

2.2.3.1 Control of enzymatic activity

There are two types of control mechanisms that affect the activity level and abilities of enzymes: product inhibition and feedback inhibition. Inhibitory substances alter enzymatic activity by affecting the enzyme binding affinity for the substrate. The origin of the product classifies inhibition as product or feedback inhibition.

Product inhibition works at the level of each individual enzymatic reaction. As the reaction proceeds forward, the product accumulates. The increased concentration allows for interaction with the substrate or the substrate-enzyme complex in such a way that the reaction is prevented from proceeding forward. This continues until the product concentration decreases sufficiently to allow the reactants (in this case enzyme and substrate) to react. In the case where the product is the substrate for another enzyme, it will be removed from the system continuously and thus inhibition will not occur.

Feedback inhibition works on the regulation of entire biosynthetic pathways. This type of inhibition works with the same principles of product inhibition except the inhibitory product is the end product of a pathway. The end product usually inhibits the activity of the first enzyme of the pathway (Madigan *et al.*, 1997).

In the case of product inhibition, the inhibitory substances frequently resemble the structure of the substrate targeted by the enzyme. Because feedback inhibition works within an entire pathway, the final products can be much different than the starting substrate and as a result inhibitory substances of feedback inhibition can be structurally very different from substrate targeted by the enzyme. Allosteric enzymes are common in catabolic pathways (Madigan *et al.* 1997). These types of enzymes typically have two binding sites: an active site for the substrate and an allosteric site for the inhibitor. When the inhibitor binds to the allosteric site, the shape of the active site changes significantly enough that the substrate no longer fits the catalytic site.

In both cases of product and feedback inhibition, the presence of the inhibitory compound affects the ability of the enzyme to bind to the substrate. There are three mechanisms used to describe how they interfere with binding: competitive inhibition, non-competitive inhibition and mixed inhibition. These mechanisms are illustrated with the following equations.

$$E+S+I \rightleftharpoons ES+I \longrightarrow P+E+I \qquad (2\text{-}6)a$$

$$E+S+I \rightleftharpoons EI+S \quad \text{(No Reaction)} \qquad (2\text{-}6)b$$

$$E+S \rightleftharpoons ES+I \rightleftharpoons ESI \quad \text{(No Reaction)} \qquad (2\text{-}7)$$

$$E+S \rightleftharpoons ES+I \rightleftharpoons ESI \quad \text{(No Reaction)} \qquad (2\text{-}8)a$$

$$E+S+I \rightleftharpoons EI+S \quad \text{(No Reaction)} \qquad (2\text{-}8)b$$

In the mechanism of competitive inhibition (Equations 2-6 (a) and (b)) the substrate (S) competes directly with the inhibitor (I) for the binding site on the enzyme (E). Formation of product is inhibited because the concentration of enzyme available to the substrate is decreased. In this case the inhibitor is similar enough to the substrate that it usually fits in the same binding site, but it is unreactive. In the case of non-competitive inhibition (Equation 2-7), the reaction is prevented as the inhibitor binds to the enzyme-substrate complex (ES) causing enough structural distortion of the active site that the enzyme is catalytically inactive. Non-competitive inhibition (Equation 2-8 (a) and (b)) or mixed inhibition is a combination of the previous two mechanisms. The inhibitor binds to both the enzyme and the enzyme-substrate complex (Voet and Voet, 1995).

Most enzymes are protein molecules and frequently they require non-protein molecules called cofactors to function. Another method of enzyme regulation involves these cofactors. The enzyme is altered when the modifying group binds to it with a covalent bond: the attachment process results in changing the shape of the enzyme enough to change its catalytic activity. Examples of such regulatory molecules include nucleotide adenosine monophosphate (AMP), adenosine diphosphate (ADP) and inorganic phosphate (Madigan *et al.* 1997).

Biochemical reactions may be catalysed by multiple enzymes. Isozymes are enzymes that catalyse the same reaction but that are controlled by different end products. The benefit of having multiple enzymes responsible for one reaction is that the reaction is only completely stopped when all the inhibitory products are in excess. Higher levels of only one product simply reduce the activity: the reaction is turned down rather than stopped.

2.2.3.2 Cellular control of enzyme production

Controlling the amount of enzyme available in the cell also controls the chemical reactions of a cell. Cells commonly achieve this control by regulating the process of transcription. Transcription is the process through which the genes encoding the instructions for synthesizing a particular enzyme are copied from DNA to messenger RNA (mRNA). The enzyme RNA polymerase is responsible for catalyzing the mRNA synthesis. The correct sequence of the DNA required for transcription is identified by a promoter, at the starting position, with a transcription terminator at the end. To start transcription, the RNA polymerase must first recognize and then bind to the correct promoter (Madigan *et al.*, 1997).

Transcription can be regulated by both positive and negative control. In the case of positive control the controlling element activates transcription whereas the controlling element involved with negative control stops transcription. Transcription with a positively controlled promoter is controlled by an activator protein. This type of promoter has nucleotide sequences that are difficult for the RNA polymerase to recognize; however, when bound to the DNA, the activator protein makes the promoter identifiable. As illustrated in Figure 2-2, binding between the activator protein and the RNA polymerase is only accomplished with the addition of an inducer. In this case, the controlling element, the activator protein, brings about transcription thus it is termed positive control. In the case of negative control, the promoter can be recognized by the RNA polymerase without the involvement of any additional proteins. As illustrated in Figure 2-3, in its resting state the repressor protein prevents transcription: transcription occurs only when as inducer molecule inactivates the repressor protein. This type of control is termed negative control because the regulatory protein, the repressor, prevents transcription.

Repression and induction are control mechanisms for the expression of genes. Repression reduces the synthesis of a particular enzyme whereas induction increases the synthesis of a particular enzyme. The compound responsible for repression is referred to as a co-repressor and that responsible for induction is an inducer. These compounds, or effectors, affect transcription by combining with the specific regulatory proteins that in turn affect mRNA synthesis. Effectors can be substrates, end products or analogs of either. Figure 2-4 illustrates how a co-repressor acts to attach to the repressor and stop transcription. Both Figure 2-2 and Figure 2-3 illustrate the actions of inducers.

When the concentration of a particular compound (X) is sufficient for the cells' requirements or if X is merely present in the system, a corepressor can help prevent transcription of the mRNA required to synthesize the enzymes needed for the reaction producing X. As illustrated in Figure 2-4, the co-repressor combines with the repressor protein and the two then bind to the operator region of the targeted DNA segment. This region is located next to the promoter. While bound to the operator, the co-repressor/ repressor combination block transcription of mRNA and mRNA is not produced. Without the encoded instructions provided by the mRNA the proteins required for that specific enzyme are not produced.

One particular type of repression is called catabolite repression. Catabolism is the biochemical process responsible for converting organic and inorganic compounds into energy. In the repression of this process, the products generated during catabolism of one substrate repress the synthesis of the enzymes required to use another substrate that would give the same products (Alexander, 1994). This regulation can involve the repression of several enzyme systems that may be unrelated (Madigan *et al.*, 1997).

In contrast, an inducer will drive transcription of information needed to make enzymes that produce certain products. In the case of a negatively controlled promoter (Figure 2-3), the repressor protein blocks transcription until the inducer attaches to this protein and it is removed from the operator. In the case of a positively controlled promoter (Figure 2-2), the inducer is needed to start transcription. The inducer attaches to the activator protein that in turn binds to the activator binding site making it recognizable to RNA polymerase which starts transcription.

Figure 2-2 Induction of a positively controlled system. (A) In the absence of an inducer, neither the activator protein nor the RNA polymerase can bind to the DNA and transcription does not occur, (B) An inducer binds to the activator protein which in turn binds to the RNA polymerase. The RNA polymerase is then able to recognize and bind to the promoter, activating transcription (after Madigan *et al.*, 1997).

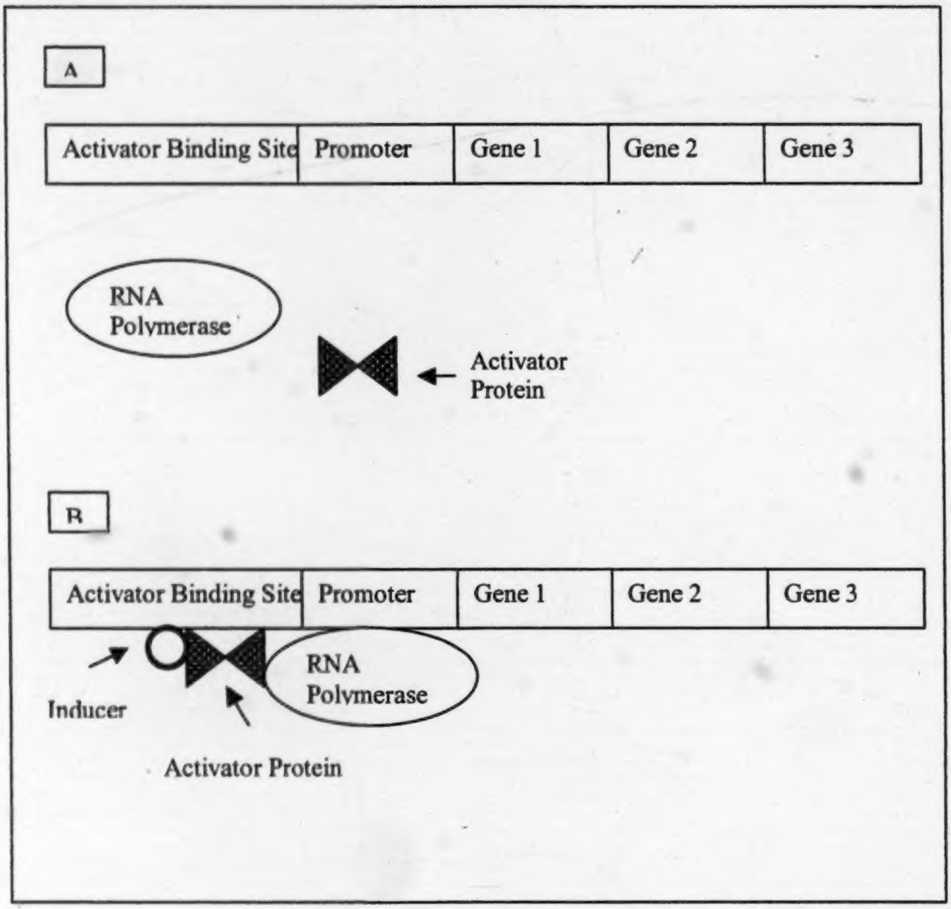
A
Activator Binding Site
Promoter
Gene 1
Gene 2
Gene 3
RNA Polymerase
Activator Protein
B
Activator Binding Site
Promoter
Gene 1
Gene 2
Gene 3
Inducer
RNA Polymerase
Activator Protein

Figure 2-3 Induction of a negatively controlled system. (A) In the absence of an inducer, a repressor binds to the operator region and blocks transcription. (B) An inducer binds to the repressor protein and inactivates it, allowing transcription (after Madigan et al., 1997).

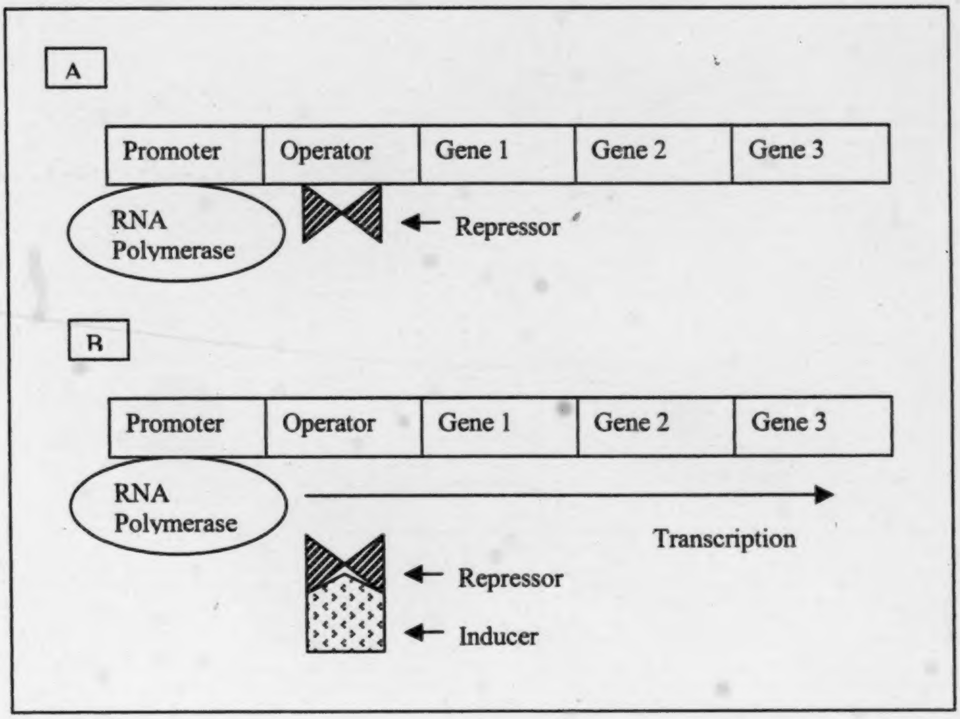
A
Promoter
Operator
Gene 1
Gene 2
Gene 3
RNA Polymerase
Repressor
B
Promoter
Operator
Gene 1
Gene 2
Gene 3
RNA Polymerase
Transcription
Repressor
Inducer

Figure 2-4 The process of gene repression. (A) Transcription occurs because the repressor cannot bind with the operator. (B) Transcription is blocked. The repressor is able to bind to the operator only after the corepressor binds to the repressor (after Madigan *et al.*, 1997).

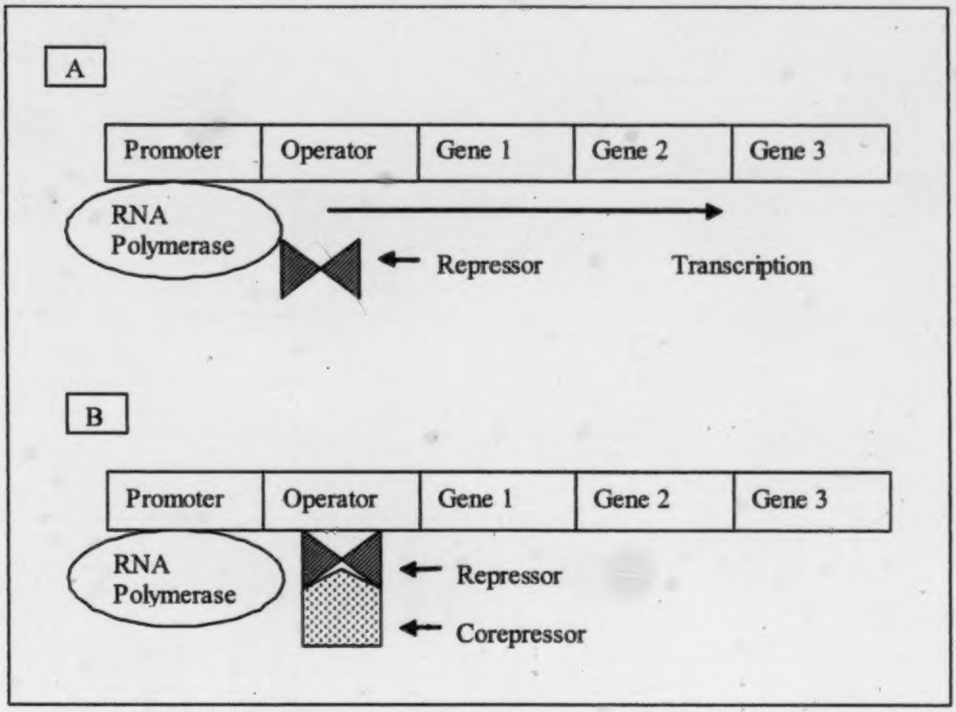
A
Promoter
Operator
Gene 1
Gene 2
Gene 3
RNA Polymerase
Repressor
Transcription
B
Promoter
Operator
Gene 1
Gene 2
Gene 3
RNA Polymerase
Repressor
Corepressor

2.3 Biochemical transformation of polycyclic aromatic compounds

Many microorganisms have the ability to metabolize a variety of aromatic compounds, and use these compounds as a source of energy and nutrition. Microorganisms also have the ability to cometabolize an even wider range of aromatic compounds. The process of cometabolism involves the transformation of a compound without extracting energy or carbon from the chemical reaction. This reaction requires the presence of a second carbon source that is suitable for catabolism. Biotransformation of aromatic compounds is also possible in a buffered cell suspension where additional energy sources are not supplied.

In the aerobic process of transforming aromatic hydrocarbons or aromatic compounds into a useful substrate for the cell, microorganisms frequently convert the complex structures into one of two products: a protocatechuate or a catechol. Transformation of the initial aromatic compound begins with oxidation by monoxygenase or dioxygenase enzymes, where either one or both atoms of an oxygen molecule are added to the compound, respectively. The addition molecular oxygen to the aromatic compound often makes it less harmful to the surrounding cells hence the initial attack can be a detoxification mechanism (Alexander, 1994). In the case of hydrophobic aromatic compounds, the attack is usually achieved by multi-component dioxygenases (Pieper and Reineke, 2000) where the resulting oxidation product is a labile *cis,cis*-dihydrodiol that converts into a catechol (Atlas and Bartha, 1998).

In oxidative catabolism, the catechol ring is subsequently opened with an intradiol enzyme via *ortho*-cleavage, or it is opened with an extradiol enzyme via *meta*-cleavage (Figure 2-5). The final products, succinate, acetyl-CoA and pyruvate, then enter central metabolic pathways (Madigan *et al.*, 1997), the final process of harnessing and storing the energy from these organic compounds.

Figure 2-5 Microbial metabolism of catechol. Catechol is an intermediate product in the degradation of aromatic hydrocarbons and related heterocyclic aromatic compounds (after Atlas and Bartha, 1998).

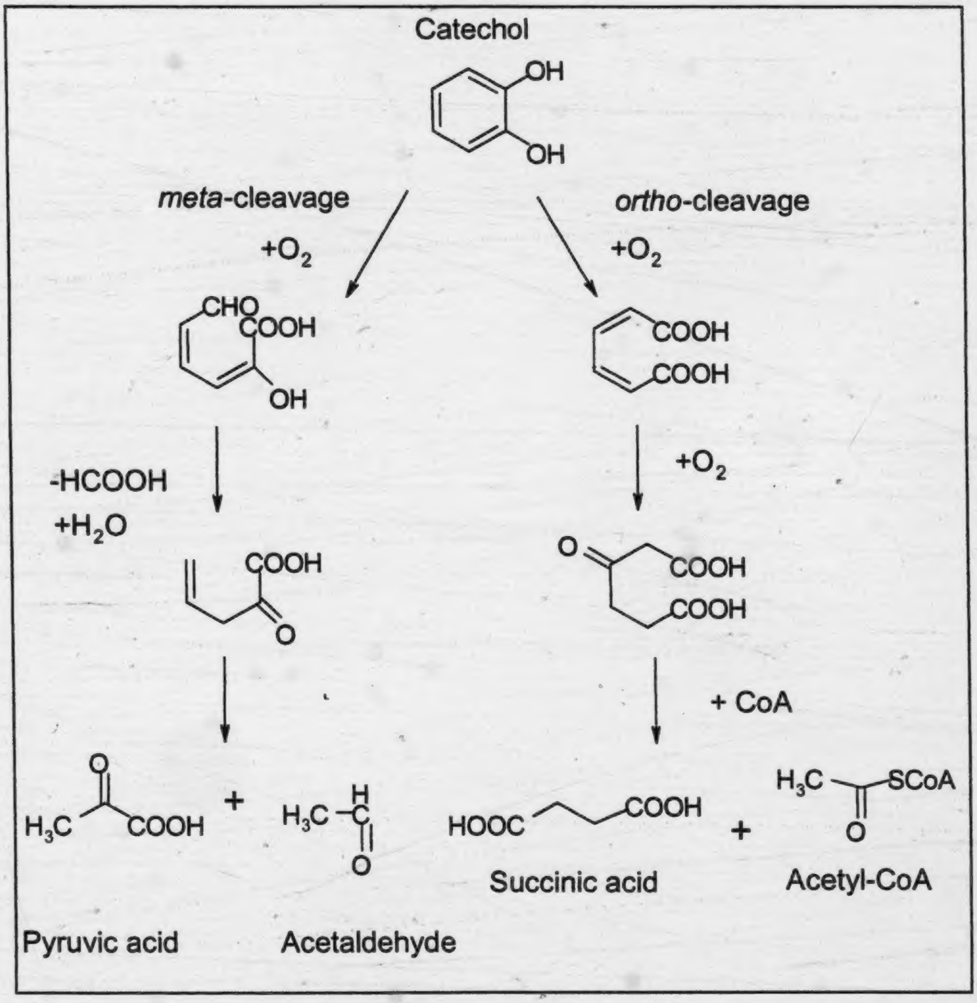
Catechol
OH
OH
meta-cleavage
$+O_2$
ortho-cleavage
$+O_2$
CHO
COOH
OH
COOH
COOH
-HCOOH
$+H_2O$
$+O_2$
COOH
O
O
COOH
COOH
+ CoA
O
H_3C
COOH
+
H_3C
H
C
O
HOOC
COOH
+
H_3C
SCoA
O
Pyruvic acid
Acetaldehyde
Succinic acid
Acetyl-CoA

2.3.1 Biotransformation of naphthalene

Naphthalene is a useful example to describe the process of biotransformation, as it is the simplest polycyclic aromatic hydrocarbon (PAH). Information about this compound is valuable for understanding and predicting the pathways of more complex PAHs and the corresponding polyaromatic compounds (PACs). The enzyme systems responsible for the transformation of other multi-ring compounds often resemble that of naphthalene (Bressler and Fedorak 2001). For example, the naphthalene dioxygenase isolated from *Pseudomonas* sp. NCIB9816 is similar to that for transformation of benzene and toluene (Ensley *et al.*, 1982). The genes encoding the naphthalene-degrading enzymes have been isolated and investigated by Eaton and Chapman (1992). Using recombinant *Escherichia coli* JM109 carrying cloned genes from plasmid NAH7, they showed the *nah* operon to have a gene order of p, A,B,F,C, and E, D. By cloning and testing the ability of each enzyme they were able to properly identify reaction steps between 2-hydroxychromene-2-carboxylate and *trans-o*-hydroxybenzylidene pyruvate (Figure 2-6). Until this particular study was completed, this step had caused some confusion. Naphthalene transformation follows the pathway illustrated in Figure 2-6.

Figure 2-6 Microbial metabolism of naphthalene, an example of a PAH (after Denome *et al.*, 1993; Eaton and Chapman, 1992). The letters refer to the enzymes that catalyze that reaction step: A. naphthalene 1,2-dioxygenase; B. 1,2-dihydroxy-1,2-dihydronaphthalene dehydrogenase; C. 1,2-dihydroxynaphthalene dioxygenase; D. 2-hydroxychromene-2-carboxylate isomerase; E. *trans-o*-hydroxybenzlidenepyruvate hydratase-aldolase; F. salicylaldehyde dehydrogenase.

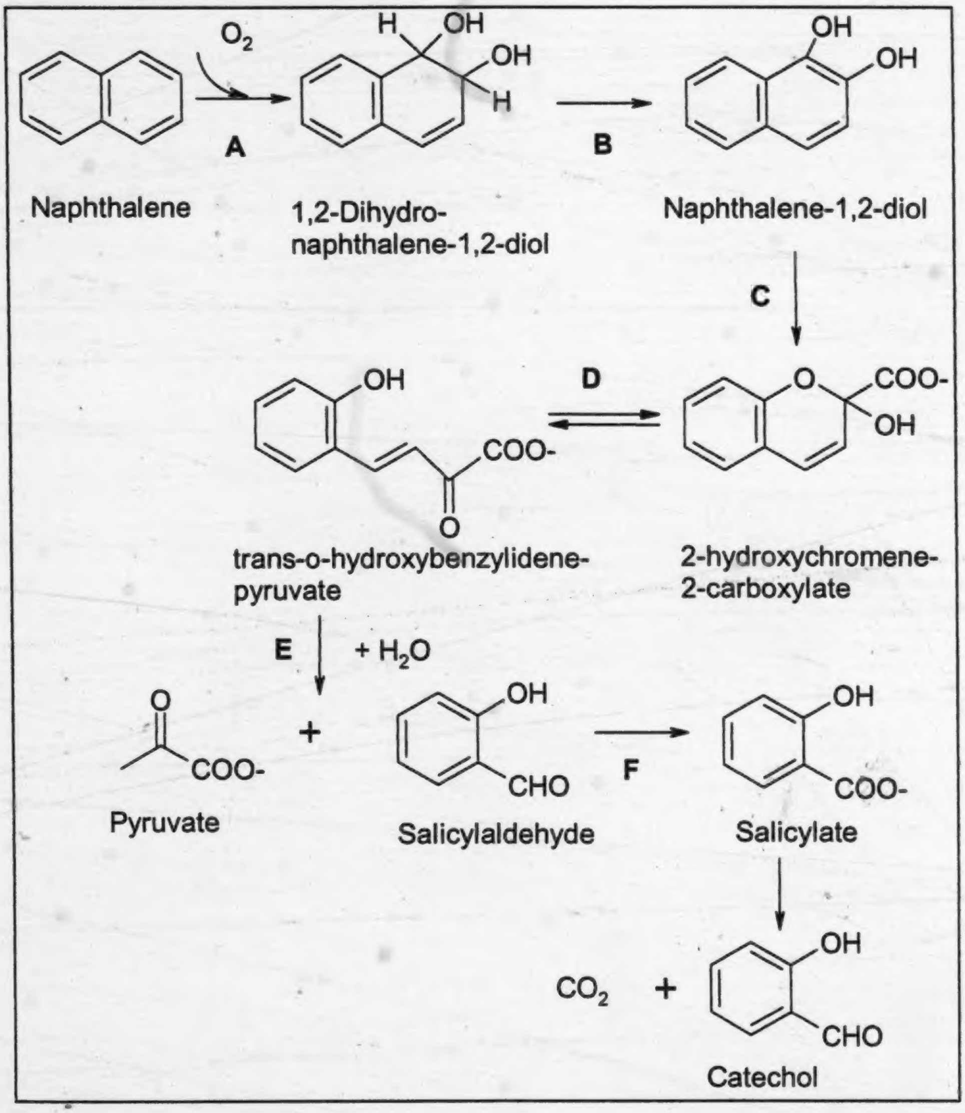
O2
A
H
OH
OH
H
B
OH
OH
Naphthalene
1,2-Dihydro-naphthalene-1,2-diol
Naphthalene-1,2-diol
C
OH
D
O
COO-
OH
COO-
O
trans-o-hydroxybenzylidene-pyruvate
2-hydroxychromene-2-carboxylate
E
+ H2O
O
COO-
+
OH
CHO
F
OH
COO-
Pyruvate
Salicylaldehyde
Salicylate
OH
CO2
+
CHO
Catechol

Figure 2-6 illustrates the types of chemical conversions that are characteristic of microbial transformation reactions. The products clearly show alterations in the chemical structures, changing aromatics to open ring structures with various degrees of degradation to the carbon skeleton. These same conversions of the carbon backbone are the objective of various upgrading processes, including thermal treatments and hydrotreating. The objectives of thermal treatments are to break large compounds into small ones and to convert saturated cyclic structures into open chained structures. Hydrotreating is employed to remove the contaminants of sulphur, oxygen and nitrogen from the valuable carbon structures. In light of these similarities, the feasibility of harnessing the microbial activities responsible for these transformations and applying them to oil feedstocks is the topic of various investigations. The first step of evaluation is to understand the biochemical pathways responsible for the transformations.

The pathways of dibenzothiophene (DBT) and carbazole transformation will be examined in the next two sections. Dibenzothiophene is of interest because of the extensive studies of microbial desulphurization processes and because it is an analogue of carbazole.

2.3.2 Dibenzothiophene biotransformation

There are three modes of attack on the fluorene analogues carbazole, dibenzothiophene and dibenzofuran (Bressler and Fedorak, 2000). One pathway starts similarly to that of naphthalene: a dioxygenase attacks two carbon atoms of one six-membered ring. These carbons are located directly opposite from the heteroatom: position 1 and 2 in dibenzofuran and dibenzothiophene and position 3 and 4 in carbazole. Another attack mechanism is termed the five-membered ring attack in which case initial oxidation starts at the heteroatom. The third mode, involves angular oxidation of the compound. Angular dioxygenases oxidize two carbon atoms directly adjacent to the heteroatom: positions 4 and 4a in dibenzofuran and position 1 and 9a in carbazole.

Figure 2-7 Numbering convention of atoms that make up the oxygen, sulphur and nitrogen analogues of fluorene.

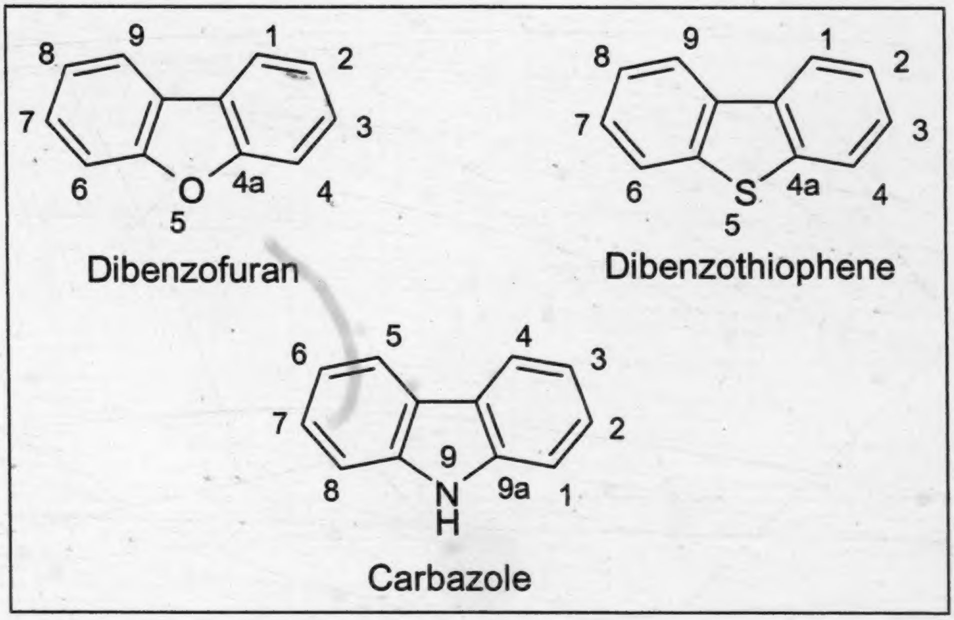
8
9
1
2
7
3
6
O
4a
4
5
Dibenzofuran
8
9
1
2
7
3
6
S
4a
4
5
Dibenzothiophene
6
5
4
3
7
2
9
8
N
H
9a
1
Carbazole

These three attack modes are illustrated in the three published pathways of dibenzothiophene biotransformation (Figure 2-8). The naphthalene type attack is found in the Kodama pathway (Kodama *et al.*, 1973), the five-membered ring attack begins the 4S pathway (Omori *et al.*, 1992) and the angular oxidation attack mode is found in the pathway described by van Afferden *et al.* (1993).

Degradation of dibenzothiophene following the Kodama pathway proceeds through ring opening of the carbon structures followed by subsequent mineralization of one carbon ring. The similarities between this degradation pathway and that of naphthalene do not stop at the initial mode of attack; in fact, it has been shown that the entire upper pathways of transformation are almost identical. The genes that encode the enzymes responsible for this activity in *Pseudomonas* sp. C18 have been cloned and sequenced. They show high similarity with naphthalene degradation (Denome *et al.*, 1993). The arrangement of the *dox* genes (dibenzothiophene oxidation) shows similarity to those of the naphthalene gene sequence, NAH that was isolated by Eaton and Chapman (1992). The main difference is that the *dox* genes contain one more open reading frame than the NAH sequence. This particular frame, *dox*H, is thought to be involved in the conversion of structure C to D (Figure 2-8). The activities of isolate *Pseudomonas* sp. C18 suggest that a single genetic pathway may control the metabolism of dibenzothiophene, naphthalene and phenanthrene (Denome *et al.*, 1993).

Perhaps the most interesting dibenzothiophene degradation pathway is that called the "4S pathway". The novelty of this reaction is that it allows direct desulphurization of organosulphur compounds and thus it has the potential for industrial implementation (Shennan, 1996). Characterized by the five-membered ring attack (Bressler and Fedorak, 2000), the 4S pathway starts with oxidation of the heteroatom. The sulphur atom is oxidized with two oxygen atoms, at which point the C-S bond is cleaved. The remaining sulphur functional group is removed via a desulphinase enzyme. Carbon is left intact in the form of 2-hydroxybiphenyl and the sulphur is released in the form of sulfite (Omori *et al.*, 1992).

This mode of dibenzothiophene transformation was detected in isolate *Rhodococcus* sp. IGTS8 (Kayser *et al.*, 1993). IGTS8 has the ability to desulphurize dibenzothiophene as well as a variety of other organosulphur compounds with minimum carbon degradation. In fact, the isolate cannot use these compounds as carbon sources. The enzymes responsible for this activity were shown to be subject to repression and induction. An appropriate organosulphur source was required to induce the expression of the enzymes, while sulphate repressed the sulphur specific activity.

The dibenzothiophene pathway characterized by van Afferden *et al.* (1993) represents a unique degradation pathway in that it has characteristics similar to both the Kodama and 4S pathways. As shown in Figure 2-8, the initial attack starts with oxidation of the heteroatom as found in the 4S pathway; however, the carbon structure is completely destroyed as in the Kodama pathway. The turning point occurs at the C-S bond cleavage. Instead of direct cleavage, the two carbon atoms adjacent to the sulphur atom are oxidized by angular dioxygenation. The sulphur atom is not released until the carbon ring is subjected to microbial degradation.

Figure 2-8 Biotransformation pathways of dibenzothiophene following Kodama et al. (1973), van Afferden et al. (1993) and Omori et al. (1992). The legend of the intermediates appears in Table 2-3.

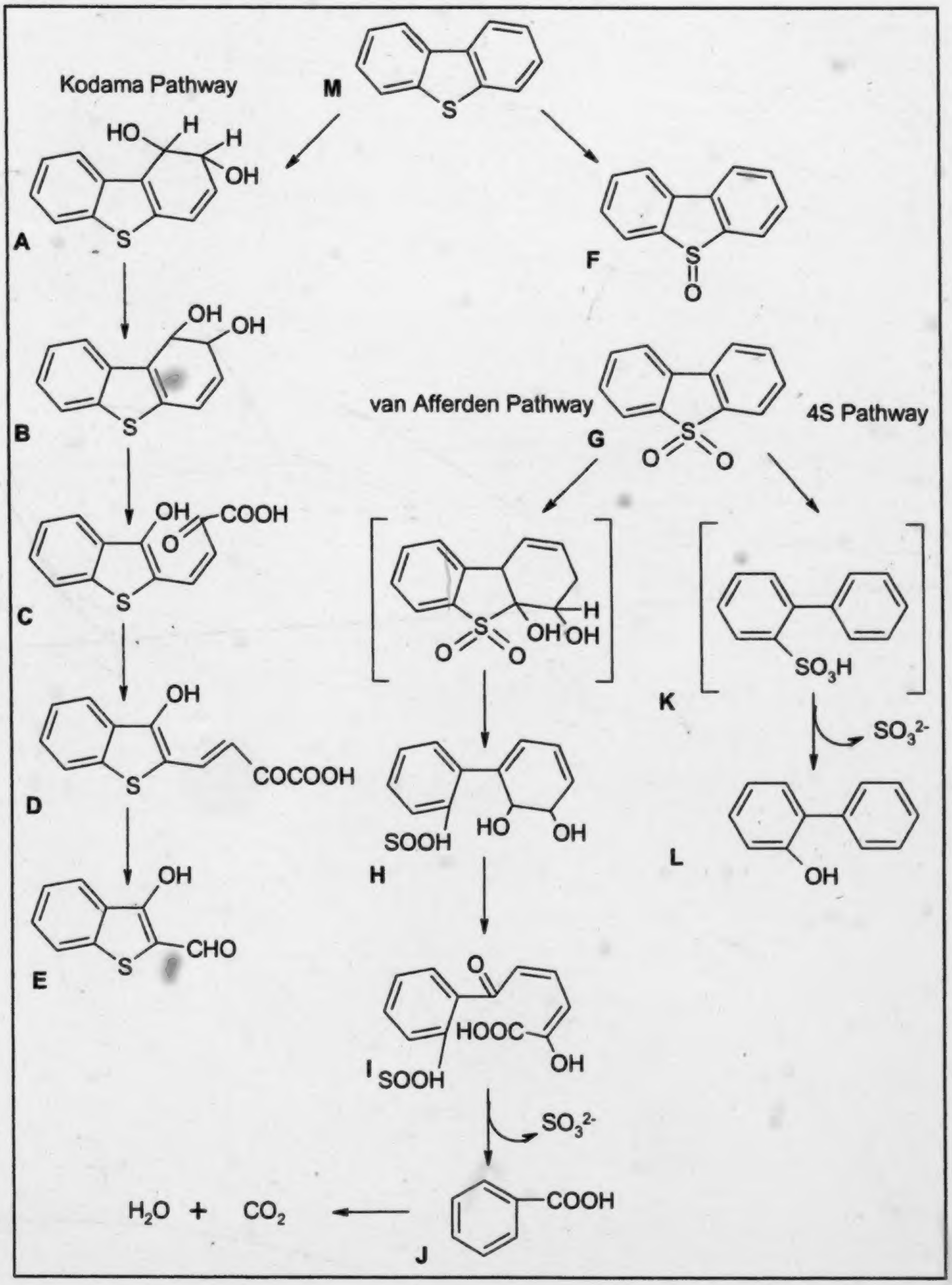
Kodama Pathway
M
S
HO
H
H
OH
A
F
OH
OH
B
van Afferden Pathway
G
4S Pathway
O
O
OH
COOH
C
OH
OH
H
SO3H
K
SO3 2-
OH
COCOOH
D
SOOH
HO
OH
H
L
OH
CHO
E
O
HOOC
OH
I
SOOH
SO3 2-
H2O + CO2
COOH
J

Table 2-3 Intermediates in dibenzothiophene metabolism as outlined in Figure 2-8.

Designation	Compound
A	*Cis*-1,2-Dihydro-1,2-dihydroxydibenzothiophene
B	1,2-Dihydroxydibenzothiophene
C	*cis*-4[2-(3-Hydroxy)-thianaphthenyl]-2-oxo-3-butenoic acid
D	*trans*-4[2-(3-Hydroxy)-thianaphthenyl]-2-oxo-3-butenoic acid
E	3-Hydroxy-2-formylbenzothiophene
F	Dibenzothiophene-5-oxide
G	Dibenzothiophene sulphone
H	2′,3′-Dihydroxybiphenyl-2-sulphinic acid
I	6(2′-Sulphinophenyl)-6-oxo-2-hydroxy-hexa-2,4-dienoic acid
J	Benzoic acid
K	2-Phenyl benzene sulphonic acid
L	2-Hydroxybiphenyl
M	Dibenzothiophene

2.3.3 Carbazole biotransformation

Benedik *et al.* (1998) reviewed the biological degradation of carbazole and other organonitrogen compounds. Unlike the desulphurization attack of the 4S pathway of dibenzothiophene transformation, the literature detailing microbial attack of carbazole does not include nitrogen specific activity. Excluding the products that have already undergone extensive carbon degradation, the identified metabolites of carbazole degradation show ring opening with a free amine group remaining intact.

Microbial consortia (Fedorak and Westlake, 1984; Grosser *et al.*, 1995), bacterial isolates (Finnerty *et al.*, 1983; Gieg *et al.*, 1996; Habe *et al.*, 2001; Kilbane *et al.*, 2002; Kirimura *et al.*, 1999; Kobayashi *et al.*, 1995; Nakagawa *et al.*, 2002; Ouchiyama *et al.*, 1993;

Ouchiyama *et al.*, 1998; Schneider *et al.*, 2000; Shotbolt-Brown *et al.*, 1996) and fungi (Bressler *et al.*, 2000) have shown the ability to biotransform or degrade carbazole.

Fedorak and Westlake (1984) examined the fate of carbazole and 26 alkyl carbazoles, in Norman Wells crude oil exposed to a carbazole enriched microbial consortium. Their findings showed complete removal of C_1 –C_3 carbazole isomers within 8 d. Grosser *et al.* (1995) showed 25-50 % mineralization of carbazole within 64 d using a bacterial consortium exposed to a variety of PACs.

A variety of bacterial isolates with the ability to biotransform and biodegrade carbazole has been identified. Their origins are diverse because they have been isolated in soil and sludge samples from various locations. Excluding one group (Kobayshi *et al.*, 1994), all isolates have been cultivated under aerobic conditions. Kobayshi *et al.* (1994) identified eight carbazole degraders under microaerobic conditions, where the liquid cultures and head space were purged with nitrogen gas. The isolates found in aerobic conditions have all been Gram negative bacteria, belonging mostly to the genera *Sphingomonas* and *Pseudomonas,* with one *Ralstonia.* One Gram positive bacterium, a *Bacillus*, was isolated under the microaerobic conditions. All these bacteria were isolated for their ability to mineralize carbazole, to use carbazole as a carbon source or to use carbazole as both a carbon and nitrogen source.

2.3.3.1 Carbazole degradation pathways

Two research groups have proposed carbazole degradation pathways: Ouchiyama *et al.* (1993) with *Pseudomonas* sp. strains CA06 and CA10; and Gieg (1996) with *Pseudomonas* sp. LD2. The former group proposed an initial angular dioxygenation attack of carbazole. The metabolites formed with the LD2 suggested the same initial attack. However other metabolites from LD2 had the structure of indole derivatives. These products were similar to those found in the Kodama pathway proposed for dibenzothiophene. The genes encoding the enzymatic activity responsible for carbazole transformation by *Pseudomonas* sp. strain CA10 were completely identified and characterized by Sato *et al.* (1997b). The genes responsible for carbazole degradation in *Pseudomonas* sp. LD2 were isolated and identified by Riddle *et al.* (2003) who used a rifampicin-resistant derivative of LD2, designated MB1332, for the genetic work.

Using isolates *Pseudomonas* sp. strains CA06 and CA10, Ouchiyama *et al.* (1993), proposed a ring opening pathway for carbazole degradation outlined in Figure 2-9. This pathway is similar to those of the carbazole analogs fluorene and dibenzofuran proposed by Strubel *et al.* (1991). Carbazole degradation starts with angular dioxygenation, leaving a product of 2′-aminobiphenyl-2,3-diol. From here the upper pathway (carbazole to anthranilic acid) follows *meta*-cleavage of 2-aminobiphenyl-2,3-diol into 2-hydroxy-6-oxo-6-(2′-aminophenyl)hexa-2,4-dienoic acid via an extradiol dioxygenase. Hydrolysis of this compound gives anthranilic acid. The lower degradation pathway is thought to continue via *ortho*-cleavage of catechol to *cis,cis*-muconic acid.

Figure 2-9 Carbazole degradation pathway proposed by Ouchiyama *et al.* (1992). 1. Carbazole; 2. 2′aminobiphenyl-2,3-diol; 3. 6-(2-aminophenyl)-2-hydroxy-6-oxo-hexa-2,4-dienoic acid; 4. 2-hydroxy-4-pentenoate; 5. anthranilic acid; 6. catechol; 7. *cis,cis*-muconic acid

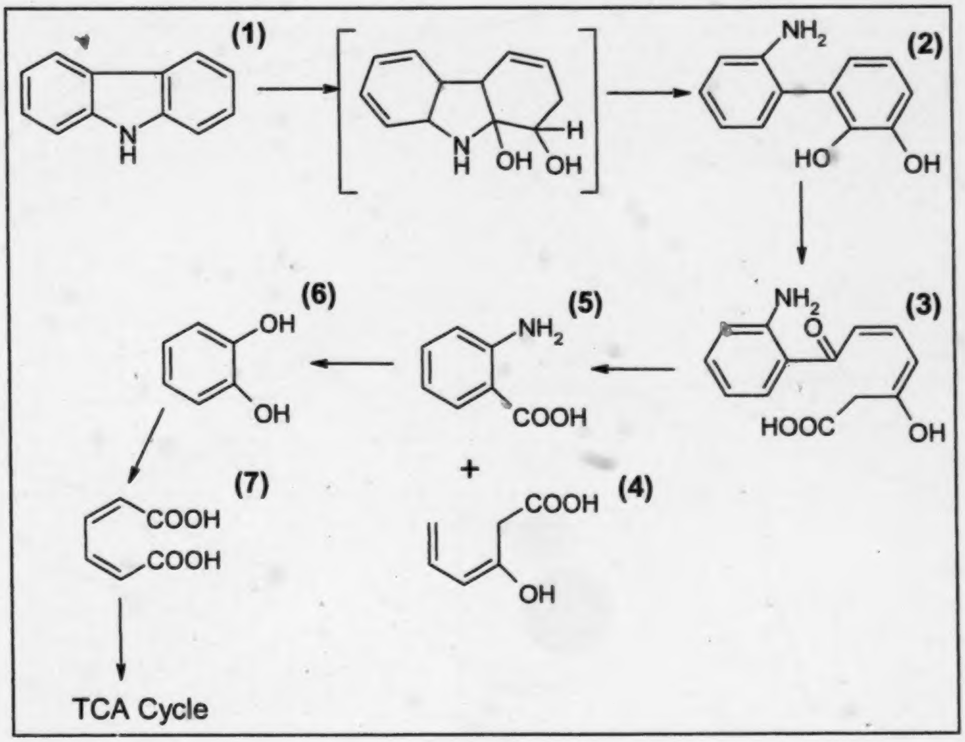
(1)
N
H
N
H
OH
OH
H
NH2
(2)
HO
OH
(6)
OH
OH
(5)
NH2
COOH
(3)
NH2
O
HOOC
OH
+
(7)
COOH
COOH
(4)
COOH
OH
TCA Cycle

Using *Pseudomonas* sp. LD2, Gieg (1996) proposed carbazole degradation to follow the pathway outlined in Figure 2-10. She identified 3a, 4-dihydro-2-methoxy-pyrrolo[1,2-a]quinoline-1,5-dione in the culture extract and attributed its accumulation to the intramolecular cyclization of 6-(2-aminophenyl)-2-hydroxy-6-oxo-hexa-2,4-dienoic acid because she did identify the methyl ether of this compound. These findings coupled with the identification of other 2-aminobenzoyl type compounds as metabolites, led to the conclusion that LD2 followed the same angular attack pathway as that described by Ouchiyama *et al.* (1993) even though she did not detect 2′-aminobiphenyl-2,3-diol. Work with anthranilic acid also confirmed that LD2 followed the same lower degradation pathway as that proposed by Ouchiyama *et al.* (1993). In addition, the genetic sequencing completed by Riddle *et al.* (2003) showed that *carAa* through *carBa* of MB1332 were identical to *carA* through *carBa* of CA10 and that the two sequences of *carC* matched.

One interesting discovery by Gieg (1996) was that indole derivatives were also identified in the supernatant of carbazole-grown LD2. These compounds do not appear in the pathway proposed by Ouchiyama, and suggest a possible alternate pathway. Similar indole derivatives were found as products of *Ralstonia* sp. RJGII.123, formerly known as *Xanthomonas ampelina* RJGII.123 (Schneider *et al.*, 2000). When incubated with carbazole as sole carbon source, 12 product peaks were detected using GC-MS. One metabolite was identified as 5-(2-aminophenyl)-5-oxopentanoic acid. This suggested that this organism followed a pathway similar to that proposed by Ouchiyama *et al.* (1993). Indole-2,3-dicarboxylic acid and indole-3-carboxylic acid were also found as metabolites, indicating that this organism may follow a second pathway similar to the one postulated by Gieg (1996).

Recombinant strains constructed with plasmids carrying portions of the carbazole degradation genes from MB1332 were used by Riddle *et al.* (2003) to produce selected carbazole metabolites. *Pseudomonas* sp. RR149 contained a plasmid carrying the gene *carA* and thus carbazole degradation stopped at 2′-aminophenyl-2,3 diol whereas *Pseudomonas* sp. RR150 contained a plasmid with *carABC* and thus degraded carbazole to anthranilic acid.

As illustrated in Figure 2-9 and Figure 2-10, neither of the published pathways for carbazole shows nitrogen-specific activity. Nitrogen-specific activity has been shown for the basic compound quinoline. Kilbane *et al.* (2000) showed that *Pseudomonas ayucida* IGTN9m targets quinoline as a nitrogen source, but it cannot use it as a carbon source. Figure 2-11 illustrates this denitrogenation reaction.

Figure 2-10 Carbazole degradation pathway proposed by Gieg (1996) using *Pseudomonas* sp. LD2. 1. Carbazole; 2. 2′-aminobiphenyl-2,3-diol; 3. 6-(2-aminophenyl)-2-hydroxy-6-oxo-hexa-2,4-dienoic acid; 4. 3a,4-dihydro-2-methoxy-pyrrolo[1,2-a]quinoline-1,5-dione; 5. 5-(2-aminophenyl)-5-oxo-pent-3-enal; 6. 2-(2,3-dihydro-4-oxo-1*H*-quinoline-2-yl) acetic acid; 7. 5-(2-aminophenyl)-5-oxo-pentanoic acid; 8. 3-(2-aminophenyl)-3-oxo-propanoic acid; 9. indole-3-acetic acid; 10. anthranilic acid; 11. catechol; 12. *cis,cis*-muconic acid.

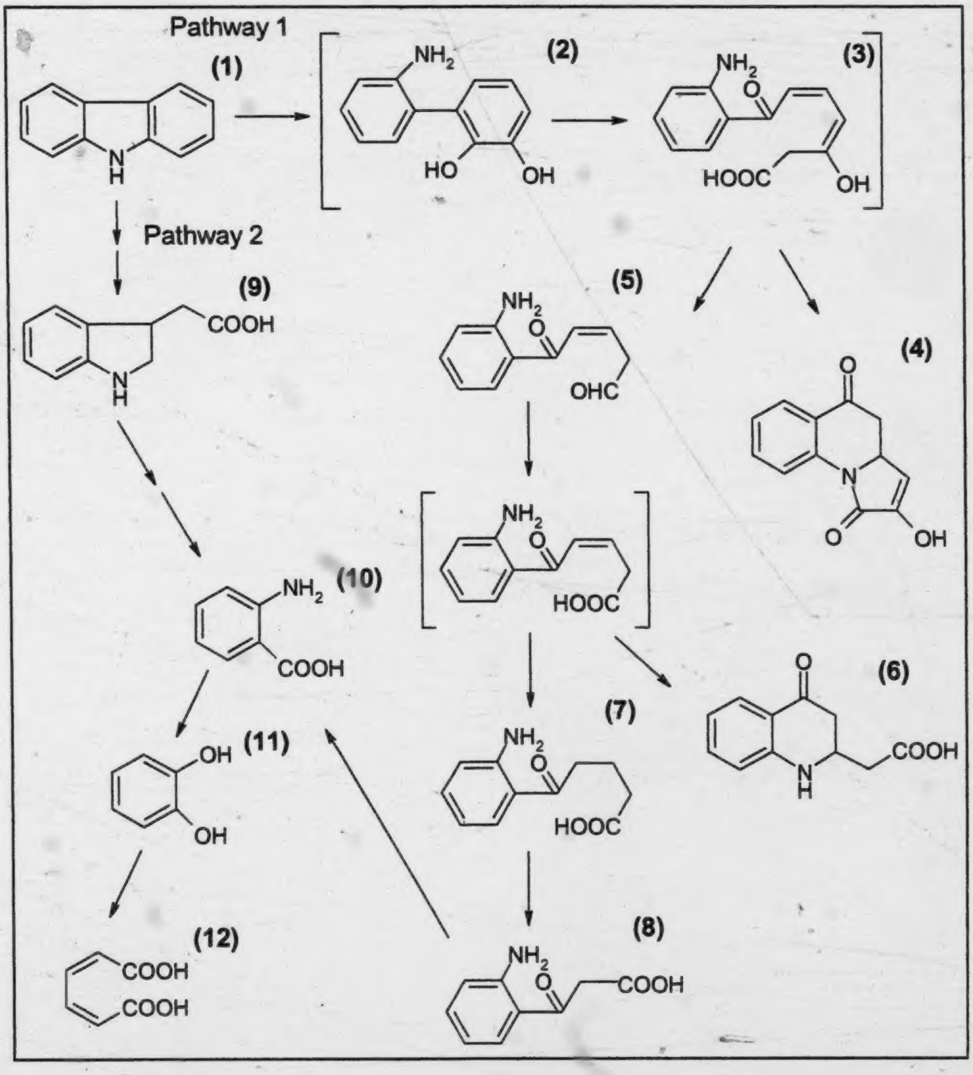
Pathway 1
(1)
(2)
(3)
Pathway 2
(9)
(5)
(4)
(10)
(6)
(7)
(11)
(12)
(8)
NH2
HO
OH
HOOC
COOH
OHC
O
N
H

Figure 2-11 Selective removal of nitrogen from quinoline using isolate *Pseudomonas ayucida* IGTN9m (Kilbane *et al.*, 2000).

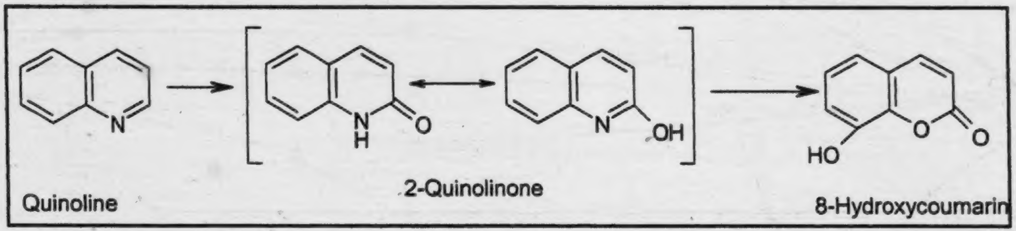

2.3.3.2 Genetic analysis of carbazole genes

A detailed genetic analysis of the activity responsible for carbazole degradation by *Pseudomonas resinovorans* strain CA10 was completed by Kimura *et al.* (1996) and Maeda *et al.* (2003). The first group isolated the genes encoding carbazole catabolism. Through transposon mutagensis, they determined that the process was encoded on two different gene clusters: one for the upper pathway converting carbazole to anthranilic acid and one for the lower pathway converting catechol to *cis,cis* muconate. The second group completed the nucleotide sequence of the Plasmid pCAR1.

The upper pathway was further studied by Sato *et al.* (1997a and b). In the first publication they detailed the results of cloning the DNA fragment encoding the *meta*-cleavage enzymes (*carBa* and *carBb*) and the *meta*-cleavage compound hydrolase (*carC*). *carBb* was found to have higher affinity for *meta*-cleavage activity of 2,3-dihydroxybiphenyl than for catechol derivatives. In comparison to other hydrolases, *carC* was found to have greatest homology with those genes involved in the degradation of monoaromatic compounds versus those involved in biphenyl degradation.

Sato *et al.* (1997b) examined the genes encoding carbazole 1,9a-dioxygenase (CARDO), which is the enzyme responsible for the initial attack on carbazole. This is a multicomponent enzyme system similar to naphthalene and toluene dioxygenases. The nucleotide sequences for these genes were given the designations *carAaAcAd*. This paper was the first to report cloning genes encoding dioxygenases that attack at the angular position adjacent to the heteroatom.

Substrate specificity of CARDO was examined by Sato *et al.* (1997b) using a recombinant plasmid that encoded only the first portion of the upper pathway genes: *carAaAcAd*, those responsible for the initial oxidation. This enzyme was able to oxidize a variety of polycyclic aromatic compounds including dibenzofuran, dibenzothiophene, fluorene, anthracene, dibenzo-*p*-dioxin, phenanthrene, fluoranthene, and others. Nojiri *et al.* (2001) characterized the final portion of the carbazole degradation gene of *Pseudomonas* sp. CA10. They revealed that the *car* gene cluster was composed of 10 genes (*carAaAaBaBbCAcAdDFE*). They also confirmed that the *car* gene cluster was located on the megaplasmid pCAR1.

Ouchiyama *et al.* (1998) cloned the nucleotide sequence of carbazole catabolic genes in *Pseudomonas stutzeri* OM1. The upper pathway of carbazole degradation was similar to that of CA10 but the lower pathway used *meta*-cleavage of catechol instead of *ortho*-cleavage. This was the first study to provide evidence of a biochemical pathway that differs to those proposed by Gieg (1996) and Ouchiyama *et al.* (1992).

The *car* locus of *Sphingomonas* sp. CB3 was isolated by Shepherd *et al.* (1998). This locus encoded the first four enzymes of carbazole catabolism. This group determined that the amino acid sequence of Car was closer to that responsible for biphenyl catabolic genes than to those of CA10. The activity of this extradiol dioxygenase showed induction by carbazole and biphenyl. This same activity showed repression when acetate or succinate was added as a carbon source. This organism was not able to use biphenyl and other PAH as growth substrates. For that reason, this gene cluster was suggested to be a unique set of *car* genes.

Habe *et al.* (2002) completed genetic analysis of carbazole degradation genes in *Sphingomonas* sp. KA1 which was isolated on carbazole as sole carbon source. The 1,9a-dioxygenase of *Sphingomonas* sp. strain KA1 was found to be a CARDO homologue. The *car* genes of KA1 were found to be very similar to those of CA10 with differences lying in the *carAa* component of CARDO. When compared to the *carAa* and *carBa* nucleotide sequences of *Sphingomonas* sp. GTIN11 (Kilbane *et al.*, 2002) this portion of the KA1 gene matched identically to strain GTIN11.

In summary, many carbazole-degrading bacteria have been isolated through metabolite identification and gene isolation and characterization. Carbazole degradation by all these bacteria has been shown to follow one major pathway starting with angular attack on the nitrogen atom producing ring-opening products. Some also use a pathway resulting in indole derivatives products. The bacterial activity targeted in this research is not evident in the literature to date, as neither carbazole pathway shows nitrogen-specific activity.

2.3.4 Abiotic transformation of biological oxidation products

Biological degradation pathways are investigated through the collection and identification of metabolites, combined with knowledge of the preferential mode of conversion. The mode of conversion is determined by testing the organism of interest on carefully selected functionalized compounds. In order to hypothesize pathways, an organism that degrades the compound must exist.

In the case of dibenzothiophene degradation, Bressler and Fedorak (2001) showed that the analysis was not as straightforward. Following the Kodama pathway, benzothiophene-2,3-dione was found to be a product of DBT metabolism. At neutral pH, 2-mercaptophenylglyoxalate was present but it cyclized at acidic pH to form benzothiophene-2,3-dione. The concentrations of both these compounds were very low and not reflective of the amount of DBT converted, thus Bressler and Fedorak (2001) investigated the formation of other products. Using HPLC analysis of aqueous samples, a time course showed that the concentrations of benzothiophene-2,3-dione and 2-

mercaptophenylglyoxalate disappeared under neutral, abiotic culture conditions. At the same time a third product formed, identified as a disulfide (Figure 2-12). The resulting molecular formula indicated that it was an oxidation product of 2-mercaptophenylglyoxalate.

Similar types of abiotic reactions have been studied with *o*-diphenol structures that contribute to the formation of humic substances in soils. Sàchez-Cortés *et al*. (2001) studied the oxidative polymerization of catechol. Catechol was used to represent the group of polyphenol compounds, often found in nature, that contain the reactive *o*-diphenol group. As outlined in Figure 2-6 catechol is a typical product of biological transformation of polycyclic aromatic compounds. Sàchez-Cortés *et al*. (2001) found that the oxidation-condensation reaction of catechol is catalyzed by silver colloids. They suggested that the predominant mechanism of condensation at neutral pH was the formation of C-C and C-O-C bonds between aromatic rings (Figure 2-13).

In terms of microbial activity on polycyclic aromatic compounds, this information suggests that the ultimate sink of some transformed products could be in the form of structures resulting from abiotic reactions occurring with various biological transformation products.

Figure 2-12 **Abiotic oxidation of a biological product of dibenzothiophene degradation (after Bressler and Fedorak, 2001).**

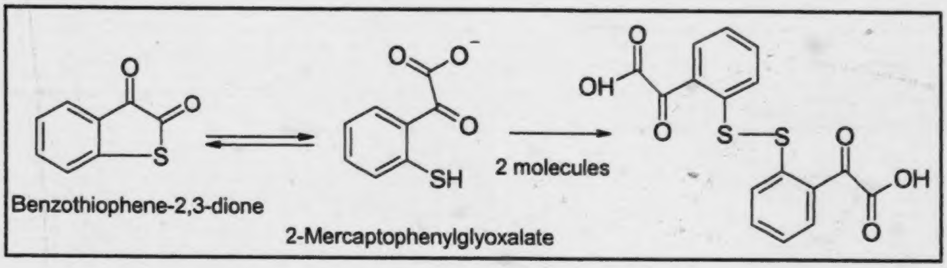
Benzothiophene-2,3-dione
2-Mercaptophenylglyoxalate
2 molecules
SH
OH
S
O

Figure 2-13 Condensation products of catechol. A. catechol, B. catechol product formed from C-C condensation, C. catechol product from C-O-C condensation (Sáchez-Cortés *et al.*, 2001) .

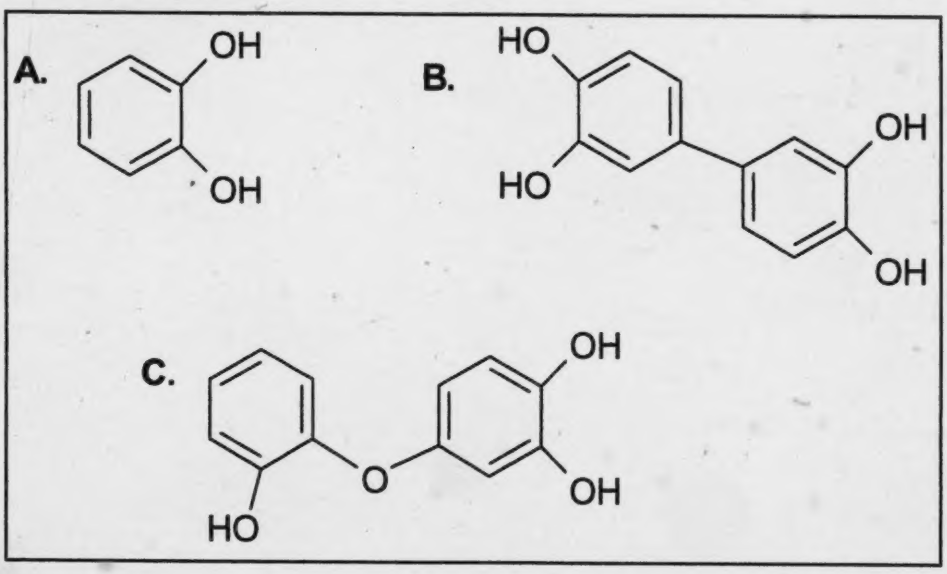

2.3.5 Hydrotreating biological oxidation products of carbazole

The process of hydrotreating is poor for converting non-basic nitrogen compounds such as carbazole. Biological systems have shown activity for the degradation of carbazole. A concept developed by several research groups (reviewed by Benedik *et al.*, 1998) is that the biological products of carbazole conversion should be more susceptible to hydrotreatment than the parent compound. A mutant strain, able to carry out the first few steps of the degradation pathway, would release the nitrogen atom from the five-membered ring leaving it as an amine functional group that is more vulnerable to removal upon hydrotreatment. Limiting the degradation pathway to only the first few steps would conserve the calorific value of the carbon structure.

The notion that carbazole metabolites are less resistant to hydrotreating than carbazole itself was investigated by Bressler and Gray (2002). Model compounds representing the types of functional groups found in biological oxidation products were exposed to conditions similar to hydrotreating. In a micro-batch reactor, both thermal deamination and hydrotreating over a Ni-Mo/γ-Al_2O_3 were accomplished. The reaction of carbazole was used as a benchmark for conversion. The compounds with free amine groups, such as 2-aminobiphenyl, anthranilic acid and 2-aminophenol, were more susceptible than carbazole to nitrogen removal under hydrotreating conditions. However, additional leaving groups located on an alkyl side chain in the β-position to the aromatic attack reacted to give products with closed-ring structures because the functional groups participated in intramolecular reactions. In the case of compounds with a free amine and a proximate leaving group, the ring closure mechanism resulted in the production of a nitrogen compound with a ring structure as stable as the initial compound, carbazole. Figure 2-14 illustrates these results.

Figure 2-14 Hydrotreatment of a carbazole biological oxidation product (after Bressler and Gray, 2002).

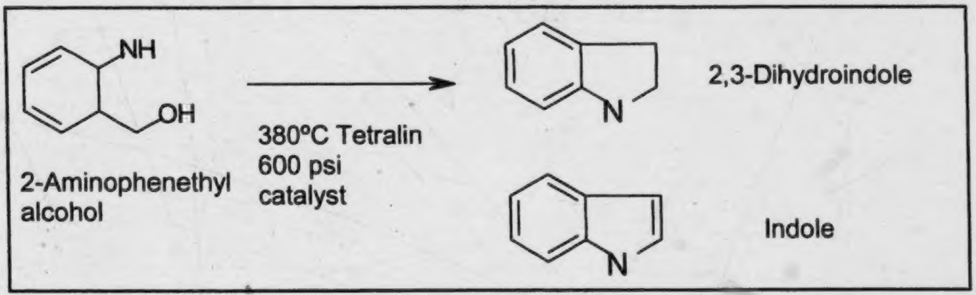

The findings of this study imply that pretreating carbazole with a biocatalyst would improve hydrotreating conversions if the microorganism converted carbazole into structures with only free amine groups. However if the product also has proximate functional groups, the pre-treatment is not suitable because ring closure reactions are likely to occur upon hydrotreatment.

This work concluded that the ideal biocatalyst should remove the nitrogen atom from carbazole completely, leaving functionalized products more susceptible to hydrotreatment than carbazole. In the absence of denitrogenation ability, a suitable bacterium would be required to produce amines without any proximate functional groups.

3.0 MATERIALS AND METHODS

3.1 Materials

3.1.1 Growth medium and buffers

Mineral salts medium was used in all testing conditions. The formulations of the various liquid media, buffers and plate media are listed in Appendix A. The pH of all media was adjusted to 7 before autoclaving. An Accumet model 25 pH/ion meter (Fisher Scientific) was used for pH determination.

Purified water was obtained through a series of water purification systems: tap water was run through the RiO_s/Elix Model 10 system followed by the Milli-Q Academic model (Millipore, Molsheim, France). This water was used in all buffer and media recipes as well it was used to rinse glassware.

The enrichment cultures and the majority of testing conditions were completed with mineral salts medium (B+8P) with carbazole supplied as sole nitrogen source and acetate as a soluble, readily assimilated carbon source. Acetate was added in the form of sodium acetate trihydrate, whereby 2 g L^{-1} was added to the medium before autoclaving.

The objective of these conditions was to select a bacterial population able to use carbazole as sole nitrogen source with minimal damage to its carbon backbone. Acetate and carbazole concentrations were chosen to supply the bacteria with excess amounts of carbon. The molar ratio of $C_{acetate}$: N of 20:1 far exceeds typical bacterial requirements for growth (Madigan *et al.* 1997). The abundance of free carbon in the form of acetate was added to ensure that any growth limitations were due to the particular nitrogen supply. The acetate also made it unnecessary for the bacteria to use the carbon backbone structure of carbazole. If the bacteria had that particular capability of using the carbazole carbon it would be unnecessary to express those enzymes. As outlined in Figure 2-6, the number of steps required to transform an aromatic compound into something suitable for the metabolism cycle are many. There are substantially fewer steps required to use acetate because acetate fits directly into the TCA cycle (Madigan *et al.*, 1997).

Agar plates were used for isolation, testing the purity of cultures and checking for activity on various carbon and nitrogen sources. The first two techniques listed involved using half-strength Plate Count Agar plates. The latter technique employed the use of mineral salts medium plates made with B+8P or B+N8P medium with or without sodium acetate trihydrate. Noble Agar (Difco, Becton Dickinson Company, Sparks, MD) was used to as a solidifying agent in these plates.

3.1.2 Chemicals and solvents

The target compound carbazole was purchased from Aldrich Chemical Co. (99 %). Before use, the carbazole was further purified using a two-step re-crystallization procedure in ethyl acetate, with the final product having a purity of >99 % according to gas chromatography. Ethyl acetate (HPLC grade, Fisher Scientific) was also the primary solvent in liquid-liquid extractions. Acetonitrile (HPLC grade, Fisher Scientific) was used as part of the mobile phase for HPLC analysis. Thianthrene (97 %, Aldrich) was dissolved in ethyl acetate to be distributed into cultures as the internal standard for liquid/liquid extraction and gas chromatography.

N,N-dimethylformamide (99 %, Sigma Chemical Co.), was used to disperse the PACs in liquid medium. The origin and purity of all the PACs used in this experiment are listed in Appendix A. Diethyl ether (99 %, EM Science, Darmstadt, Germany) was used to disperse carbazole in the test tube experiments and in the radioactive tracer experiments. Technical grade hydrochloric acid (12 N HCl) (Fisher Scientific) was diluted to 4 N make the acid wash for pre-treatment of glassware.

Radioactive experiments were completed using uniformly labeled ^{14}C-carbazole (97 % radiochemical purity, Amersham International) in a carrier solvent of dichloromethane (DCM). The activity showed approximately 310 000 DPM/10 μL of DCM.

3.1.3 Microorganisms

Carbazole-transforming bacteria were isolated from enrichments cultures from creosote-contaminated soil. The soil was collected from a site located outside of Edmonton, Alberta. The site was selected based on the number of years it had remained contaminated (decades), characteristics of the oil which was spilt there (creosote oil) and the lack of attempted site remediation. Eight samples were collected from various locations on the site. Thirty grams from each sample was then mixed together to become the initial enrichment inoculum.

The carbazole-degrading bacterium *Pseudomonas* sp. LD2, isolated by Gieg *et al.* (1996), was used as the positive control in all screening conditions.

3.2 Methods

3.2.1 Glassware preparation

Bacteria were isolated based on their ability to grow on carbazole as sole nitrogen source. To ensure that the growth media and flasks were free of any other trace nitrogen sources, all glassware involved in media preparation and all that used for growing cultures was pretreated by acid washing. Residual inorganic nitrogen was removed by first washing the glassware in 4 N HCl solution for 10 min followed by rinsing with purified water. Once dry, the glassware was rinsed with DCM to remove traces of organic nitrogen and finally rinsed thoroughly with purified water.

3.2.2 Preparation, inoculation and incubation of cultures

3.2.2.1 Test Tube Cultures

To maintain accuracy and consistency when dispensing a crystalline substrate, carbazole was dispensed into the acid-washed screw cap test tubes as an ether solution. Five millilitre of ether solution was dispensed into each tube to give a final residue of 1.25 mg carbazole. The tubes were left overnight in a fume hood to allow the ether to evaporate. After ether evaporation, 5 mL of mineral medium was added to each tube and they were autoclaved. The mineral medium recipe was completed by adding 25 μL of sterile 0.04 g $MgSO_4 \bullet 7H_2O$ mL^{-1} (aq) solution to each tube. Each cap contained a Teflon liner (Thomas Scientific, Swedesboro, NJ) as a precaution against chemical contamination between experiments.

Test tube cultures were grown in 5 mL of mineral salts medium and they were inoculated with a buffered cell suspension. Cells were taken from two well-isolated colonies growing on a half-strength PCA agar plate. Two loops filled with culture were added to a sterile 2 mL Eppendorf tube containing 1.8 mL of phosphate buffer (pH 7) and mixed. Using sterile technique, 500 μL of the cell mixture was dispensed into each tube.

The glass culture tubes measured 16 x 150 mm (Fisher Scientific). The tube cultures were incubated at room temperature for 7 d. Aeration was maintained through the use of a roll tube rack (Model TO-7, New Brunswick Scientific Co., New Brunswick) that operated on setting 5. This setting corresponded to a speed of approximately 28 RPM with an outside diameter of 35.56 cm. Each test condition contained a sterile control and a positive control of *Pseudomonas* sp. LD2.

At the end of 7 d incubation, half-strength PCA plates were streaked with a loop filled with culture and incubated until enough culture had grown to detect the presence of any possible contaminants.

3.2.2.2 *Erlenmeyer Shake Flask Cultures (500 mL)*

Shake flask cultures were prepared by adding 50 mg of crystalline carbazole to the flask containing 200 mL of medium. Flasks were covered with foam plugs and aluminum foil. After autoclaving, 1 mL of sterile 0.04 g $MgSO_4 \bullet 7H_2O$ mL^{-1}(aq) was aseptically added to each culture. Cultures were not inoculated until at least 24 h after the medium had been autoclaved to ensure significant time for proper cooling and oxygenation.

3.2.2.3 *Enrichment Cultures*

Enrichment cultures were started from creosote-contaminated soil. Eight shake flasks were inoculated with 10 g of the soil composite. These cultures were incubated at room temperature and maintained on a rotary shaker moving at 200 RPM. Transfers were made every 7-10 d with 10 % inoculum (by volume) into fresh mineral medium with carbazole. To ensure suitable conditions were maintained, each set of transfers included a sterile control and a positive control of *Pseudomonas* sp. LD2.

3.2.2.4 *Isolate CP19*

Isolate CP19 was studied in 500-mL shake flask cultures. This bacterium was selected for further characterization of its carbazole degradation activity. Inoculum for these cultures was grown on Trypic Soy Broth (TSB). Every 2 weeks, half-strength PCA plates were streaked for isolated colonies from glycerol stocks maintained at -70 °C. These plates were incubated at 28 °C for 3-4 d and then stored at 4 °C. From these plates, 2 loops filled with culture were used to inoculate 200 mL of TSB in a 500 mL shake flask. After 43 h, the cells were harvested by centrifugation three times at 27 000 x g for 10 min, using a Sorvall® Refrigerated Superspeed Centrifuge model RC-5B fitted with the GSA rotor. After each spin cycle, the supernatant was decanted and the pellet was washed with phosphate buffer (pH 7). The final pellet was suspended in approximately 100-mL of buffer with appropriate adjustments made to give a final OD_{600} reading of 10. Two millilitres of this solution was added to each sterile shake flask to give an initial OD_{600} of 0.1.

Isolates in 500-mL shake flasks were incubated at a temperature of 28 °C and a gyratory speed of 200 RPM. Incubation times varied depending on the experiment. Each experiment contained heat-killed controls in which the inoculum was autoclaved before being added to the culture flask. At the end of every experiment, a loop filled with culture was removed from each flask and streaked on half-strength PCA plates. The plates were incubated for 3-4 days at 28 °C and examined for purity.

3.2.2.5 Biometers (250 mL)

Clean 250-mL biometers flasks (Bartha and Pramer, 1965) along with their syringes and rubber stoppers were autoclaved. Once the flasks cooled, an ether solution containing a mixture of dissolved, crystalline carbazole and radiolabeled carbazole (in DCM) was dispensed. Each flask contained 6.25 mg of unlabeled carbazole and 310 000 DPM of radiolabel. Forty eight h after the carbazole was dispensed, 50 mL of sterile, mineral salts medium with acetate was added to each biometer flask. Ten millilitres of 1 N KOH was added to each side arm.

Biometer flasks used in the screening process were inoculated with 1 mL of liquid cell suspension and then capped with a neoprene stopper. The cell suspension was prepared by flooding a grown half-strength PCA plate with 5 mL of phosphate buffer and suspending the colonies. Cultures were incubated for 7 d at 28 °C and a shaker speed of 200 RPM. Experiments included a sterile control and a positive control of *Pseudomonas* sp. LD2.

Biometer flasks used with isolate CP19 were inoculated prepared as outlined in 3.2.2.2. To give an initial OD_{600} of 0.1, 500 μL of cell suspension was added to each 50 mL culture. These cultures were incubated for 7 d at 28 °C on a rotary shaker moving at 200 RPM. Purity of these cultures was tested on half-strength PCA plates. Experiments included heat-killed controls.

3.2.2.6 *Screw-Cap Shake Flasks (500 mL)*

To prevent the release of any vapours, experiments involving mixtures of various PACs were completed in screw cap shake flasks. Each cap was lined with a Teflon liner. Before sterilization, 100 mL of mineral salts medium with acetate was dispensed into each flask. After autoclaving, 1 mL of sterile 0.04 g $MgSO_4 \bullet 7H_2O$ mL^{-1} (aq) was added to each flask. Substrates were dispensed in a solution of N,N-dimethyl formamide using a glass syringe. The solution was made to give a concentration of 0.12 mg μL^{-1} of all compounds. Each flask received 400 μL of the solution. Equivalent amounts of substrate solution were dispensed into 8-mL glass vials with screw caps lined with Teflon liners. These vials were stored for use as extraction controls.

TSB grown cells were used as inoculum in these experiments. Similar to the procedure outlined in section 3.2.2.2 above, culture from a half-strength PCA inoculum plate (started every 2 weeks from the -70 °C glycerol stocks) was used to inoculate TSB. In this case, larger volumes were required so 2-L Erlenmeyer flasks, containing 1 L of TSB were used, as were 250-mL polypropylene centrifuge bottles. The pellet in each bottle was re-suspended in 50 mL of sterile mineral medium with acetate. The suspensions were collected in a sterile, 1-L Erlenmeyer flask and mixed thoroughly. The final OD_{600} was adjusted to 10 using sterile medium for dilution.

Using a sterile volumetric cylinder, each flask received 100 mL of inoculum giving an initial OD_{600} of 5. The cultures were incubated at 28 °C on a rotary shaker operating at 200 RPM for a period of 50 h. A positive control containing solely carbazole accompanied each set of experiments as did heat-killed control flasks. Before the cultures were stopped by acidification to pH 2 with 6 M HCl, a half-strength PCA plate was streaked and grown to ensure purity.

3.2.3 Isolation methods

At the completion of five transfers of soil enrichments, several individual colonies were isolated from each enrichment culture. Using the spread plate method, morphologically different colonies were picked and re-streaked for purity. One half PCA plates were used for isolation and purification.

3.2.4 Evaluation of screening results

3.2.4.1 Isolate Screening

Stable bacterial consortia exist with certain community dynamics that enable individual bacterium to survive in environments that they cannot withstand alone. After the establishment of a bacterial community able to exist in the very selective conditions of the enrichment cultures, it was necessary to determine which of the many individual cells possessed the ability to break the carbon-nitrogen bond of carbazole. In order to identify these bacteria, a series of growth conditions were selected whereby both carbon and nitrogen sources were varied in combination and structure. Bacterial growth and substrate loss were used to evaluate the usefulness of each bacterium.

Table 3-1 describes the screening conditions that were used for each purified bacterium. Visible colour formation and growth (OD_{600}) were monitored daily whereas pH and substrate loss were measured at the completion of the assay.

Table 3-1 Summary of conditions for screening isolates and the hypotheses tested.

Condition	Hypothesis Tested
A. Mineral medium with carbazole as sole nitrogen source and acetate as available carbon source. (CAR+ACT)	Bacteria can use carbazole as a nitrogen source and thus they have the ability to break the targeted C-N bond. Growth and carbazole loss will be seen in this condition regardless of the bacterium's ability or inability to use carbazole carbon.
B. Mineral medium with carbazole as sole nitrogen and carbon source. (CAR)	Bacteria have the ability to use carbazole as both a carbon and nitrogen source. Bacteria growing in this medium are capable of using the carbon backbone of carbazole.
C. Mineral medium with acetate, nitrate and ammonium as available carbon and nitrogen sources, respectively. Carbazole present in the system. (CAR+ACT+N)	The enzyme system has the potential to be regulated therefore, with both nitrogen and carbon supplied in other forms, the need to use carbazole is eliminated. Only an enzyme system that is not regulated by ammonium, nitrate or acetate will show substrate loss. Growth will be present regardless of the nature of the enzyme system.
D. Mineral medium with acetate as an available carbon source. No nitrogen source supplied. (ACT)	Most bacteria rely on the simplest forms of nitrogen such as ammonium and nitrate, to carry out the cells metabolic processes. Most are unable to fix nitrogen from the air and thus their survival is dependent on their ability to utilize the nitrogen sources supplied to them as substrates. Only nitrogen fixers will exhibit growth in these conditions.

Individually, the testing conditions are somewhat limited in their description of the biochemical activity of each isolate. However, the combined results of all four conditions in Figure 3-1 provide a much more interpretive illustration of the enzyme systems being expressed. To summarize, there were three fundamental questions asked: 1) Can the bacterium use nitrogen from carbazole? 2) At what point in the carbazole degradation pathway is the nitrogen atom being removed (what is the condition of the carbon backbone)? 3) Are the genes responsible for carbazole degradation always expressed (constitutive) or is their expression dependent on the surrounding environment (regulated)? Figure 3-1 provides a logic diagram of how the screening results were combined to answer these questions.

The most interesting isolates from this stage of screening proceeded to the second stage of screening in which the degree of utilization of carbazole-carbon was evaluated. Substituting radiolabelled carbazole into condition A (Table 3-1), the isolates were monitored for their ability to mineralize carbazole-carbon. Mineralization implies complete degradation of the carbon structure to the end product of $^{14}CO_2$. Thus, the release of $^{14}CO_2$ is a direct measurement of carbazole-carbon utilization.

Although it does not reflect the order in which testing was completed, Figure 3-1 outlines how the results from the testing conditions and the radioactive work were used collectively to evaluate each isolate.

Figure 3-1 Strategy for evaluating isolates from enrichment cultures. The combined results of growth and substrate loss measurements in the four testing conditions in Table 3-1 along with the release of $^{14}CO_2$ were used.

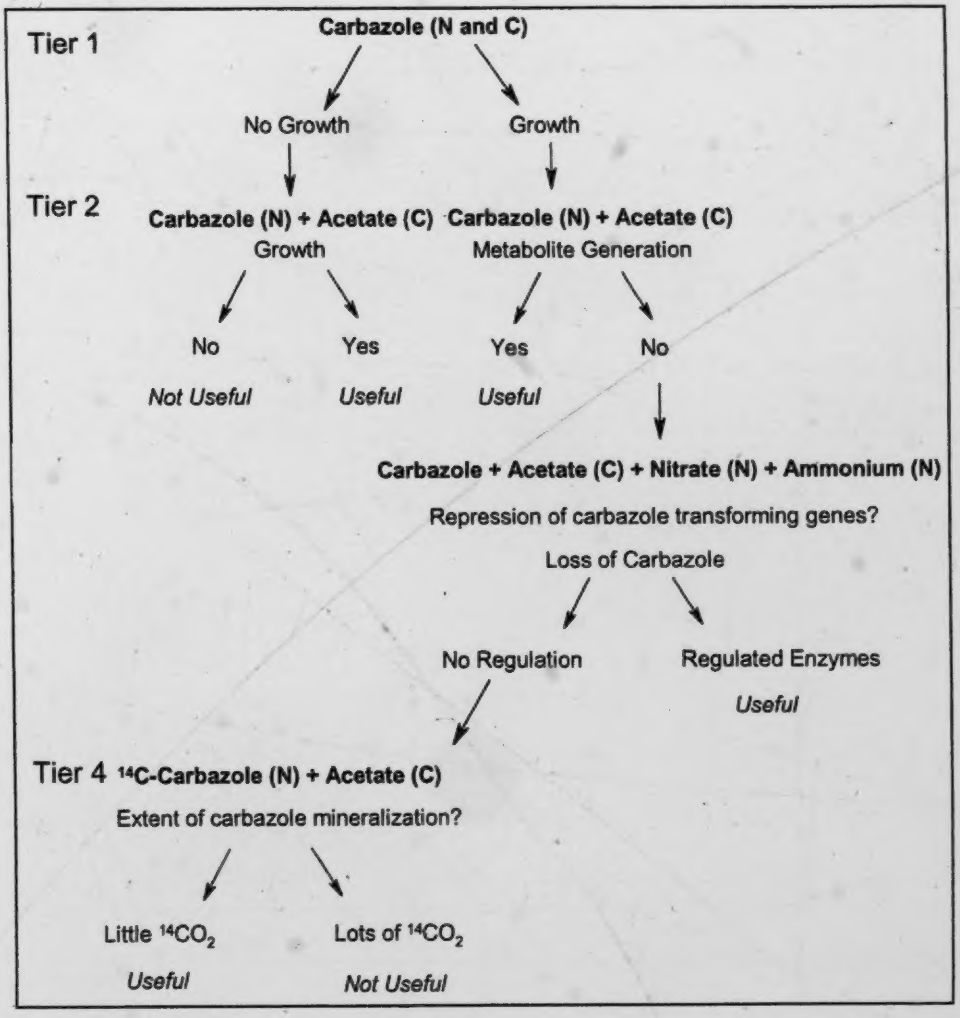
Tier 1
Carbazole (N and C)
No Growth
Growth
Tier 2
Carbazole (N) + Acetate (C)
Growth
Carbazole (N) + Acetate (C)
Metabolite Generation
No
Yes
Yes
No
Not Useful
Useful
Useful
Carbazole + Acetate (C) + Nitrate (N) + Ammonium (N)
Repression of carbazole transforming genes?
Loss of Carbazole
No Regulation
Regulated Enzymes
Useful
Tier 4
^{14}C-Carbazole (N) + Acetate (C)
Extent of carbazole mineralization?
Little $^{14}CO_2$
Useful
Lots of $^{14}CO_2$
Not Useful

3.2.4.2 Profile of Suitable Candidates

A suitable candidate for bioconversion of carbazole can be identified by this screening process in a number of places. The **ideal bacterium** would have a constitutive gene system that implies that the genes are always expressed regardless of the surrounding environment. This activity would attack carbazole as a nitrogen source, targeting the nitrogen atom and not the remaining carbon. It would not be able to use carbon from any other compound in the oil feed. Therefore growth would only be possible in the presence of an alternative carbon source such as sodium acetate, a readily assimilated carbon source. This particular organism would show up in Tier 2 of Figure 3-1. It would not show any growth in an environment with only carbazole but it would show growth in the presence of an additional carbon source (Figure 3-2).

Another suitable organism is one that uses a regulated enzyme system to grow on carbazole carbon. This candidate potentially could be genetically modified to block the expression of the carbazole carbon degradation genes thereby sparing the carbon backbone. The application of this organism would depend on the starting point and direction of the degradation pathway because the steps of ring opening and nitrogen atom utilization would have to occur early in the degradation pathway. Such a candidate would reveal itself in Tier 3 of screening conditions in Figure 3-1.

Other useful carbazole degraders would be those that produce unique metabolites that accumulate in the system. Such candidates would show up at Tier 2 on the right-hand side of Figure 3-1. At this point, the carbazole structure would be degraded to some degree but accumulation would suggest that some carbon would still be intact. A unique metabolite could potentially be more susceptible to hydrotreating than the known biological oxidation products of carbazole.

Figure 3-2 Hypothetical growth characteristics of an ideal carbazole degrader under the testing conditions.

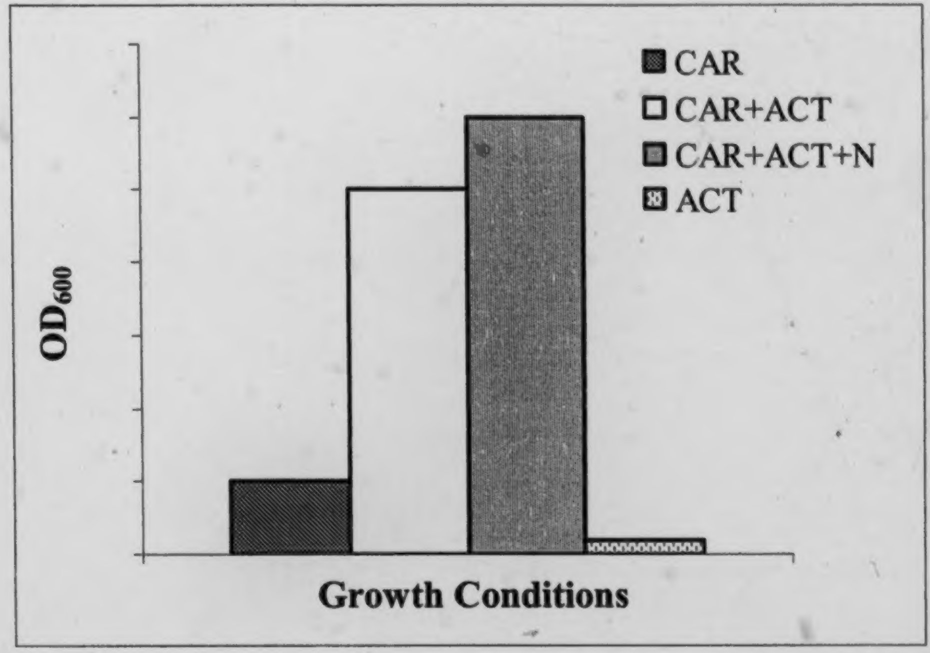

3.2.5 Chemical analysis

3.2.5.1 Carbazole loss

Unconverted carbazole was analyzed in spent culture, medium using two different methods. In most experiments, liquid-liquid extraction was used. In some cases, carbazole was also analyzed by adding ethanol such that all crystals were dissolved in solution. Analysis was completed in this fashion when simultaneous measurements of biomass were required.

3.2.5.2 Liquid-Liquid Extraction

Liquid-liquid extraction was completed with ethyl acetate as the solvent. Ethyl acetate was selected based on its ability to extract both carbazole and any possible carbazole metabolites that may have been formed from the purified isolates in the screening process. It was used throughout this work to maintain consistency. Cultures were first acidified to pH 2 using 6 M HCl to stop biological activity. Thianthrene was then added in a solution of ethyl acetate as an internal standard at a ratio of $C_{\text{Thianthrene}}$: $C_{\text{Carbazole (maximum)}}$ of 1:2.

In the 5-mL cultures in test tubes, carbazole was collected in the following sequence of steps: 1 mL of internal standard solution was added, followed by 1 mL of ethyl acetate to the test tube. The sample was vortexed and the organic layer was collected with a Pasteur pipette. Another 1 mL of ethyl acetate was added followed by mixing with a vortex and collections of the organic layer with a Pasteur pipette. The organic fraction was collected in 4 dram vials fitted with a Teflon liner. Any emulsions that formed were broken by repeated passes through a Pasteur pipette. Unbroken emulsion was left in the original test tube.

The cultures from the shake flasks of 200-mL volume were extracted in 500-mL separatory funnels. After 5 mL of internal standard solution was added to the Erlenmeyer flask, the culture was transferred to the separatory funnel. Fifty millilitres of ethyl acetate was used to rinse the flask: it was then collected in the funnel. The aqueous-solvent mixture was agitated well and left stationary until separation between the organic and aqueous phase was very distinct. The aqueous fraction was removed first and collected in the original Erlenmeyer flask. The organic fraction was then passed through a drying agent (granular anhydrous sodium sulphate) and collected in a round bottom flask. After three repetitions of this procedure, both the separatory funnel and drying agent were rinsed well with solvent to ensure that any trace of carbazole adhering to the surfaces was collected. The final extract was then concentrated using a rotary evaporator model Rotavap R-112 (Buchi, Switerland) and water bath model Waterbath B-480 (Buchi, Switzerland). The evaporator was operated under vacuum at 30 °C. The concentrated extract was collected in 8 mL screw cap glass vials with Teflon liners. All extracts were then dried under nitrogen and dissolved in 5 mL of ethyl acetate.

Solvent extracts were analyzed by gas chromatography (GC). Using a syringe, 1-μL samples were injected into the instrument with 1 μL of air preceding and 0.1 μL of air following the extract. A Hewlett Packard Series II Model 5890 gas chromatograph fitted with a flame ionization detector (FID) and a HP-1 column made of crosslinked methyl silicone gum was used for the analysis. The column was 30 m in length, 0.25 mm in diameter with 0.25 μm film thickness. At a flow rate of 1.3 mL min^{-1} through the column, helium was used as the carrier gas. The temperature program started at 100 °C for 2 min followed by ramping at 10 °C min^{-1} to 250 °C and held for 10 min. The injector was set at 250 °C, the detector was set at 300 °C and the equilibrium time was set to 3 min. Carbazole gave a retention time of 15.18 min and the internal standard, thianthrene, a retention time of 16.7 min. Peak areas were calculated using an integrator (Hewlett Packard model 3396A).

Extraction efficiency was measured by comparing the internal standard GC peak areas to those of samples that did not undergo extraction. Carbazole concentration was determined using the area ratios as compared to the internal standard.

3.2.5.3 Aqueous solubilization of carbazole using ethanol

Similar to the procedure of solvent extraction, cultures were first acidified to pH 2 using 6 M HCl to stop biological activity. Following acidification, 200 mL of 95 % ethanol was added to the 200 mL culture. The foam plug was replaced with a rubber stopper and sealed with Teflon tape. The culture was then placed back on the shaker platform and allowed to mix for 24 h. This additional mixing time was needed to ensure all the crystalline carbazole was dissolved into the water/ethanol solution. After mixing, 1 mL of the solution was removed and stored in a 1.5-mL Eppendorf tube in the dark at -4 °C until it was analyzed by high performance liquid chromatography (HPLC). A 50-µL sample was used in this analysis.

HPLC analysis was completed using a Hewlett Packard model 1050 liquid chromatography system equipped with a LiChrospher 100RP-18 column (Merck 50943, LiChroCART 125-4) and a UV detector set at 254 nm. A mobile phase of 50/50 acetonitrile/water was used at a flow rate of 2 mL min^{-1}. Total run time was set to 8 min where the water and ethanol peaks were seen between 0.5 and 0.6 min and carbazole at 3.33 min. Peak areas were calculated using an integrator (Hewlett Packard model 3396A).

A calibration curve of acetonitrile standards of known carbazole concentration were run with each sample run on the HPLC. The best-fit curve of the standards was then used to convert the carbazole areas into concentrations. Sample calibration curves can be found in Appendix E Figure 12-4.

3.2.5.4 Acetate consumption

Acetate concentration was measured using 1 μL aqueous injections into a Varian 3600 model GC-FID. The column was a DB-FFAP Megabore column (Chromatographic Specialties, Brockville, Ontario) 15 m x 0.53 mm. The temperature program started at 50 °C for 0.1 min followed by ramping at 10 °C min^{-1} to a final temperature of 110 °C. Both the injector and detector operated at a temperature of 250 °C. Gas flow rates were as flows: 305 mL min^{-1} of air, 32 mL min^{-1} of hydrogen, 30 mL min^{-1} of helium as carrier gas and 30 mL min^{-1} of nitrogen as make up gas. Total run time of this program was 6.1 min with the acetate peak coming off at 2.7 min whereas the water peak was detected at approximately 1 min. The method was linear in the range of 32 mg mL^{-1} to 250 mg mL^{-1}. This method was developed by Melissa Haveron and Dr. Phil Fedorak in the Department of Biological Sciences, University of Alberta.

Using sterile technique, 1-mL samples were taken from the 200-mL culture before the culture was acidified for extraction and stored in a sterile 1.5-mL Eppendorf tube at -20 °C until analysis was possible. Particulates were removed from the aqueous sample using an Eppendorf Microfuge model 5415C operated at 14 000 RPM for 10 min. Ninety microlitres of the supernatant were removed and acidified with 10 μL of 4 N phosphoric acid. This acidification step converts acetate to acetic acid that is then detected on the volatile fatty acid column. Samples that had concentrations outside of the range of the method were diluted with purified water before acidification.

Peak areas were determined using Varian GC Star Workstation Version 5.51 Software. A set of standards with known acetate concentration was run with each set of samples. The best-fit line of the standards was then used to calculate acetate concentration from the sample areas. An example of the concentration curve can be found in Appendix B, Figure 9-1.

3.2.5.5 *Conversion of polycyclic aromatic compounds (PACs)*

Unconverted PACs were collected using liquid-liquid extraction, again using ethyl acetate as the solvent. The structures of these compounds are outlined in Figure 3-3. Due to the large biomass of cells in each flask, the addition of solvent to the aqueous culture resulted in very stable emulsions. Separatory funnels were ineffective in separating the organic layer from the aqueous layer and thus centrifugation was required.

Following the previous extraction protocols, each culture was first acidified to pH 2 using 6 M HCl. A solution of thianthrene in ethyl acetate was then added, as internal standard, to the screw-capped flask. The culture was then transferred to a 500-mL polypropylene centrifuge bottle. Approximately 50 mL of solvent was used to rinse out the screw-capped flask and it was collected in the centrifuge bottle. The sample was mixed well, followed by centrifugation for 10 min at 10 000 RCF using a Sorvall Evolution $_{RC}$ centrifuge (Mandel Scientific, Ontario, Canada) fitted with the SLA-3000 Super-Lite model rotor. The resulting organic layer was removed from the centrifuge bottle using glass pipettes. The extract was passed through drying agent (granular, anhydrous sodium sulphate) and collected in a round bottom flask. After the third repetition, the aqueous fraction was poured back into the screw-capped flask. The centrifuge bottle, pipette and drying agent were rinsed well with ethyl acetate to ensure all traces of substrates had been removed from all the surfaces and collected in the extract.

The final extract was concentrated to small volumes using the vacuum rotary evaporator as previously described in section 3.2.5.1. The concentrated sample was analyzed by GC-FID using the procedure described in section 3.2.5.1. Alterations to the temperature program were required to ensure that all components were completely separated. The temperature started at 100 °C for 2 min, increasing by 5 °C min^{-1} to 250 °C for 10 min. Table 3-2 lists the retention times of all the compounds used in this study. Substrate conversions were reported in comparison to the concentrations in the heat-killed controls.

Figure 3-3 Structures of PACs used in the selectivity experiments with CP19.

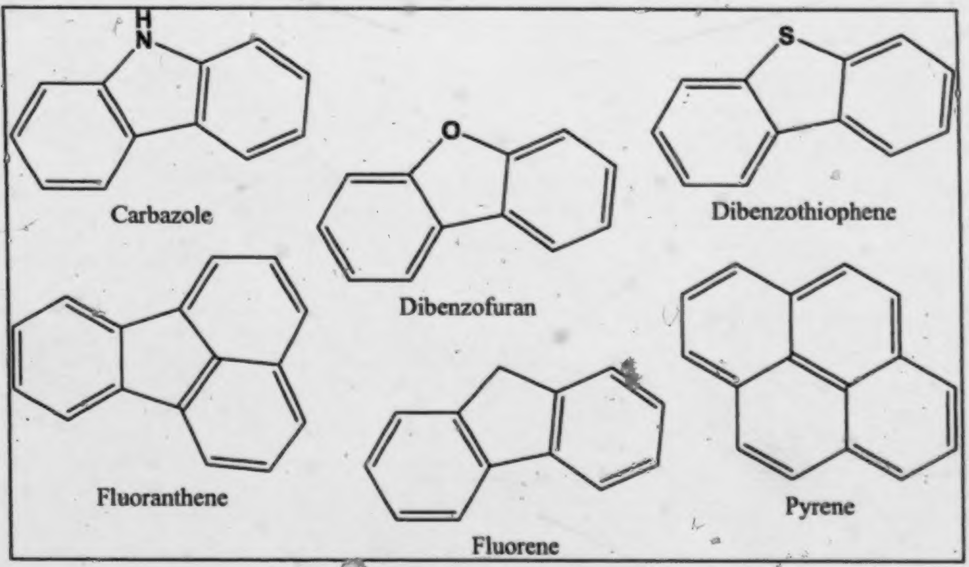
Carbazole
Dibenzofuran
Dibenzothiophene
Fluoranthene
Fluorene
Pyrene

Table 3-2 Retention times of the PACs tested as substrates with strain CP19. Compounds were analyzed using GC-FID.

Polyaromatic Compound	*Retention Time (min)*
Dibenzofuran	15.57
Fluoranthene	17.18
Dibenzothiophene	17.85
Carbazole	22.53
Thianthrene	25.15
Fluorene	27.53
Pyrene	28.52

3.2.5.6 Radiolabelled carbazole

Uniformly radiolabelled carbazole was used to quantify the amount of carbazole carbon mineralized by each isolate. In the presence of non-radiolabelled carbazole and mineral salts medium with acetate, the radiolabelled compound was added as a tracer. The extent of mineralization was monitored by sampling and measuring $^{14}CO_2$ daily. Before adding the KOH sub-sample, each scintillation vial was prepared by adding 1.5 mL of water, 0.1 mL of acetic acid and 10 mL of ACS fluor (Amersham). After mixing the KOH by plunging the syringe up and down several times, a 0.5-mL sample was taken from the KOH side of each flask. Samples were added to the prepared vials and left to set for several minutes before measurements were taken. Liquid scintillation counting was performed with a Beckman Model LS 3801 liquid scintillation counter. Percentage of radiolabel released as $^{14}CO_2$ was calculated based on the amount of radiolabel originally added. Sterile controls were used in the screening experiments while heat-killed controls were used in the CP19 mineralization study.

The final distribution of radiolabel was determined at the completion of the experiment. Before any extraction was completed, the scintillation vials required for counting were prepared. Unlike the $^{14}CO_2$ counts, these vials required only 10 mL of fluor. Controls of measuring background activity and 100 % of added activity containing solely 10 mL of fluor and fluor plus the residue from 10 mL of the original ether suspension, respectively, were counted at each time interval.

During the original screening process the following procedures were followed. At day 7, cultures were acidified to pH 2 using 6 M HCl and extracted with ethyl acetate. The final amount of $^{14}CO_2$, ^{14}C in the organic portion and the aqueous portion were analysed for DPM counts.

A modified version of this procedure was followed in the mineralization study with isolate CP19. Before the cultures were extracted, a small portion of each sample was plated on half-strength PCA plates and incubated to check for purity. Extraction was completed using DCM at neutral pH. The solvent was changed to reduce the amount of emulsion formed thus reducing the amount of pellet lost. The extraction was completed with the culture at pH 7. At this pH, the majority of the solvent extract would consist of unconverted carbazole and any other non-polar metabolites. The resulting extract was collected in a graduated test tube and the volume was recorded. One millilitre from both the extract and aqueous fraction was added to the prepared scintillation vials and counted.

The remaining aqueous fraction was then separated into biomass and supernatant. One millilitre of sample was added to a 1.5-mL Eppendorf tube. The sample was centrifuged in the microfuge for 2 min at 10 000 RPM. One half of a millilitre of supernatant was removed from the tube and added to a prepared scintillation vial for counting. The remaining supernatant was carefully pipetted away from the cell pellet and discarded. Depending on the amount of pellet collected, this washing procedure was completed several times. The total volume of aqueous culture required to build the cell pellet was recorded and used to quantify the total amount of biomass in the culture. To ensure all the ^{14}C was removed from the cell to be counted, the pellet was lysed by adding 500 µL of 1 M KOH to the final pellet and heating it for approximately 20 min at 60 °C. Heating was completed in a 500 mL glass beaker of water heated on a hot plate. The Eppendorf tubes were kept accessible by fitting then in a Styrofoam plate whereby the top was kept out of the water and the sample in the water. After heating, the sample was mixed by a vortex and then added to a prepared scintillation vial for counting. The scintillation vial required for this measurement mirrored those used in the CO_2 counts.

Sample calculations used to convert these sample measurements into the total fraction counts are outlined in Appendix C.

3.2.5.7 Mass spectrometry and derivatization methods

Metabolites were collected in both neutral and acidic solvent extracts as explained in detail in section 3.3.3. Where necessary the extracts were derivatized with diazomethane and analyzed with gas chromatography with mass spectrometry. The programs, procedures and instruments used are those outlined by Bressler and Fedorak (2001). This section of experimental analysis was completed by Dr. David C. Bressler.

3.2.6 Biomass measurement

3.2.6.1 Optical density (OD_{600})

Along with visible changes in turbidity, optical density at 600 nm was used to measure the growth of isolates during the screening process. A desk-top spectrophotometer model Spectronic 21 (Bausch and Lomb, Rochester, NY) was used for these measurements. A background of the corresponding medium was used to zero the instrument. All samples were mixed for 30 sec using a Vortex model Genie 2 (Fisher Scientific) and let to sit for 5 min before the measurement was recorded. The exterior of each tube was thoroughly cleaned with ethanol to remove any residues from the glass.

The growth curve of strain CP19 on TSB was constructed using OD_{600} measurements completed on the $Spectra_{max}$ Plus (Molecular Devices, Sunnyvale, CA). A quartz cuvette with a light path of 10 mm was used. The instrument was referenced with sterile TSB before measurements were taken. Samples were serially diluted ten-fold with sterile TSB to ensure the readings were between 0.1 and 0.6 OD_{600} units.

The optical density of inoculum suspensions was measured using a Philips Model PU 8740 UV/VIS Scanning Spectrophotometer. The instrument was referenced with either sterile buffer or sterile medium depending on what was used to make the cell suspension. All samples were diluted with sterile medium (or buffer) in increments of 10 to ensure the readings were between 0.1 and 0.6 OD_{600} units.

3.2.6.2 Dry cell weight

Accurate cell weights could only be determined once the crystalline carbazole was removed from the culture medium. As previously described in section 3.2.5.1, carbazole was dissolved into the aqueous culture with the addition of 95 % ethanol. Once the HPLC samples had been removed, the remainder of the culture was vacuum filtered though a Millipore filtering system fit with a 42.5 mm diameter, glass microfibre filters (GF/C from Whatman International Ltd., Maidstone, England). To dissolve any salts that may have accumulated on the filter, 10 mL of distilled water was run through the filter at the end of each run. The wet filter papers were left for 24 h in an oven maintained at 70 °C. Dry cell weights were calculated by subtracting the mass of the dry filter paper from the mass of the filter and cells. Before use, filters were stored in a dry oven maintained at 70 °C. Depending on the amount of biomass, multiple filters were used for one culture: the resulting dry cell weights were then added to give the total for the culture.

3.2.6.3 Protein content

Protein was extracted by mechanically breaking the cells in suspension using sonication and quantified with a bicinchoninic acid assay kit (Pierce, Rockford, IL).

The cell pellet from 200 mL of culture was collected and washed with three repetitions of: centrifugation at 27 000 x g for 10 min, decanting of the supernatant and re-suspension of the pellet in 50 mL of phosphate buffer. The volume of buffer was reduced to 10 mL in the final re-suspension. The concentrated cell suspension was transferred to a sterile 50 mL disposable centrifuge tube. The original centrifuge bottle was rinsed several times with phosphate buffer. The final volume of suspension was recorded. Cells were lysed by 10 min of sonication using a Branson Sonifer 450 fitted with the micro tip (VWR Scientific, West Chester, PA). One millilitre of the resulting suspension was removed to a 1.5 mL Eppendorf centrifuge tube. Particulates were separated from the supernatant by centrifugation in a microfuge at 16 000 x g for 10 min. To ensure readings were in the linear range of the concentration curve, 1/10 and 1/100 dilutions of each sample made in phosphate buffer were analysed.

Using a 96 well polystyrene microplate (Costar, Corning, NY), samples and standards were all analyzed in triplicate. Standards were made from the bovine serum albumin stock (2000 μg mL^{-1}) supplied with the kit. Dilutions ranging from 500- 0 μg mL^{-1} were made in phosphate buffer and used to make a concentration curve. Per the manufacturer's instructions, 10 µL of samples and standards were dispensed into the microplate. Two hundred microlitres of working reagent was added to each well, after which the plate was mixed for 30 sec followed by 30 min of incubation at 37 °C in the $\text{Spectra}_{\text{max}}$ Plus microplate reader. After incubation, the plate was allowed to cool to room temperature and the absorbance was measured at 562 nm.

The best-fit line of the BSA concentration curve was used to convert the adsorbance reading of each sample to protein concentration. The protein concentration found in the phosphate buffer was subtracted from each sample. Total protein was then calculated using this concentration and the total sample volume determined after sonication. Sample calculations for the procedure are outlined in Appendix C.

3.2.6.4 Elemental carbon, hydrogen and nitrogen analysis

To complete the material balance in the carbon regulation experiment, elemental carbon, nitrogen and hydrogen contents were determined on a subsample from the culture at the final time point. Fifty millilitres of each culture were passed through the Millipore filtering apparatus as outlined in section 3.2.6.2. In order to remove any residual components, the glass fiber filters (24 mm diameter) were baked at 400 °C for 3 h prior to use. Each filter was placed in an individual snap-sealed petri dish and brought to the Limnology service unit in the Department of Biological Sciences (University of Alberta) for analysis.

3.3 Characterization of *Sphingomonas* sp. CP19

3.3.1 Identification

A variety of biochemical tests were performed on isolate CP19 including: 3 % KOH test, catalase test, oxidase test, urease test, acid-fast test and the endospore stain (American Society of Microbiology, 1974). The bacterium was then identified using a full-length 16S rRNA sequence analysis. This work was completed by MIDI Labs in Newark, DE.

3.3.2 Solubilization mechanisms

Strain CP19 was examined for its ability to increase the solubility of carbazole in aqueous conditions. The analysis was completed on cultures and the appropriate heat-killed controls grown in mineral medium with carbazole and acetate. Preparation, inoculation and incubation of these cultures were done using the procedures as outlined in section 3.2.2.2. Cultures were grown for 7 d after which time approximately 5 mL of sample was filtered through a 0.22 μm pore size, sterile Millipore filter Millex-GS into sterile Eppendorf tubes. The filtering procedure was used to remove both the bacterial cells and any carbazole crystals. Using the same HPLC instrument and operating conditions as previously mentioned in section 3.2.5.1, a 50-μL aliquot of the filtered sample was analyzed for its carbazole concentration. After the first measurement was completed, crystalline carbazole was added to the sample and the carbazole concentration was measured again.

3.3.3 Recovery of metabolites

The recovery of metabolites from cultures of strain CP19 was accomplished using two main procedures. Starting with 200-mL culture of CP19 grown on carbazole and acetate, the coloured metabolite (Metabolite A) was extracted at neutral pH, three times using 50 mL of DCM. This extract was concentrated to dryness under nitrogen and re-suspended in 0.5 mL of pentane. Pentane extraction was used to remove carbazole from the sample. Carbazole remained in the crystalline form and the coloured metabolite was dissolved in the liquid extract and further analyzed. The liquid extract was then dried again under nitrogen and dissolved in DCM.

To confirm this product as an abiotic condensation product from 2-aminophenol, crystals of 2-aminophenol were added to culture medium containing acetate. This abiotic mixture remained untouched for 72 h. The sample was extracted with DCM at neutral pH and analyzed using GC-MS. See section 3.2.5.7 for procedures.

Other metabolites were recovered from the aqueous fraction after neutral extraction. With 2 mL of 5 M H_2SO_4, the culture was acidified to pH 2 and extracted three times with 50 mL of DCM. This extract was concentrated to dryness under nitrogen and re-dissolved in 0.5 mL of ether. The sample was derivatized using diazomethane followed by GC-MS analysis for metabolite identification.

4.0 RESULTS[2]

4.1 Validation of experimental procedures

Due to the nature of the model compound, carbazole, and the properties of isolate CP19, a variety of different experimental procedures were used throughout this work. The choice of procedure very much depended on the measurements required to answer a particular hypothesis and the feasibility of completing such an experiment with sufficient replications and time points. The following sections provide estimates of the errors in the experimental methods.

4.1.1 Error analysis and experimental controls

The majority of the results presented in this thesis are the average of three replicates. Excluding some portions of the isolating and screening work, all experiments completed on isolate CP19 were done in triplicate flasks at each time point and for each condition. The errors associated with the reported values are given as the absolute standard deviation for each set of replicates as a measure of the repeatability. The accuracy of the experimental procedure was quantified by including a triplicate set of heat-killed controls at each time point. This set of samples provided information on the influence that the presence of cells had on the measurements, excluding the effect of metabolic activity. These controls also showed the quantity of any abiotic losses or transformation of substrate that occurred during incubation, without any biological activity.

The effects of the heat-killed controls were incorporated into the live culture at each time point. The following equation illustrates how error for each value was calculated.

$$C = (A - B) \pm \sqrt{a^2 + b^2} \qquad (4\text{-}1)$$

---

[2] Unless indicated otherwise, the graphs presented in this section are illustrations of experimental data.

C= Corrected value of carbazole removal at in a live culture, % Removal.
A= Average value of carbazole removal in a live culture, % Removal.
B= Average value of carbazole removal in the heat-killed control, % Removal.
a= Standard deviation of culture value
b= Standard deviation of heat-killed control value

A variety of measurements required calculating the product or quotient from two measured values. For example the transformation of carbazole per gram of dry cell weight and the conversion factor of protein content to dry cell weight were calculated by dividing two measured variables. The error for these calculations was found with the following equation.

$$J = \frac{H}{I} \pm \left(\sqrt{\left(\frac{h}{H}\right)^2 + \left(\frac{i}{I}\right)^2} \right) * J \qquad (4\text{-}2)$$

J= Transformation of carbazole per gram of dry cell weight (μmol (mg DCW)$^{-1}$)
H= Mean amount of carbazole transformed (μmol)
I= Mean amount of dry cell weight (mg)
h= Standard deviation of H
i= Standard deviation of I

Sample calculations of both equations 4-1 and 4-2 are found in Appendix C section 10.1.

4.1.2 Analysis of carbazole concentrations

4.1.2.1 Ratio of internal standard to substrate

Liquid-liquid extraction was done using an internal standard to quantify the efficiency of the extraction and to correct for any volume inconsistency between injections and between analytical instruments.

Thianthrene was chosen as the internal standard for these analyses based on its retention time relative to carbazole. The concentration of thianthrene added the samples before extraction was based on the linearity of response of the GC to each component. The ideal concentration occurred when the area ratios of the compounds were equivalent to their mass ratios. In order to determine the most suitable concentration ratio, samples of carbazole and thianthrene in ethyl acetate at various ratios were injected into the GC. The ratio of the resulting areas to the initial masses was then plotted to determine the most linear response. Figure 4-1 shows the results of this analysis. The line fitted to these data show an R^2 of 0.9993, indicating a good linear fit. A ratio of 2, at the higher end of this curve, was chosen for this procedure in order to ensure that as the concentration of the substrate decreased, the response would still be linear.

After analysis of each set of samples, a calibration sample was analysed to verify the standard curve. The ratio of substrate to internal standard was known and set to 2. The resulting areas were then used to determine the instruments' response (area ratio/mass ratio) to the compounds during that particular run. To simplify each set of analyses, it was assumed that the y-intercept of this response line was essentially equivalent to zero. This assumption is validated with the results of Figure 4-1. Figure 4-1 shows that the y-intercept of this response line is actually only a fraction (0.345 %) of the total ratio (2) of compounds used. When the linear regression line is forced through zero the slope of standard curve is essentially left unchanged, with 0.33 % difference.

Figure 4-1 Calibration curve of carbazole and thianthrene in ethyl acetate on the GC-FID. The line represents the best fit, linear regression through the data points.

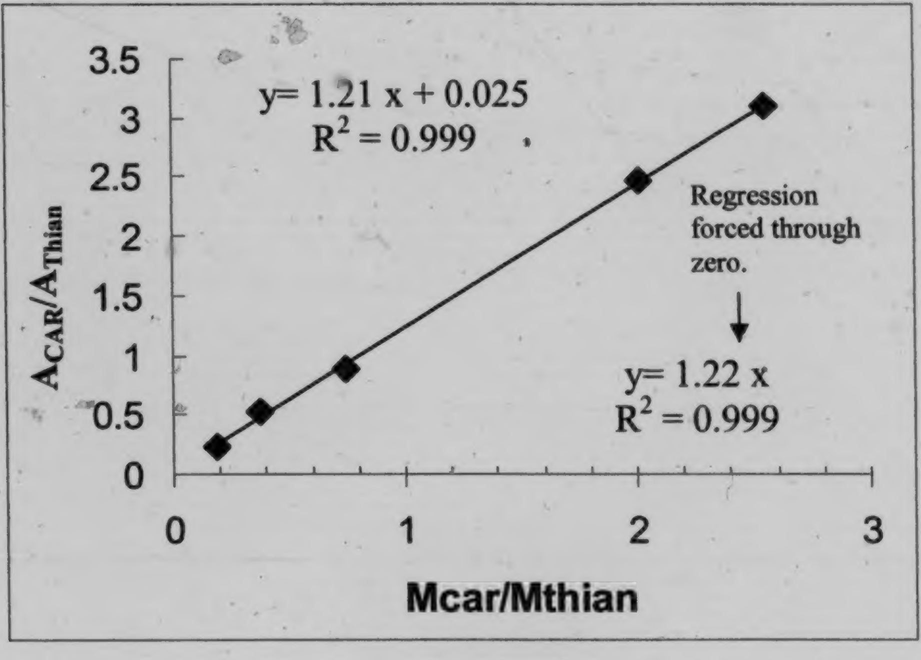

4.1.2.2 Sensitivity of gas chromatography

In order to properly evaluate the method sensitivity of GC-FID to quantify carbazole concentrations, a calibration curve was completed with samples of carbazole in ethyl acetate. The dilution series was started with a high concentration and diluted several times until a concentration undetectable by the gas chromatography method was reached. As shown in Figure 4-2, the detector was able to maintain a linear response to a carbazole at concentrations as low as 0.14 mg mL^{-1}. This linearity was confirmed with the R^2 value of 0.986.

Figure 4-2 Calibration curve of carbazole determined by GC-FID. Standards were made from solutions in ethyl acetate. The line represents a linear regression through the data points.

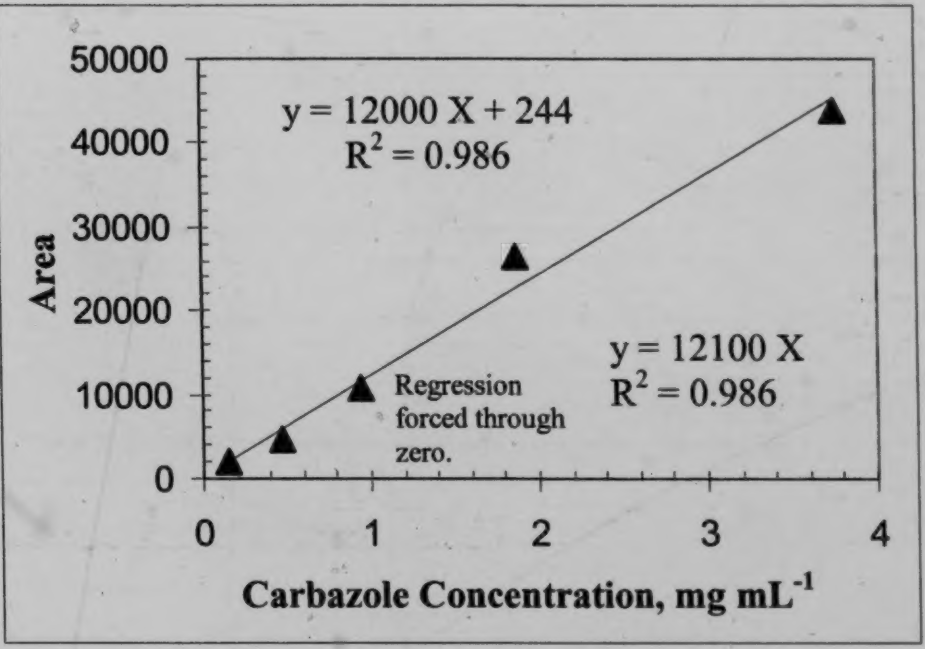

4.1.2.3 Effectiveness of liquid-liquid extraction in test-tube cultures

Carbazole is a solid compound that is poorly soluble in water. The aqueous solubility of carbazole is 1.209 μg mL^{-1} (Pearlman *et al.*, 1985), whereas glucose which is readily soluble in water has a solubility of 1540 mg mL^{-1} (Perry and Green, 1984). Because of this characteristic, a large portion of carbazole in the small-volume cultures (5 mL) was dispersed as a solid throughout the culture tubes and on the walls both above and below the liquid surface. Each tube contained a maximum amount of 2.5 mg of carbazole. At such a small scale it was important to ensure that the extraction procedure was effective for carbazole recovery. Also because there were a large number of cultures to be analyzed, it was advantageous to use the most effective and least labour intensive procedure.

The extraction procedure was developed and evaluated by extracting a series of sterile cultures using various volumes and number of repetitions of extracting solvent (ethyl acetate). In the end, all detectable carbazole and thianthrene was removed with two extraction steps: the first being the internal standard solution and the second being another additional millilitre of solvent.

4.1.2.4 Effectiveness of carbazole solubilization technique.

This work was started with measuring substrate loss using solely liquid-liquid extraction with ethyl acetate as the solvent, under acidic conditions followed by GC-FID analysis to quantify the final concentration. This method was used with both the test tube cultures and the 500-mL shake flask cultures. With extraction efficiencies of 91.2 ± 7.4 % (based on thianthrene recovery) this was an effective method. (See Appendix E for data and calculations.)

To ensure manageable numbers of flasks when both carbazole loss and biomass growth were measured, a method that allowed for both measurements to be taken from the same flask was developed. By adding 95 % ethanol at a volume ratio of 50/50, the particulate carbazole was dissolved. A sub-sample was then removed and analyzed using HPLC. The culture was then vacuum filtered to collect the biomass. The analytical method was evaluated by preparing 10 live cultures and 2 sterile control cultures in 500 mL shake flasks. All cultures were prepared and incubated identically. Biological activity was stopped with acidification to pH 2 using 6 M HCl. The culture set was then split in half: five cultures and a sterile control underwent the ethanol solubilization procedure followed by HPLC and five cultures and a sterile control were extracted with ethyl acetate and analyzed by GC.

The hypothesis that there was no difference between the two methods was statistically analyzed using the non-pooled t-test. It was assumed that both sample sets represented populations of normal distribution and that both populations were independent. At p=0.117, there was no statistical difference between the means of each sample. Thus we can conclude that the method of ethanol solubilization followed by HPLC analysis produces measurements comparable to the technique of solvent extraction and gas chromatography.

Table 4-1 Comparison of procedures to quantify carbazole concentration. Cultures were grown for 7 d. The concentration of carbazole remaining was measured with two methods: ethanol solubilization and solvent extraction.

		Carbazole Remaining (%)	
Method	Sample Size	Average	Standard Deviation
HPLC	5	74.5	5.35
GC	4	69.7	1.72

4.1.3 Biocatalyst measurements

4.1.3.1 Biomass measurements

The measurement of biomass after the ethanol treatment allowed for a minimum number of replicate flasks. Measurement of biomass was difficult with isolate CP19. Standard methods of growth measurements such as OD_{600} and protein content were inappropriate and very time consuming, respectively. The cells of CP19 clumped together at the bottom of the flask, and tended to agglomerate with carbazole crystals. As a result of this lack of homogeneity, OD_{600} measurements were not valid. The process of cell lysis required for completing protein content measurements was time intensive and thus was less desirable.

The preferred method of biomass determination was dry cell weight. Typically dry cell weight measurements are performed on cultures without any pretreatments. However, given that carbazole is in a solid form in the untreated culture, a measurement of dry cell weight by simple filtration would not be valid. Any carbazole particulates would bias the biomass numbers. Considering that carbazole was solubilized after the ethanol treatment, the solid substrate would not be a problem. Sub-sampling was still not appropriate as the cells aggregated, therefore, vacuum filtering of the entire sample was examined.

To ensure that all biomass was accounted for, the possibility of cell lysis during the ethanol procedure was investigated by comparing the amount of cells collected with and without ethanol treatment. Optical density measurements at 600 nm were performed on the filtrates before and after filtration to quantify the amount of cell material passing through the filter. In this instance, OD_{600} measurements were applicable because CP19 cells did not aggregate when grown on TSB.

Ten cultures (and two sterile controls) were prepared, inoculated and incubated identically. At the end of the incubation period, biocatalytic activity was stopped with acidification to pH 2 using 6 M HCl. The ethanol treatment, as described in section 3.2.5.1, was applied to five of the cultures while the other five were filtered without addition of ethanol. The final masses obtained from both procedures were compared and evaluated. Wet mounts from samples of each culture were prepared and examined, with a light microscope, for the presence of intact cell walls. Optically it was not apparent that the ethanol treatment disrupted the cells.

This preliminary experiment showed that the filtering method was able to collect more cells when the ethanol pretreatment was applied. As outlined in Table 4-2, the filtering method collected almost twice the amount of cells when ethanol was added to the culture.

Table 4-2 Summary of biomass measurements from filtering untreated TSB cells and ethanol treated TSB grown cells. Five replicates used for each determination.

Sample	Total Dry Cell Weight (mg)	
	Average	Standard Deviation
TSB	381	68
TSB+Ethanol	714	34

Examination of the OD_{600} of filtrate before and after filtering showed that the removal of material detectable at 600 nm was greater in the presence of the ethanol pretreatment. As shown in Table 4-3, the ethanol treatment increased the removal from 69-97 %. This is another indication that the filtering method was indeed more effective for the cells pretreated with ethanol.

One more piece of evidence was used to validate the effectiveness of biomass quantification and that was repeatability. Six cultures grown on carbazole and acetate in mineral medium for 7 d were treated with the ethanol procedure and then filtered. Starting with identical inoculum grown under identical conditions with identical amounts and types of substrate, the final biomass in each culture should be identical. As determined from statistical analysis, the cultures did indeed give repeatable results. The total biomass averaged 13.2 ± 2.6 mg, where the error bound gives the 95 % confidence interval.

Table 4-3 Evaluation of filtering method whereby efficiency is measured using OD_{600} readings before and after filtering. The designation "-F" indicates the cell-free filtrate.

Sample	OD_{600}		
	Average	Standard Deviation	% Removed
Untreated	11.4	2.16	
Untreated -F	3.49	0.62	69
Ethanol	7.20	1.70	
Ethanol-F	0.21	0.03	97

4.1.3.2 Validation of protein content determinations

The procedure for measuring protein content was not used routinely as a method of measuring biomass, but it was needed to correlate dry cell weights to actual cell protein content. Conventional methods of protein measurements were not successful with the bacterium CP19 so an alternate method was developed.

The procedure of protein measurements starts with lysing the cells to release the protein held within the cell wall (Izac and Tholozan, 1998). Cell lysis can occur with various procedures but a common one includes adding 1 M NaOH to the cell suspension followed by a short heat cycle. A clear, non-turbid suspension indicates cell lysis. When this procedure was conducted on CP19, it was difficult to obtain the clear suspension. In fact, once the heat cycle had been increased to 1 h at 100 °C, the cell suspension was still turbid and microscopy showed the presence of intact cells.

The next step in this process was to try mechanical disruption of the cells with sonication. The effectiveness of this procedure was determined by optically examining a sample of cell suspension after increasing exposure time to sonication. A wet mount of each sample was prepared and examined microscopically. The condition of the cells was evaluated by comparing it to the original sample, and to the sub-sample from the previous time interval. When the cells were confirmed to have been broken, by examining them under the microscope, the sonication procedure was stopped. The samples taken after each time interval were then analyzed using the protein assay. As outlined in Figure 4-3, maximum protein concentrations were obtained after 10 min of sonicating. Ten min of sonication was adopted as the means of releasing protein from the cells.

Figure 4-3 Time course evaluating the length of sonication time required to lyse CP19 and release cellular protein.

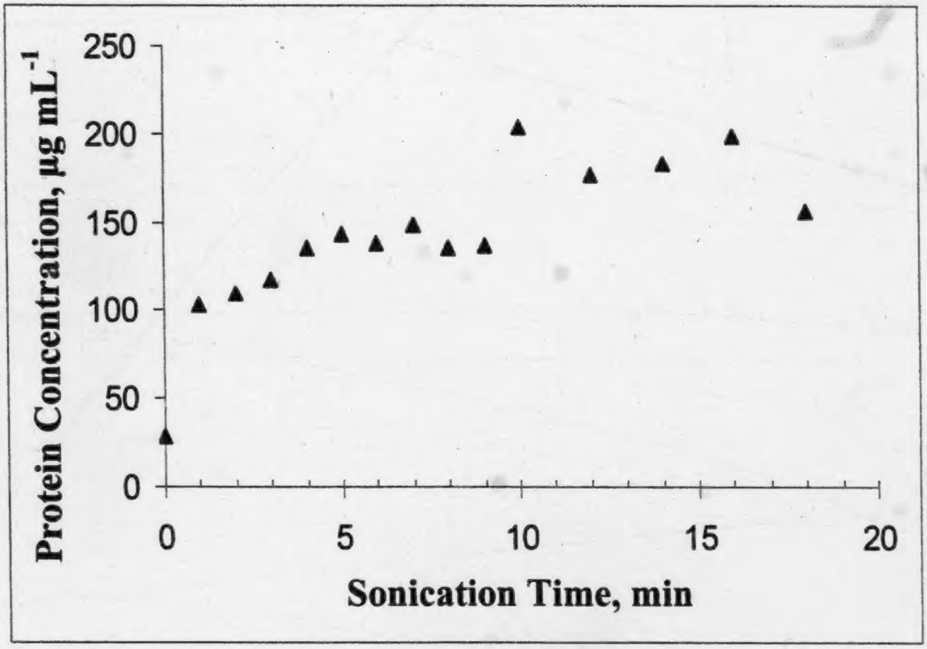

4.1.3.3 Ratio of dry cell weight to protein content

As previously explained in section 4.1.3.1, dry cell weight (DCW) was measured to monitor biomass formation. In order to convert these measurements to a protein basis, a conversion factor was determined by using the measured protein content (3.2.6.3) and DCW (3.2.6.2) from identical cultures. Eighteen, identical 500-mL cultures of CP19 were prepared (section 3.2.2.4). Three conditions were used at each time point: a heat-killed control, a culture for protein measurements, and a culture for DCW measurements. Triplicate samples of each condition were used at 2 d and 7 d of growth.

As can be seen in Figure 4-4, the ratio of DCW to protein content changed over time. The composition of biomass increased from 68 mg protein (mg DCW)$^{-1}$ to 98 mg protein (mg of DCW)$^{-1}$. At 10 % significance, these numbers are statistically different (See Appendix E for the analysis). Indeed, the amount of protein (mg DCW)$^{-1}$ increases with time. The increase in the ratio can be attributed to an increase in protein content. When the ratio is broken into its two components (Table 4-4), it is evident that there is a greater increase seen in the protein content than in the DCW. Within the 2 day incubation period, DCW increased by 4 % whereas protein content increases by approximately 33 %. This inconsistent increase suggests the possibility that the technique used to measure DCW decreased in effectiveness with higher cell densities.

Figure 4-4 Ratio between DCW and protein content of CP19 cells. HKC refers to heat-killed controls.

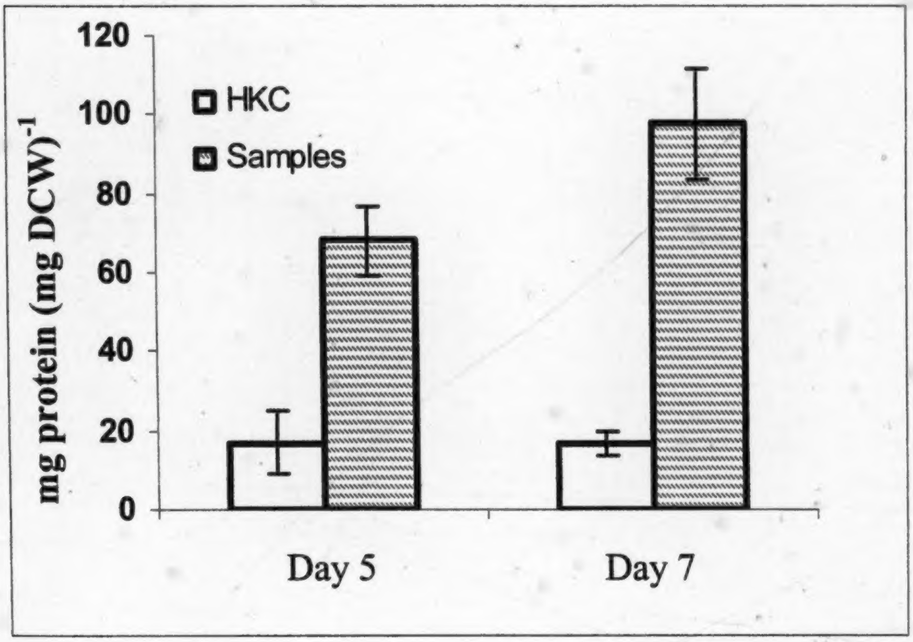

Table 4-4 Results from protein and DCW measurements of CP19 and heat-killed controls (HKC).

		Dry Cell Weight (mg)		Protein (μg)	
Sample	Time	Average	St. Dev	Average	St. Dev
HKC	Day 5	5.7	0.7	98	35
	Day 7	5.9	0.2	99	15
CP19	Day 5	32.8	1.5	2230	190
	Day 7	34.1	2.0	3330	282

4.2 Isolation and screening of carbazole degraders

Bacterial colonies were isolated from creosote-contaminated soil found at a site in Edmonton, Alberta. This site provided a carbon-rich, nitrogen-limited environment with an abundant supply of carbazoles compounds. Carbazole compounds characterize creosote oil (Mueller *et al.*, 1989) that had been the original contaminating substance. Colonies with various morphologies were purified and screened in liquid culture.

Isolates were evaluated by monitoring growth and substrate loss. The data presented are from the cultures that showed the most interesting characteristics from the initial screening, based on unusual colour formation or interesting growth patterns in the various growing conditions as compared to the positive control (*Pseudomonas* sp. LD2).

Testing conditions included mineral salts medium with carbazole and various combinations of supplemental carbon and nitrogen sources. An ideal bacterium for carbazole processing would give growth on carbazole supplemented with acetate carbon (CAR+ACT), no growth on carbazole as sole carbon and nitrogen source (CAR) and growth on carbazole supplemented with acetate and nitrogen (CAR+ACT+N). Bacteria that fix nitrogen are not desirable for this process so no growth in the acetate only conditions is required. These trends are illustrated in Figure 4-5 in the first, second, third and fourth bars, respectively.

The data of Figure 4-5 show that there was no appreciable growth in the fourth condition with acetate only. CP18, CP19 and LD2 showed some growth in this condition, but when compared to the sterile control it was not significant. Consequently, these bacteria were not capable of nitrogen fixation. All bacteria were able to grow in the acetate, nitrate and ammonium supplemented conditions. All of the strains were also able to grow in the presence of carbazole as sole carbon and nitrogen source (CAR).

When compared to the positive control LD2, the difference of growth between the supplemented cultures (first and third bar) and the carbazole only condition was most significant for isolate CP19. Figure 4-6 A and B give more detail on the growth with acetate supplements and with carbazole only, respectively. Isolate CP19 had a different growth curve from both LD2 and CP18. The typical growth curve, starting with a lag phase, followed by an exponential growth phase and finally a stationary phase, is evident in both CP18 and LD2; however, this type of growth was not observed for CP19. The zero-order growth of CP19 was consistent with a nutrient supply limited by mass transfer, (Volkering *et al.*, 1992). Isolates CP6a and CP6b were much slower growing in the acetate supplemented condition and a trend was not evident in the time period of monitoring.

Without the addition of acetate, the growth curves of CP18 and LD2 still have the same trends, but give less biomass. This result would be expected since the total amount of carbon in the culture was less than in the carbon supplemented culture. Both CP6 cultures do not show significant changes in biomass formation regardless of the amount or source of carbon supplied.

Although they did contribute to the evidence that supported the decision to select CP19 for further study, comments on the growth trends of CP19 cannot be legitimately made from the results of the OD_{600} measurements made in the screening process. Subsequent observations of its behaviour on carbazole revealed that CP19 tended to agglomerate with the crystals. This characteristic made the optical density measurements inconclusive.

Figure 4-5 Growth yield from isolates in test conditions. Growth is measured as OD_{600} after 7 d incubation. A sterile control (StCntl) was completed with each culture set.

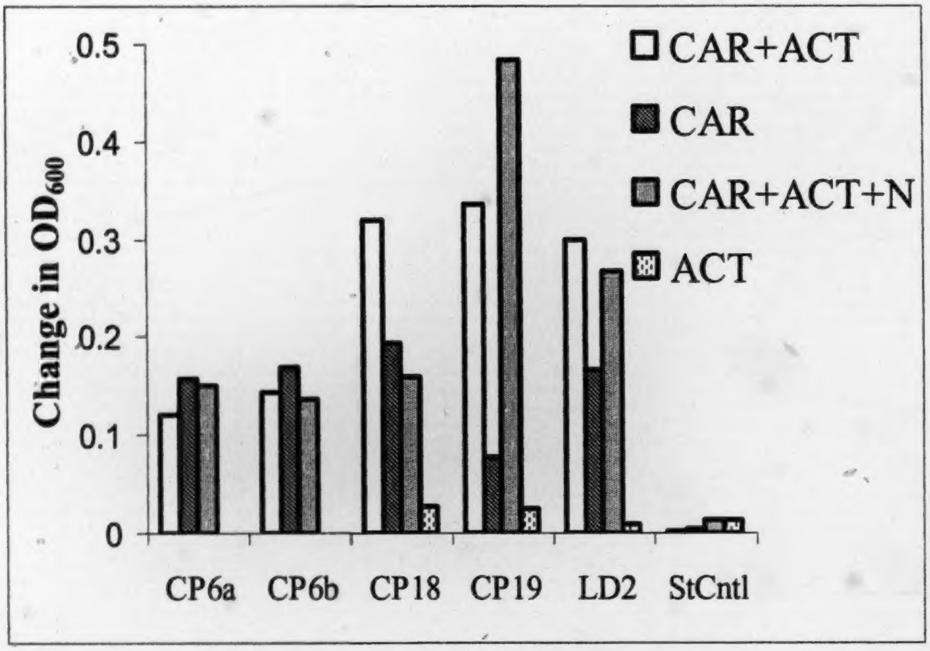

Figure 4-6 Growth of isolates with acetate supplemented conditions and only carbazole. A. CAR+ACT, B. CAR

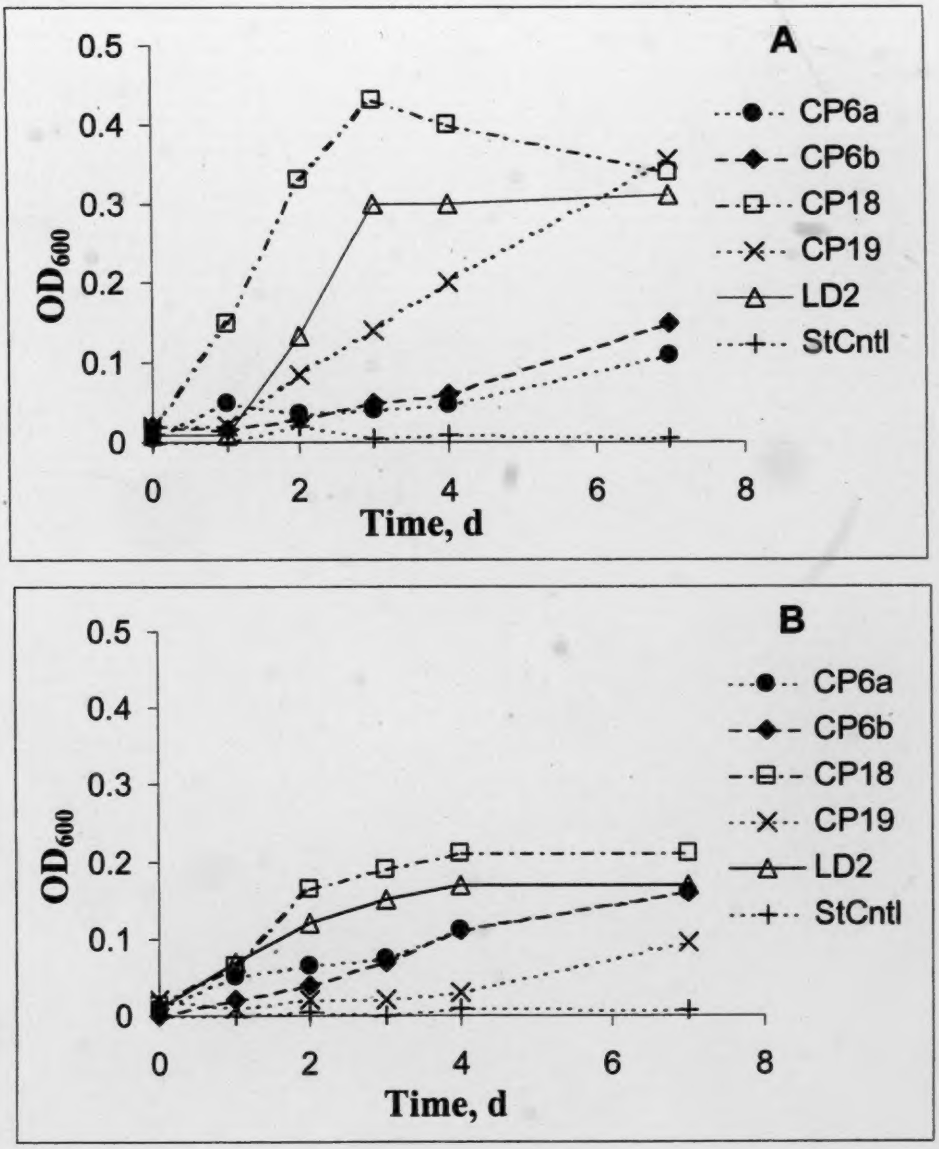

The data presented in Figure 4-5 and Figure 4-6 show that all of these cultures had the ability to use carbazole carbon. None of these isolates exhibited the desired activity of the ideal carbazole isolate. However they still may be suitable for carbazole processing following mutagenesis. Selection of promising bacteria for such a modification requires information on the enzyme pathways and the degree of mineralized carbazole.

Growth of isolates with supplementary carbon and nitrogen sources in the presence of carbazole, and the usage of carbazole, provided information on the regulation of enzyme pathways. The amount of substrate converted by the isolates in the testing conditions is outlined in Figure 4-7. The first and second bars represent the difference of carbazole transformation as a result of the presence supplementary carbon: no appreciable difference was observed. To grow, the isolates still require the nitrogen from carbazole, so regardless of whether the acetate can inhibit the use of carbazole carbon transformation of carbazole will still be seen when the nitrogen atom is used.

If the enzymes for transformation of carbazole are regulated by the presence of available carbon and nitrogen, then addition of these components should suppress conversion of carbazole. The data of Figure 4-7 show that no significant suppression of carbazole conversion was observed due to alternate carbon or nitrogen sources.

Figure 4-7 Removal of carbazole by isolates incubated with various sources of nitrogen and carbon. Cultures were incubated for 7 d.

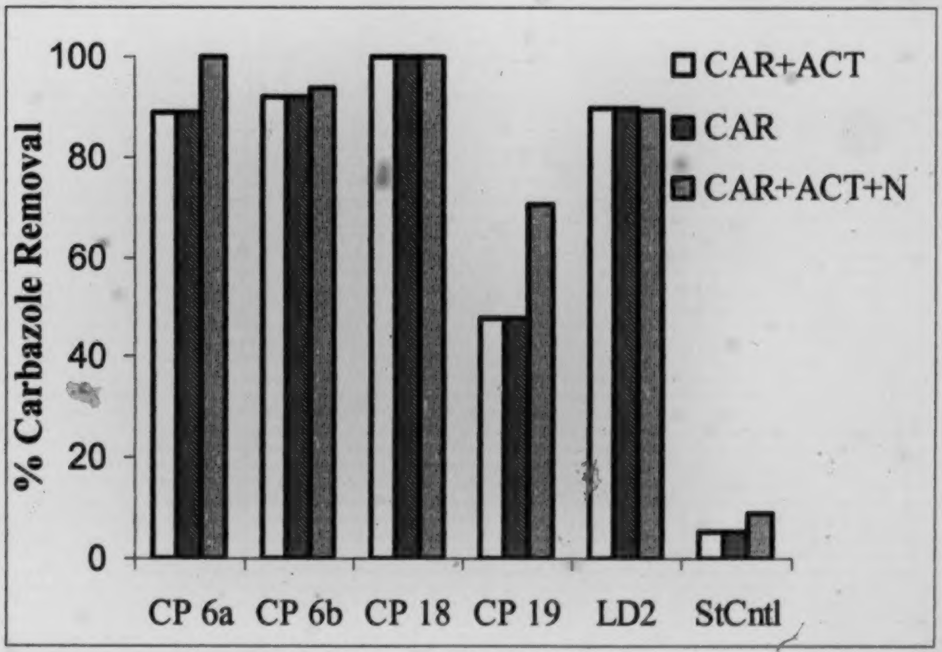

The data presented thus far show that all isolates can use carbazole carbon and the enzyme systems they use are not regulated by acetate, nitrate or ammonium. The amount of carbazole carbon degraded was evaluated using uniformly radiolabelled carbazole with acetate, monitoring the release of $^{14}CO_2$. Medium containing acetate was selected because it was necessary to determine if the additional carbon regulated the use of carbazole carbon.

The rate of $^{14}CO_2$ released by each isolate is shown in Figure 4-8. The degree of mineralization of all isolates was less than that of LD2, the positive control. When compared to LD2, both CP19 and CP6a show slower rates of mineralization. At day 1 and day 2, these cultures show less than half the amount of mineralization as LD2 however by day 7 they are similar. Both CP18 and CP6a show rates comparable to LD2.

Distribution of the radiolabel after incubation was determined by extracting the culture under acidic conditions. Along with some acidic carbazole products, all unconverted carbazole is collected in the extract. Very polar carbazole metabolites and biomass-associated ^{14}C remains in the aqueous fraction and mineralized carbazole is in CO_2 fraction. Figure 4-9 shows the results of this distribution. Overall, LD2 showed the largest amount of mineralization; however, excluding CP6b, it also showed the least amount of ^{14}C remaining in the extract, implying it actually used the most carbazole. The extract may contain some converted products, however it can provide some insight on the amount of unconverted carbazole remaining. CP6b shows the least amount of radiolabel in the extract, implying that this culture had the greatest amount of carbazole conversion. Cultures CP6a, CP18 and CP19 show a higher accumulation of ^{14}C in the aqueous fraction than LD2, implying possible accumulation of very polar metabolites. Without knowing the actual amount of ^{14}C metabolized, this trend can only be an indication.

Figure 4-8 Degradation of the carbon backbone of carbazole by isolates, determined by the production of $^{14}CO_2$ from ^{14}C-carbazole.

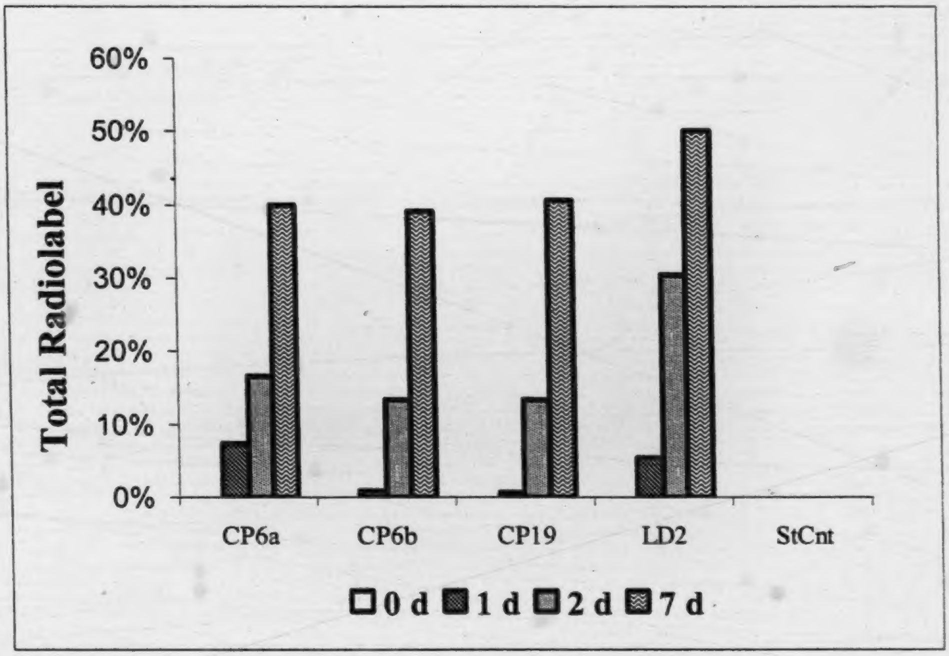

Figure 4-9 Distribution of radiolabel from ^{14}C-carbazole in ethyl acetate: extract, aqueous phase and carbon dioxide release. Isolates were grown on carbazole and acetate for 7 d. The percent of radiolabelled reflects the percent of total ^{14}C added to the culture.

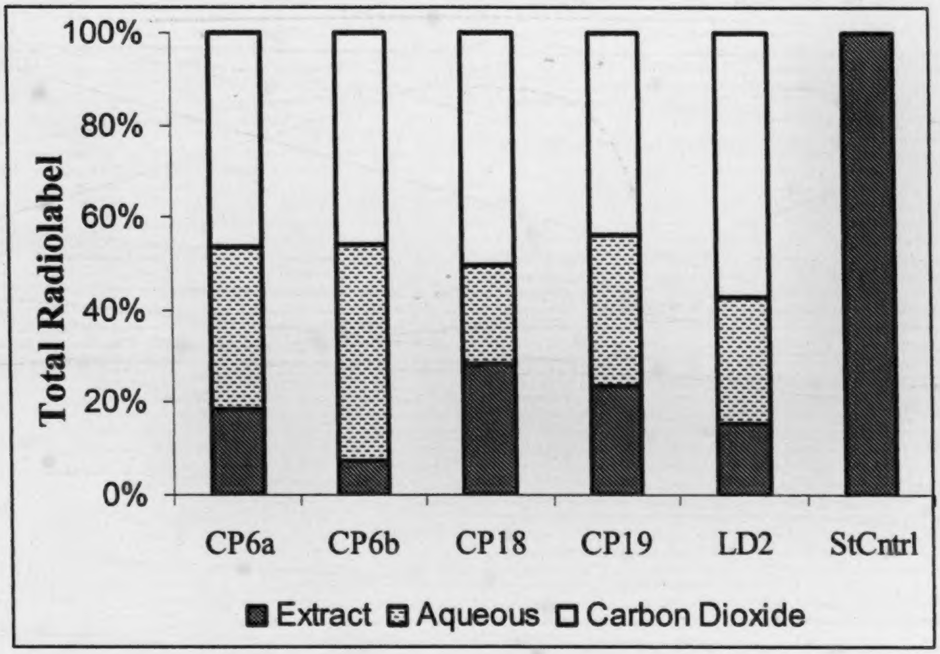

4.3 Characterization of isolate CP19[3]

Isolate CP19 was selected from the group of carbazole degraders as a bacterium suitable for further study. The selection was made based on its interesting growth characteristics as compared to the other isolates and the formation of a coloured metabolite unique to this isolate when grown on carbazole.

4.3.1 Growth characteristics

The data presented in Figure 4-5 through Figure 4-9 showed that isolate CP19 grew slowly on carbazole. Inoculum was prepared by growing isolate CP19 on TSB to a high cell density, then harvesting during the mid-exponential growth phase to inoculate cultures with carbazole.

The "clumpy" characteristics of CP19 on carbazole were not evident when the culture grew on TSB. The growth curve was constructed by measuring OD_{600} at various times until the cells reached stationary phase. Three independent batches of 200 mL TSB cultures were grown at 28 °C. At each time point, 1 mL samples were aseptically removed from the whole and analysed using the spectrophotometer. If the measurement was not within the linear range of the instrument it was diluted with sterile TSB. Figure 4-10 shows the average growth curves of all three cultures.

---

[3] Unless otherwise indicated, the error bars shown in the graphs of this section represent the standard deviation of three replicates.

Figure 4-10 Growth curve of CP19 grown on TSB. [4] **The error bars represent the standard deviation of three replicates.**

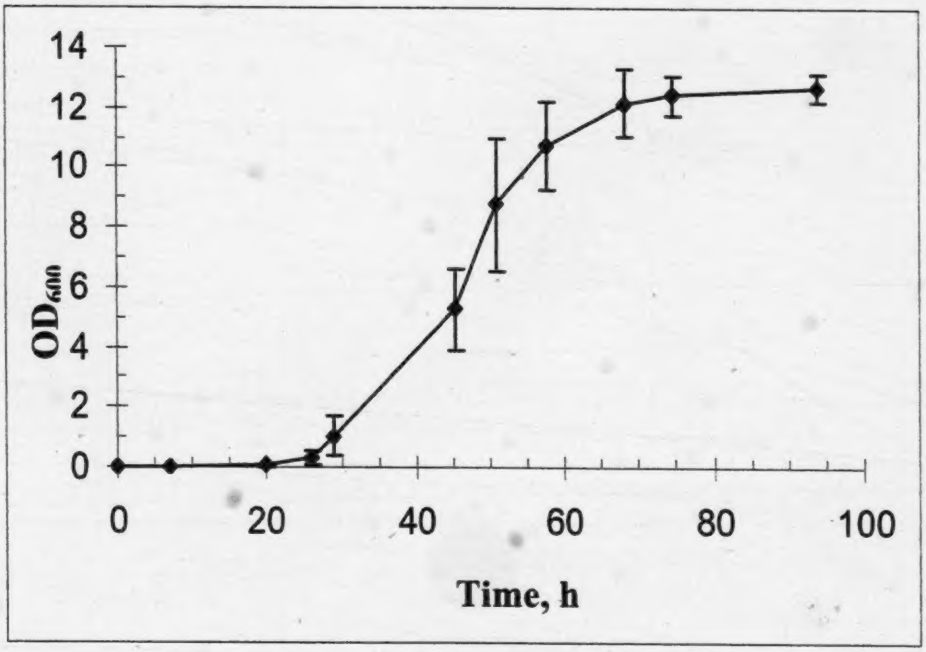

---

[4] The larger magnitude of the error bars in the mid-exponential phase was due to one of the replicates which showed a slight lag behind the other two cultures. The lag shifted the exponential phase to the right by approximately 5 h.

4.3.2 Species identification and characterization

A variety of biochemical tests was performed on isolate CP19, the first of which was Gram stain. Because of inconclusive results, the 3 % KOH test (von Graevenitz and Bucher, 1983) was performed as well. Using both positive and negative controls, this test was performed on CP19 and initially gave results indicating that the cell wall did not lyse. The cell wall did not lyse with 3 % KOH solution and thus the bacterium was labelled Gram positive. The biochemical tests performed were selected according to this initial result. After increasing the duration of the test, the KOH test showed that the cells did lyse, indicating that CP19 is actually a Gram negative bacterium.

Table 4-5 Summary of biochemical test performed on CP19

Test	Result
Gram stain	Inconclusive
3% KOH test	Gram negative
Catalase test	Positive
Oxidase test	Positive
Urease	Negative
Bile esculin	Negative
Endospore stain	Negative
Acid-fast test	Inconclusive
Morphology	Tiny rods. Round, white mucoid colonies.

The bacterium was conclusively identified as a member of the genus *Sphingomonas* by 16S rDNA sequencing by MIDI Labs. When aligned in a pair-wise manner against the MicroSeq Database, CP19 was 3.41 % different from *Sphingomonas yanoikuyae* at the genus level. A full gene alignment with the GenBank database showed 98 % similarity with *Sphingomonas* CF06 U52146 (Figure 4-11).

Bacteria belonging to the genus *Sphingomonas* are Gram negative, non-spore forming, non-motile, urease negative and catalase positive (Balkwill *et al.*, 1997). All these characteristics were evident with the biochemical tests performed on CP19 therefore the results from methods of classification were consistent. These are some of the characteristics used to identify *Sphingomonas* bacteria; however the presence of sphingoglycolipid in the cell membrane is one of the most distinctive traits.

Figure 4-11 Illustration of Neighbour Joining Tree resulting from 1500 bp concise alignment report. Reproduced from the data supplied by MIDI labs on the 16S rDNA sequencing of CP19. The percentages represent the percent difference from the sequence of CP19.

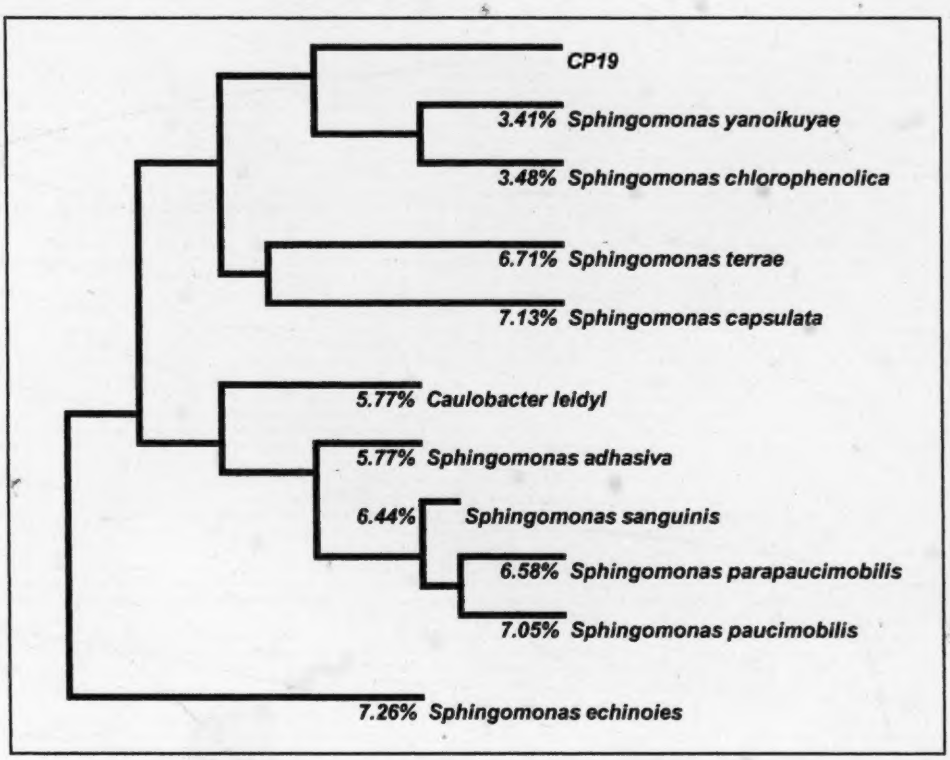
CP19
3.41% Sphingomonas yanoikuyae
3.48% Sphingomonas chlorophenolica
6.71% Sphingomonas terrae
7.13% Sphingomonas capsulata
5.77% Caulobacter leidyl
5.77% Sphingomonas adhasiva
6.44% Sphingomonas sanguinis
6.58% Sphingomonas parapaucimobilis
7.05% Sphingomonas paucimobilis
7.26% Sphingomonas echinoies

4.3.2.1 Capsule Staining

In an attempt to determine the reason behind the resistance of the cells to lysis by KOH and their tendency to adhere to carbazole, the surface properties of CP19 were examined. A capsule stain was performed on the organism to determine if it carried the sticky, polysaccharide coating which functions as a protective layer in various organisms. India ink was used to stain the background and methylene blue was used to stain the cell. Capsule layers appear as light halos around a blue, stained cell.

Using oil immersion, the capsule stained specimen was examined under a light microscope. As illustrated in Figure 4-12, the image showed that CP19 does possess a significant capsule layer around its cell wall. According to measurements completed with the microscopy photos, the cells inside the capsule are approximately 1-1.3 μm in length whereas they are approximately 3.5 μm in length including the capsule. Confirmation of the presence of the capsule layer accounts for the difficulty in lysing cells both in the protein assay and in the KOH test.

Figure 4-12 Capsule stain of *Sphingomonas* sp. CP19 using India ink and methylene blue stain. Magnification is 1000 X using a light microscope. Cultures were grown on carbazole as sole nitrogen source with acetate as a soluble carbon source.

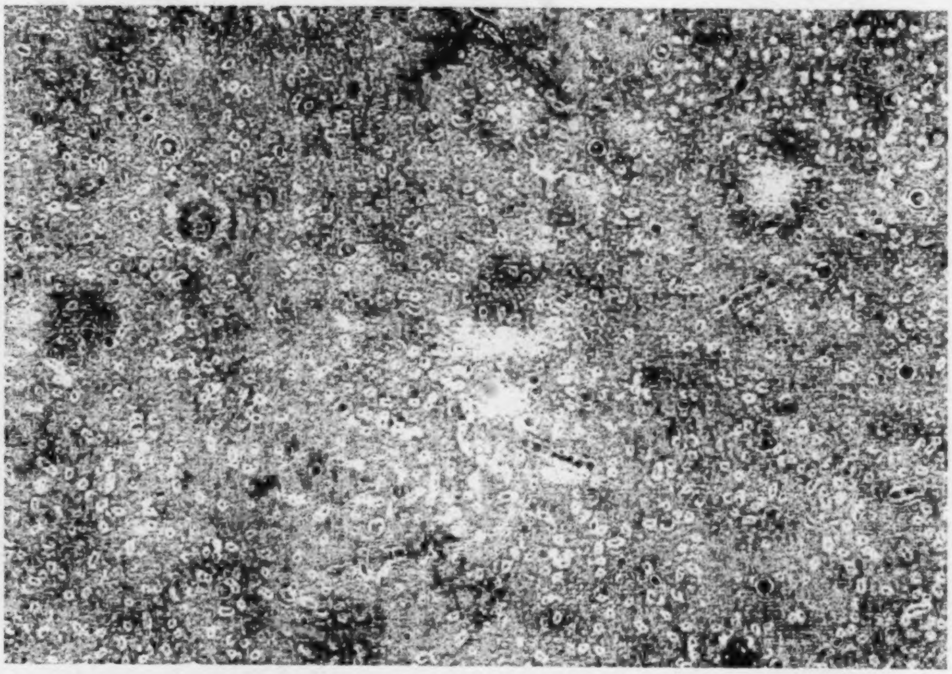

4.3.2.2 Microstructures of CP19

Sphingomonas sp. CP19 was also examined for the presence of inclusions by imaging cross sections of the cells by TEM. Two sets of cultures were grown, one in TSB and one in mineral medium and carbazole. If CP19 were to develop inclusions due to the utilization of carbazole, the inclusions would be seen only when carbazole was present, but not evident in TSB grown cells. Figure 4-13 and Figure 4-14 show the results of this procedure.

Bright, white spots were observed in both samples. This observation was attributed to the preparation procedure, which involves fixing the cells with glutaraldehyde, dehydrating them with an ethanol wash, encasing the sample in epoxy resin, and finally sectioning the sample. Polysaccharide material has the opportunity to fall out of the plastic at the time of sectioning. This will result in the white spots or "holes" that appear in these photos (Hayat, 2000).

Cells grown under both conditions show lighter areas inside the cell membrane. This observation suggests that inclusions are present in isolate CP19 under both growing conditions. The contribution of carbazole, if any, to the composition or formation of these inclusions is not clear. Cells growing on carbazole are larger in shape with "weaker" more fragile looking cell walls than those growing in TSB. This observation was consistent with the slow growth rates of cells on carbazole.

Figure 4-13 Transmission electron micrograph of *Sphingomonas* sp. CP19 grown on TSB medium.

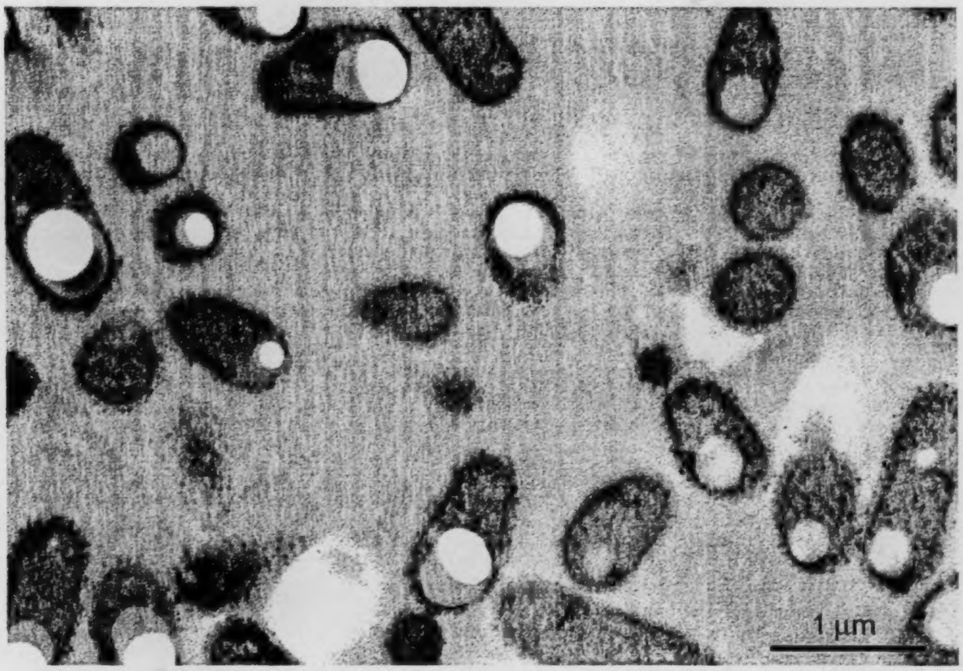

Figure 4-14 Transmission electron micrograph of *Sphingomonas* sp. CP19 grown on carbazole as sole nitrogen source.

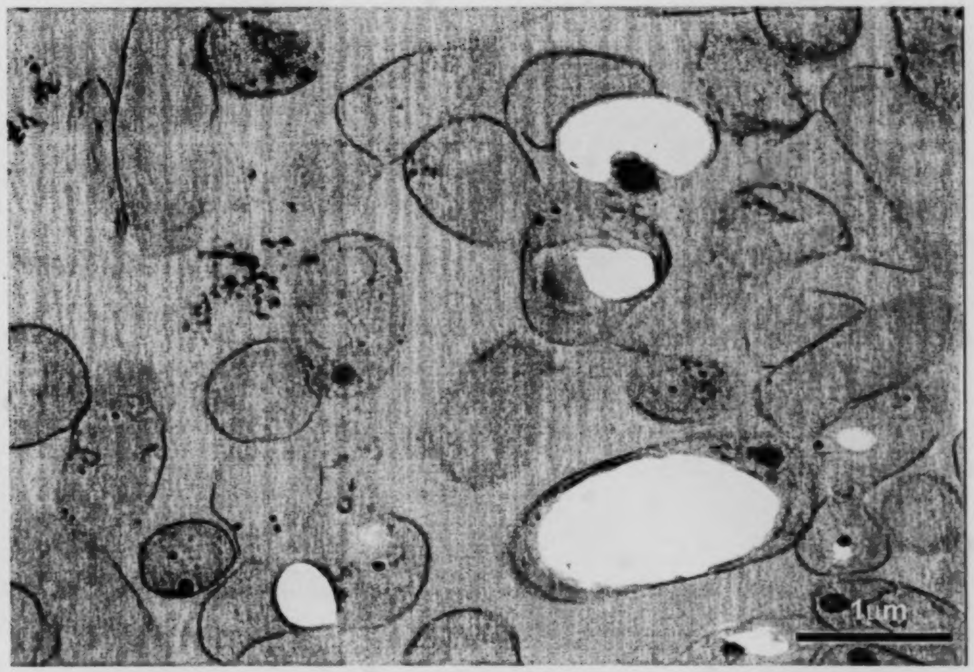

4.3.2.3 Growth of strain CP19 on carbazole crystals

CP19 exhibited tendencies to grow with adhesion to crystals of carbazole. The possibility that the cells were growing on the surface of the carbazole crystals was investigated using environmental scanning electron microscopy. Carbazole crystals incubated in sterile medium were photographed, as were the crystal structures once they had been exposed to *Sphingomonas* sp. CP19. Samples were fixed for 2 h with 4 % formaldehyde solution in buffer. The images in Figure 4-15 illustrate the findings of this procedure.

As shown in Figure 4-15 A, without *Sphingomonas* sp. CP19, the carbazole surface was very smooth. In the presence of cells (Figure 4-15 B and Figure 4-15 C), the crystals are shown to have more particulate matter on the surface. Due to the size of the particulates, they cannot be concluded to be cells. Nevertheless it can be concluded that the surface of carbazole is being affected in the presence of live cells.

Figure 4-15 Environmental scanning electron micrographs of carbazole crystals. A. In mineral salts medium B,C. Exposed to *Sphingomonas* sp. CP19.

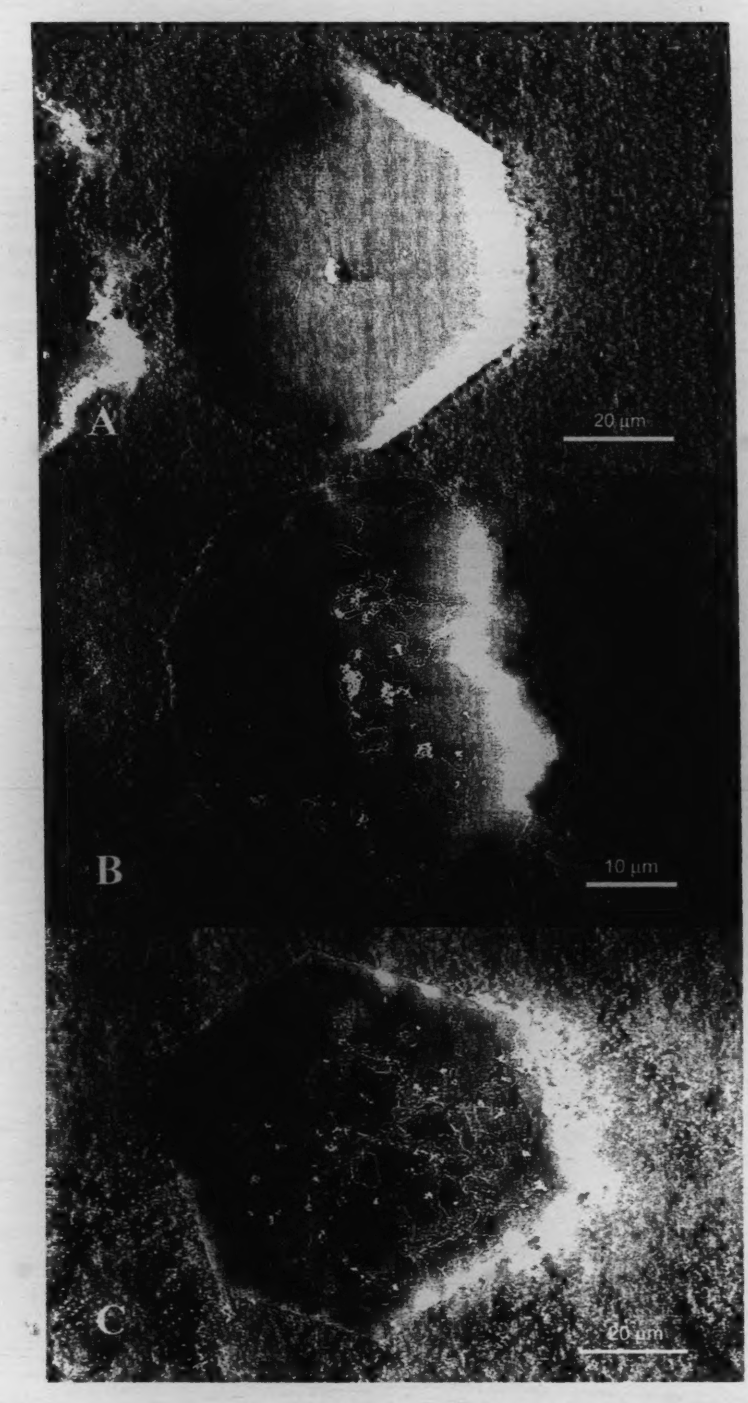
A
20 µm
B
10 µm
C
20 µm

4.3.3 Mechanisms for carbazole solubilization

In the screening process, the growth characteristics of CP19 on carbazole as sole nitrogen source suggest a mass transfer limited situation (see section 4.2). In response growing on poorly-soluble substrates, some bacteria actively produce or excrete materials that can increase the solubility of the substrate. An experiment to detect the presence of such material and to characterize its effects was established with CP19 cultures. Three heat-killed controls and three active CP19 cultures were prepared, inoculated and incubated as outlined in sections 3.2.2. At the end of 7 d, sub-samples of the cultures were filtered through 0.22 μm Millipore filters. Filtering was done first to stop the biological activity by removing the cells and second to remove any residual, insoluble carbazole. Using HPLC, the concentration of soluble carbazole was measured. After this measurement was completed, carbazole crystals were added to the sterile sample and mixed well. The resulting aqueous carbazole concentration was measured using HPLC.

Figure 4-16 summarizes the final carbazole concentration after the cultures have been filtered initially and then re-exposed to carbazole. The filtrate from culture samples showed a dramatic increase in carbazole solubility. Carbazole solubility in the culture filtrate was over 6 times greater than that of purified water. The aqueous concentration of carbazole determined with this method was 2.14 μg mL^{-1} which, when compared to literature values of 0.907-1.67 μg mL^{-1} (Pearlman *et al.*, 1984), indicated that the HPLC method gave values of the same order of magnitude.

Surface tension measurements of the supernatant from CP19 cells grown on acetate and carbazole for 7 d gave values of 60 mN m^{-1} and 61 mN m^{-1}. The same measurement of sterile, filtered water gave a value of 73 mN m^{-1}. The reduction in surface tension between the filtrate from the live cultures and from heat-killed controls was not large enough to infer the presence of a surfactant. Nevertheless, the increase in solubility between the filtrate from cultures and filtrate from heat-killed controls did indicate that live CP19 cells produced material that increased the aqueous solubility of carbazole.

Figure 4-16 Solubilization effects on carbazole by *Sphingomonas* sp. CP19 cells. This graphs shows the carbazole concentration measured in filtrate from heat-killed controls (HKC), live CP19 cultures (CP19), and carbazole concentrations in mineral medium (Medium) and distilled water (Water).

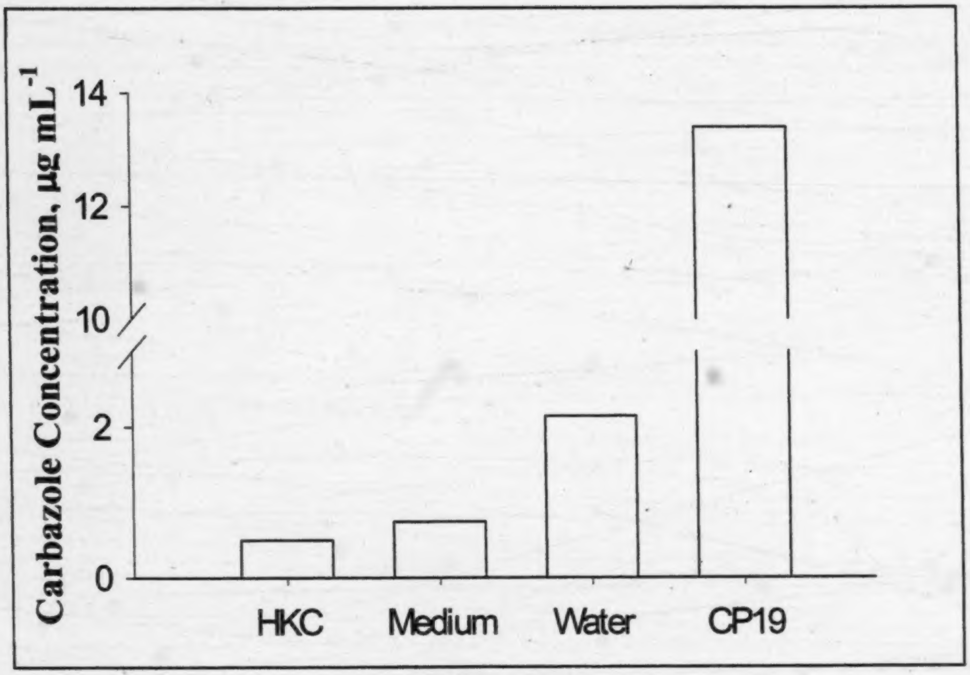

4.4 Regulation of carbazole transformation by CP19 with additional carbon and nitrogen sources.

In the screening process, it was apparent that the absolute amount of carbazole transformed in the testing conditions was not reduced by the presence of additional carbon or nitrogen sources. However it was also apparent that CP19 produced much less biomass without supplemental carbon or nitrogen. The objective of this investigation was to determine the rate of carbazole transformation in the testing conditions, normalized to biomass accumulation. This calculation will give a more detailed illustration of the effects the additional nutrient sources have on carbazole transformation.

Each condition at each time point was completed in triplicate 500-mL shake flasks. A variety of properties was measured for each sample, including final pH, concentration of soluble carbazole in the active culture, final total carbazole concentration, and dry cell weight. Despite the use of three different conditions, only one set of heat-killed controls was used. Mineral medium containing acetate, nitrate, ammonium and carbazole (CAR+ACT+N) was used for these controls as it represented the most complex medium and the medium most likely to show contamination if it was introduced during the experiment.

4.4.1 Overall conversion of carbazole and conversion rates

Normalized conversion of carbazole was calculated using carbazole conversion (Figure 4-17) and mass of accumulated cells (Figure 4-18). The results of these calculations are presented in Figure 4-19 where the values have been corrected using the results from the heat-killed controls. Strain CP19 transformed significant amounts of carbazole regardless of the presence of additional carbon and nitrogen sources. The conversion in both the carbon, and carbon and nitrogen supplemented conditions reached a constant value after 5 d, at values of approximately 8 μmol (mg DCW)$^{-1}$ and 6 μmol (mg DCW)$^{-1}$, respectively. High conversion of carbazole coupled with high accumulation of cells is the basis of this result.

Repression of carbazole enzymes by acetate was not obvious in these results, however at day 7, the normalized conversion of carbazole (12.5 μmol (mg DCW)$^{-1}$) in the carbazole only medium (CAR) was significantly higher than that of either supplemented media (Figure 4-19). This conclusion was based on the results of a non-pooled t-test completed on each of the conditions (see Table 12-16 in Appendix E).

The conversion of carbazole in the carbazole only medium (CAR) of 50 % was less than that observed in the carbon supplemented medium (CAR+ACT) and the carbon and nitrogen supplemented medium (CAR+ACT+N). As illustrated in Figure 4-17, these latter cultures showed 70 % and 85 % removal respectively. The normalized conversion in the carbazole only medium (CAR) was greater because significantly less biomass formed. The amount of biomass formed in the CAR condition is approximately 10 % and 20 % of the CAR+ACT+N condition and CAR+ACT condition respectively.

Using the same statistical analysis applied to the values at day 5, there was no evidence for inhibition by acetate, nitrate or ammonium sources. The conversions of carbazole are not statistically different at a significance level of 0.05.

Figure 4-17 Removal of carbazole by CP19 in the presence of various carbon and nitrogen sources. A. Complete set of raw data. B. Values have been corrected using data from the heat-killed controls. The error bars represent the standard deviation of three replicates.

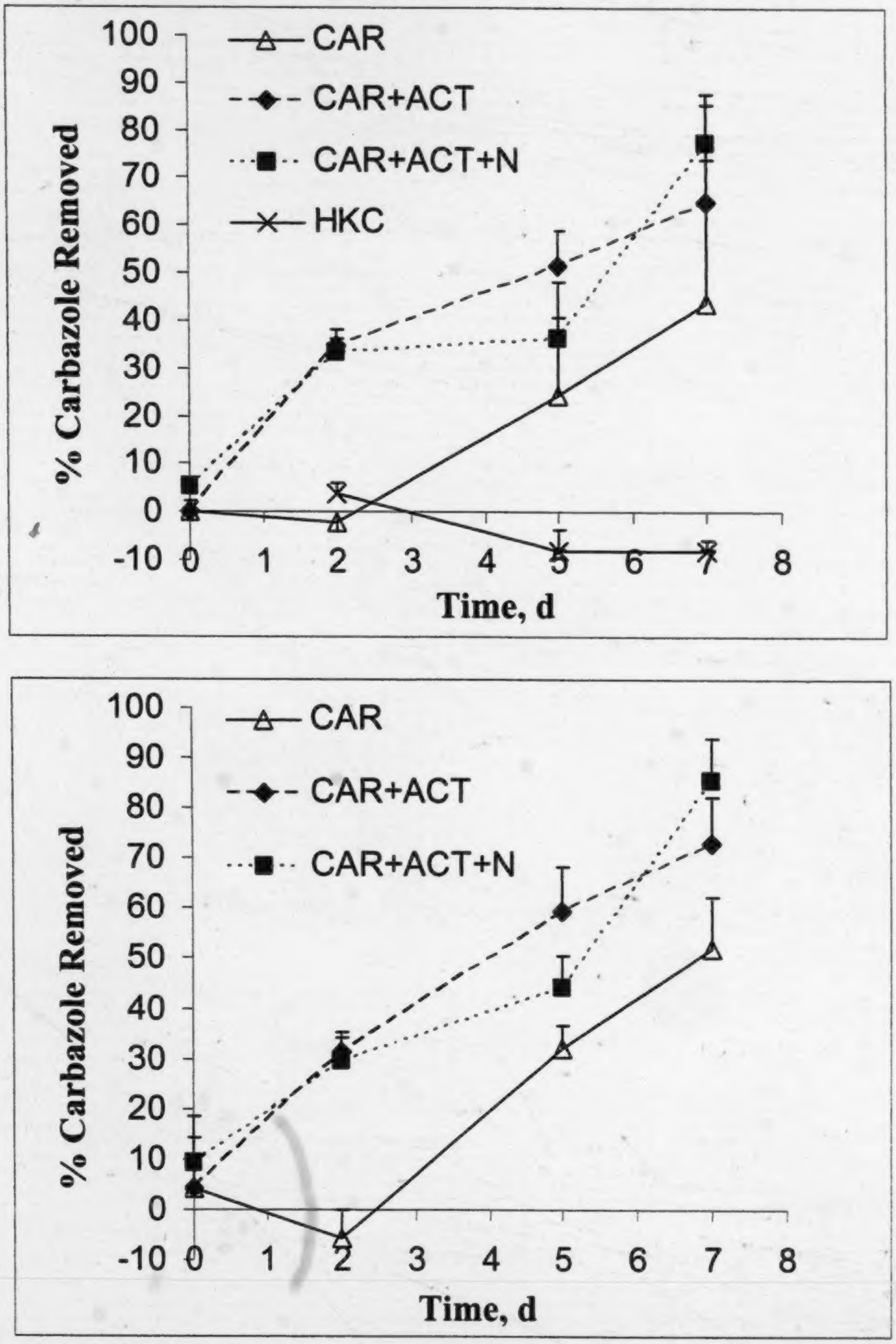

Figure 4-18 Increase in dry cell weight by CP19 with incubation. Each value has been corrected using the data from the heat-killed controls.

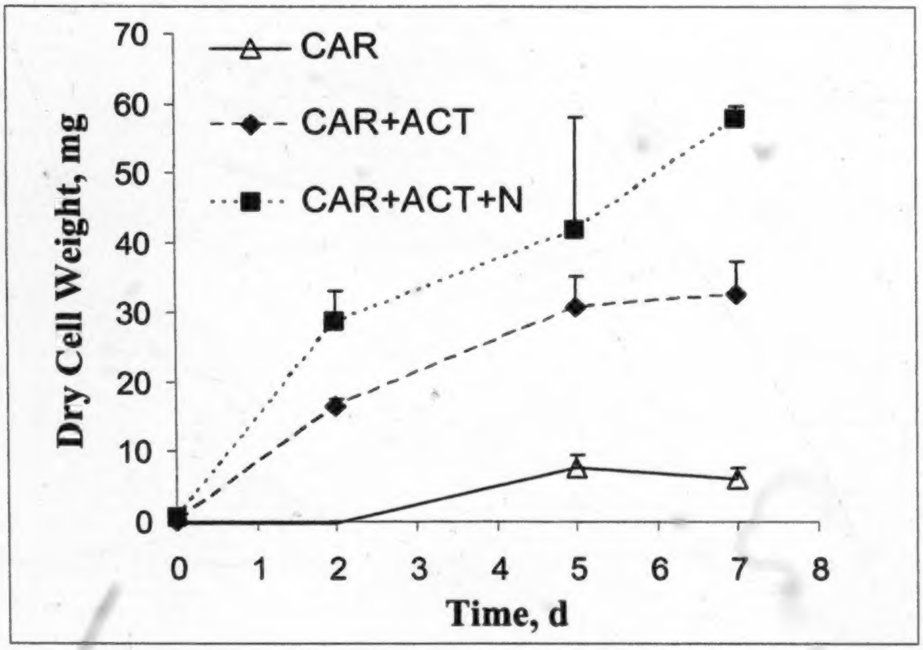

Figure 4-19 Transformation of carbazole by CP19 in the presence of various combinations of carbon and nitrogen sources. All conversions from (Figure 4-17) have been normalized with dry cell weight from Figure 4-18 in the culture setup at the same time in the conversion measurement. The error bars represent the standard deviations of three replicates.

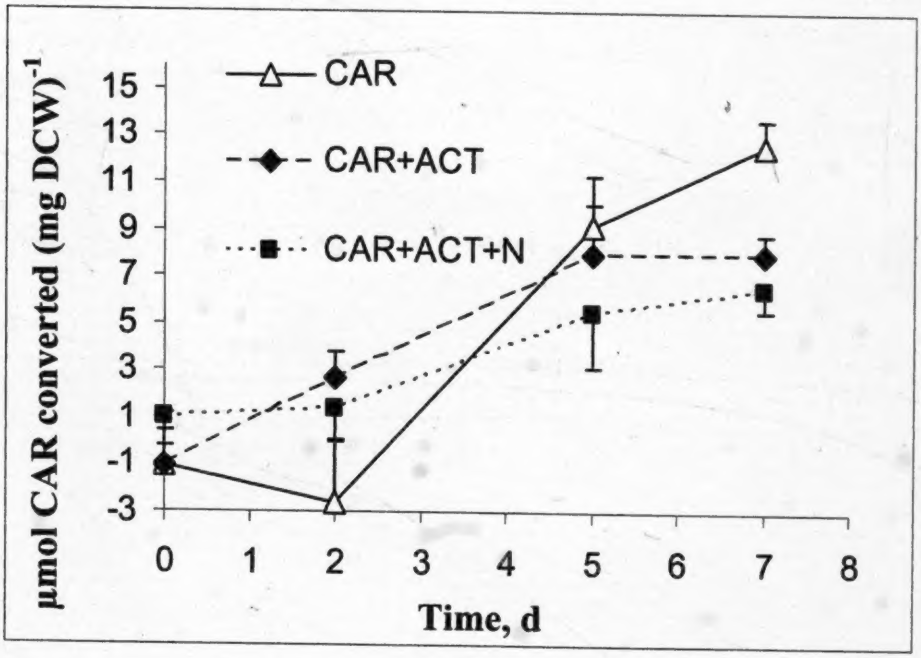

When the supplemented conditions are compared to each other, it was found that there was no significant difference between carbazole conversions at day 5. At day 7, the conversion in the acetate culture was higher ($p=0.037$). This result suggests that the free nitrogen does indeed cause some inhibition of carbazole conversion but not until day 7.

When examining carbazole conversion values, the change in pH of each medium must be considered. Despite the use of highly buffered medium, the cultures with supplemental carbon and nitrogen both experienced increases in pH over the course of the experiment. As illustrated in Figure 4-20, the carbon and nitrogen supplemented cultures experienced a pH increase from 7 to 8. The pH in the acetate cultures showed a pH increase from 7 to 7.6. Because the medium contained no acetate, the carbazole only cultures did not experience the same pH changes.

The rates of carbazole conversion were calculated for each condition at each time interval, as shown in Table 4-6. When the rates are examined as the averages between two time points, it is apparent that the rates in the cultures with only carbazole are significantly higher than those shown in the other two conditions. The interval between 0 and 2 d shows a negative conversion that is the result of an overestimation of the remaining carbazole concentration coupled with a very small amount of biomass at the 2-d time point. This same error affected the rate calculated in the next time interval as the slope of the line coming from the negative value was exaggerated giving a higher rate of conversion.

The acetate condition started with a high conversion rate of 3.8 μmol (mg DCW-d)$^{-1}$ that leveled off to 0.7 μmol (mg DCW-d)$^{-1}$ as time progresses.

The overall mean rate of conversion was calculated using the weighted averages of the rate over each interval. As can be seen in Table 4-6, the weighted mean rates all fall within the error bars of each data set and they are not statistically different from each other. Consequently, the conversion rates of carbazole, as μmol (mg DCW-d)$^{-1}$, were not significantly affected by the addition of soluble carbon or nitrogen source.

Figure 4-20 Change of culture pH during growth of CP19 under test conditions. [5]

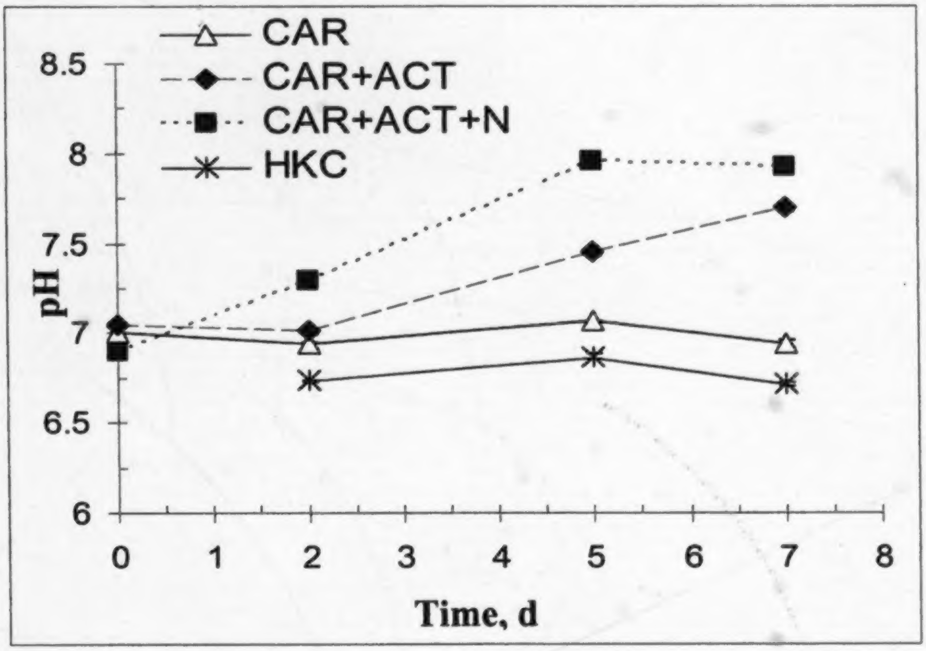

---

[5] Error bars representing the standard deviation of the measurement, are comparable to the size of the markers.

Table 4-6 Mean rate of carbazole removal from testing conditions. All values are the average of three replicates, corrected for the results of the heat-killed controls.

	Carbon and Nitrogen Sources					
	CAR		**CAR+ACT**		**CAR+ACT+N**	
	μmol carbazole (mg DCW)$^{-1}$ (d)$^{-1}$					
Time (days)	Average	Error	Average	Error	Average	Error
T=0-2	-2.7	-3.4	3.8	0.6	2.1	0.8
T=2-5	10.7	5.6	1.3	0.4	0.4	0.3
T=5-7	4.5	2.5	0.7	0.6	1.2	0.6
Mean Rate	**5.1**	7.0	**1.8**	0.9	**1.1**	1.0

4.4.2 Relationship of acetate consumption to carbazole transformation.

The time courses of both carbazole conversion and acetate consumption are given in Figure 4-21. In the nitrogen supplemented culture, the rate of carbazole conversion is very slow between day 2 and day 5 where the curve is essentially flat. The amount of acetate removed from the culture approaches and reaches 100 % in this time period. Increased carbazole conversion is seen in the next time period likely as a result of carbazole being used to meet carbon requirements.

In the acetate supplemented medium shown in Figure 4-21 , the consumption of acetate was much slower than when the nitrogen supplement was also added. However, despite the trends of acetate consumption, the overall conversion of carbazole was not statistically different; thus, nitrogen regulation was not evident. In the acetate supplemented medium, the consumption of acetate significantly increased between 5 and 7 d. Over that same time interval, the rate of carbazole conversion decreased from 1.3 ± 0.4 μmol carbazole (mg DCW-d)$^{-1}$ (between 2 and 5 days) to 0.7 ± 0.6 μmol carbazole (mg DCW-d)$^{-1}$. This suggests that carbazole degradation enzymes may be weakly carbon regulated after a significant percentage of the carbazole is removed.

Figure 4-21 Time course of acetate and carbazole transformation by strain CP19. Open symbols represent the transformation of acetate and the solid symbols represent the transformation of carbazole.

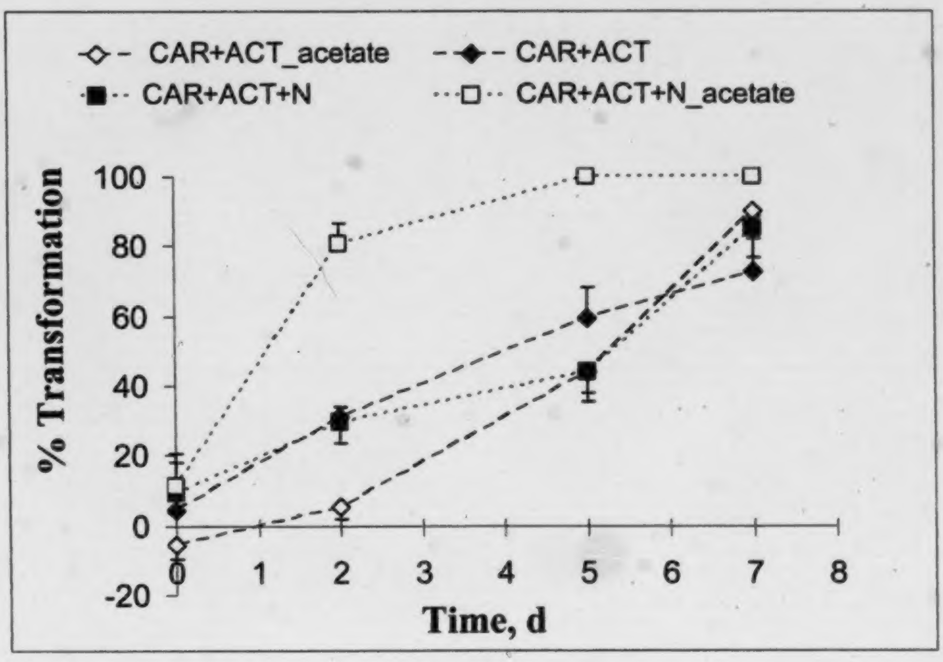

4.4.3 Elemental composition of biomass

An analysis of the elemental composition of CP19 biomass was completed at the end of 7 days incubation. This analysis was completed in order to allow balances on the carbon from the substrates. Figure 4-22 shows that the composition of the cell stayed relatively constant at all the conditions. The biomass yield resulting from the consumption of carbazole was calculated for the conditions in which carbazole was the sole carbon and nitrogen source and in the case when it was the sole nitrogen source. Strain CP19 grown on carbazole as sole nitrogen and carbon source gave biomass yields of 0.51 ± 0.1 μmol of N in biomass (μmol of CAR converted)$^{-1}$ and 2.23 ± 1.52 μmol of C in biomass (μmol of CAR converted)$^{-1}$. Strain CP19 grown on carbazole as sole nitrogen source with acetate as a soluble carbon source gave biomass yields of 0.417 ± 0.083 μmol of N in biomass (μmol of CAR converted)$^{-1}$. These coefficients indicate that the amount of nitrogen removed from carbazole that accumulated in the biomass is essentially constant regardless of additions of soluble carbon.

Figure 4-22 Elemental carbon and nitrogen concentrations in dry CP19 cells. Each bar represents the average value of three replicates and the error bars are the corresponding standard deviation.

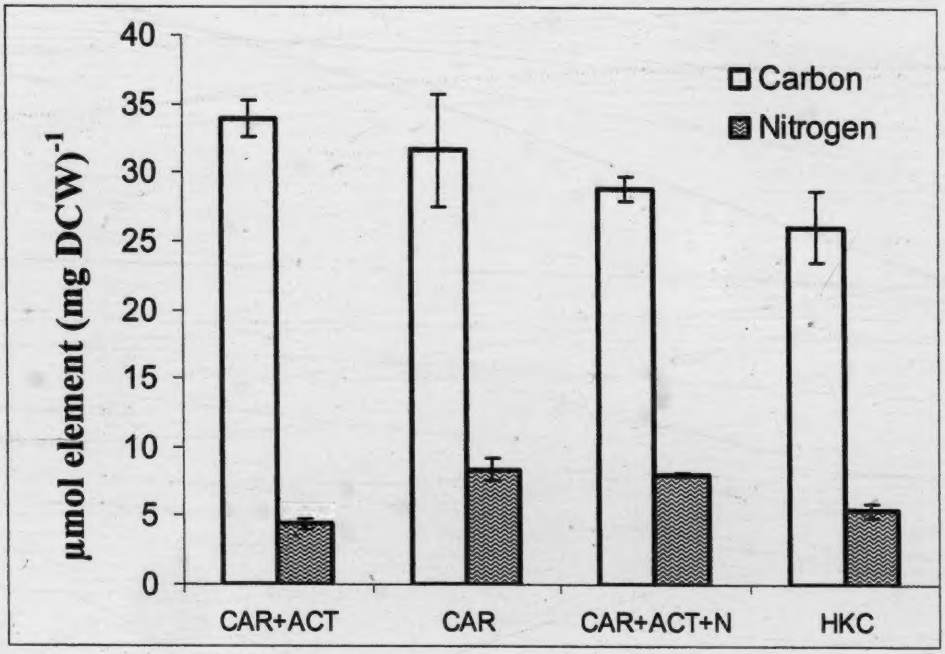

4.4.4 Aqueous concentration of carbazole in live cultures.

Figure 4-16 showed that the concentration of carbazole in the aqueous phase was approximately 6 times greater in sterilized filtrate from CP19 cells grown on carbazole than in sterile water or medium with carbazole. This implies that the cells increase the amount of carbazole available to them in the aqueous phase by producing a cellular material; however, despite this increased aqueous solubility, the growth patterns of CP19 in the initial screening process did indicate that growth was limited by mass transfer (Figure 4-6 and Figure 4-7). To clarify this characteristic, the aqueous concentration of carbazole in the presence of live cells was measured at the end of each time interval.

Figure 4-23 shows aqueous carbazole concentrations in the live cultures and in heat-killed controls. There was essentially no carbazole remaining in the aqueous phase in the presence of live cells. This provides further evidence to support the conclusion that growth of CP19 is limited by the availability of carbazole in the aqueous phase. Despite the fact that cells increased the aqueous solubility of carbazole over that in sterile water (Figure 4-16) the increased availability does not exceed the amount that the cells are able to consume. If the amount available in the aqueous phase was to exceed the amount the cells were able to consume than there would be a significant amount of carbazole remaining in the filtrate where the maximum concentration would be equivalent to that found in sterile culture supernatant (Figure 4-16).

The aqueous carbazole concentrations have been reported as 5.43, 6.17 and 10 μmol L^{-1} by Pearlman *et al.* (1984). These concentrations are equivalent to a of 0.9-1.6 μg mL^{-1}. At a value of approximately 5 μg mL^{-1}(Figure 4-23), the aqueous concentration of carbazole determined in the heat- killed control was higher than those reported in literature but it was within the same magnitude. This small increase can be linked to the solubilization mechanisms seen in Figure 4-16. The heat-killed controls were inoculated with cells which would contain a portion of the cellular material responsible for the increased aqueous concentrations of carbazole seen with sterile filtrate.

Figure 4-23 Aqueous concentration of carbazole in the presence of *Sphingomonas* sp. CP19. Average value of the concentrations found at four different time points over total incubation time of 7 d. The error bars are bound by 95% confidence interval.

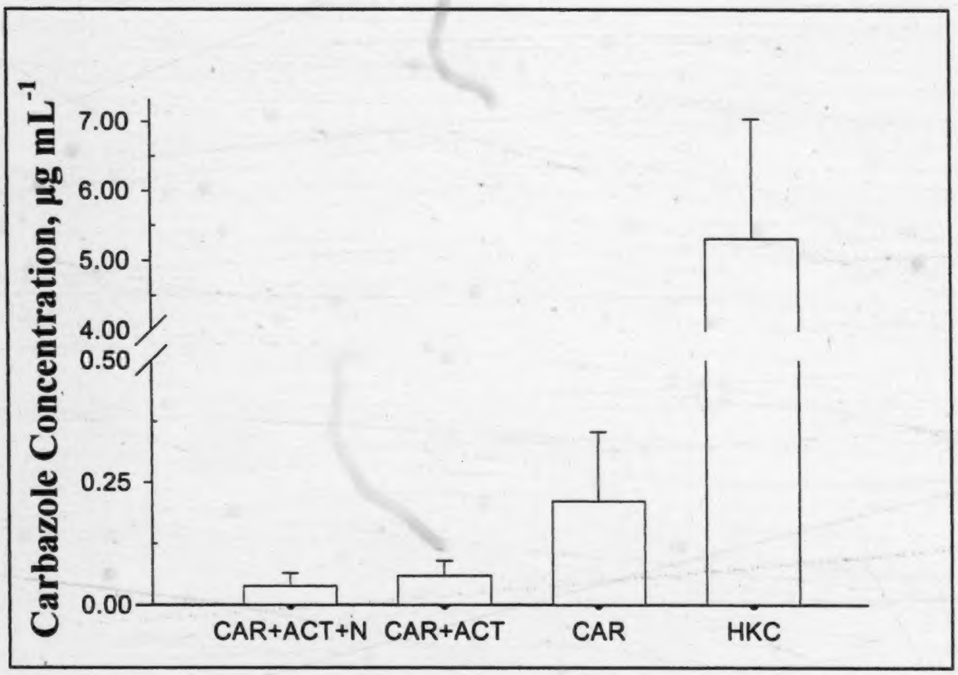

4.5 Regulation by acetate of carbazole mineralization

The experiment of section 4.4 looked at the ability of additional carbon or nitrogen to inhibit the carbazole loss; however, it did not give any information on the regulation of mineralization of carbazole carbon. Carbazole loss is strictly a measurement of the amount of carbazole that has been transformed into a different compound and is no longer in its initial state. Carbon mineralization occurs in the final steps of the degradation pathway where the substrate carbon is oxidized to carbon dioxide. Radiolabelled carbazole, in the presence and in the absence of additional carbon, was used to measure mineralization. The flasks containing acetate had 4.27 times more carbon than did those without acetate.

Cultures were prepared in two groups: one supplemented with radiolabelled carbazole and one without the radiolabel. The unlabelled group served to quantify the amount of biomass formation and the amount of unconverted carbazole remaining. Table 4-7 summarizes information collected from each fraction of the labelled cultures. Heat-killed controls were completed with the most complex medium of the two conditions: mineral salts medium containing acetate and carbazole.

Table 4-7 Composition of each fraction after liquid-liquid extraction of radiolabelled carbazole in CP19 liquid cultures. Extraction was accomplished with DCM.

Fraction	Compounds
Neutral Extract	Unconverted carbazole + Non-polar metabolites.
CO_2	Mineralized carbazole carbon.
Supernatant	Very polar carbazole metabolites in various stages of degradation.
Pellet	Carbazole carbon taken into the cell and used for various cell functions, i.e. carbon needed for cell growth.

Figure 4-24 shows the release of $^{14}CO_2$. The carbon supplemented culture steadily released $^{14}CO_2$ after an initial lag period of approximately 24 h. The carbazole only culture experienced a longer lag period of approximately 60 h before $^{14}CO_2$ was released. Despite the different lag periods, within the duration of incubation, each culture released a similar amount of $^{14}CO_2$, approximately 50 % of the total added.

Figure 4-25 illustrates the location of ^{14}C in each fraction extracted from the culture, after the data was normalized to 100 % recovery. The recovery of ^{14}C in each fraction was adjusted to reflect the percentage of recovered label as opposed to the percentage of the total radiolabel that was added. Overall, ^{14}C recoveries ranged from 91-113 %, with less than 100 % recovery in the active cultures and greater than 100 % recovery in the heat-killed controls. On average, ^{14}C recovery in active cultures was 7 ± 2 % less than 100 % recovery and ^{14}C recovery in heat-killed controls was 5 ± 11 % greater than 100 %.

The group of cultures grown in parallel without radiolabel did not show consistent behaviour. The data collected for the carbazole only growing conditions showed an outlier in replicate 3. As shown in Table 4-8, at a value of 24 % the standard deviation of the unconverted carbazole is quite high compared to the standard deviations in the other two conditions (both <4%). Plating of a culture sample on half-strength PCA plates was done at the end of the experiment and confirmed that the cells in both replicate 1 and 2 of this series were not viable. Consequently measurements of this growing condition were based solely on the values of replicate 3.

Figure 4-24 Time course of $^{14}CO_2$ released by CP19 from radiolabelled carbazole. This figure represents two conditions: carbazole supplied as sole nitrogen and carbon source and carbazole supplied as a nitrogen source. Each marker represents the mean of three replicates and the error bar is the corresponding standard deviation.

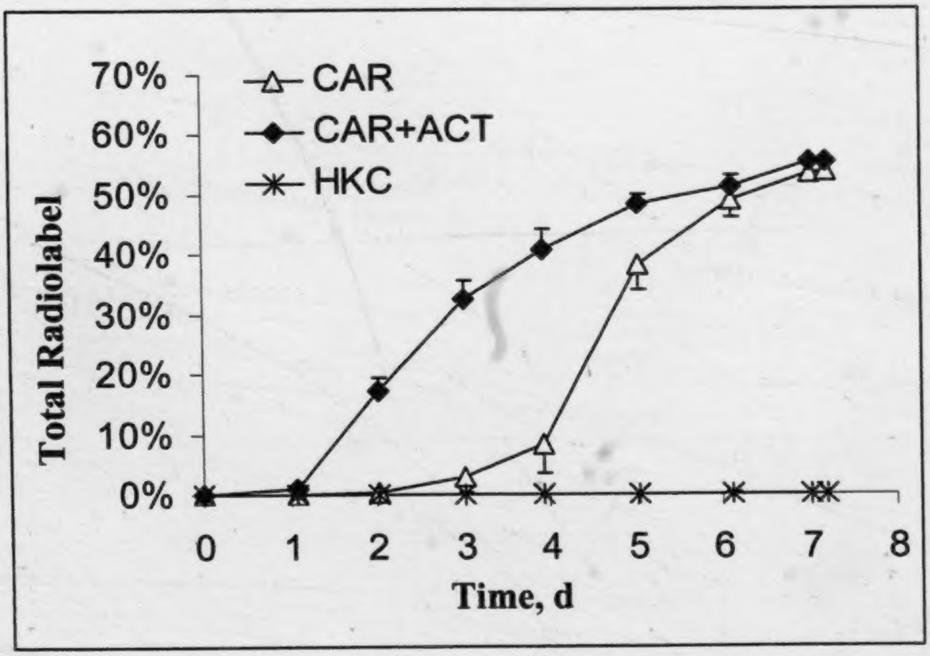

Figure 4-25 Distribution of radiolabel from CP19 cultures grown under two growth conditions. Data presented are the average of three replicates after they have been normalized to 100 % recovery. All standard deviations were less than 3 %.

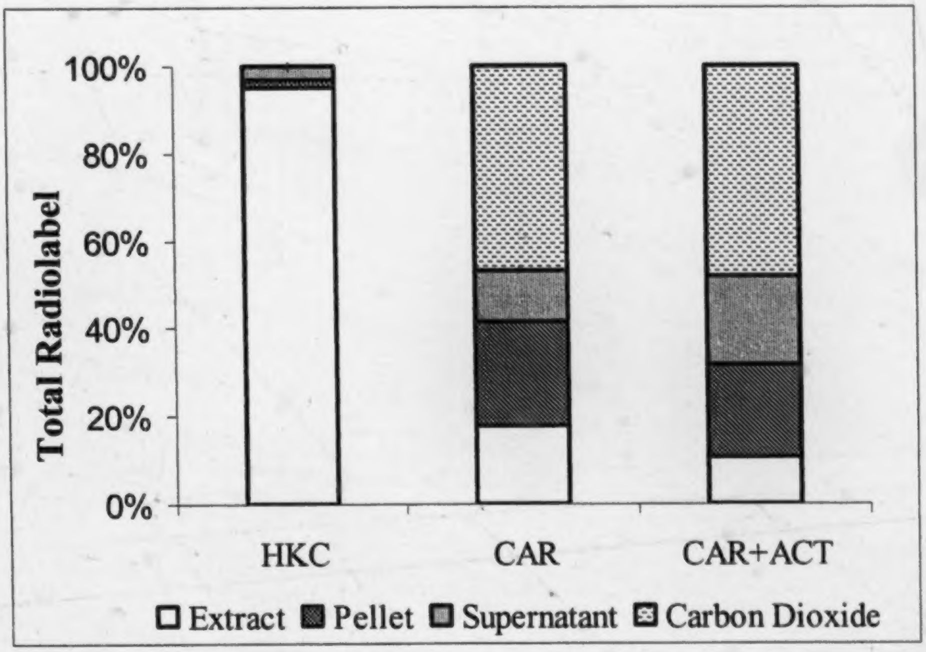

Table 4-8 Summary of measurements taken in the flasks containing un-radiolabelled carbazole that were incubated in parallel to those containing radiolabelled carbazole. Plating of cultures at the completion of the experiment showed that cells from replicate 1 and 2 in the carbazole medium were not living at the end of the 7-d incubation period.

Total Biomass (mg)					
	Average	Std Dev	Replicate 1	Replicate 2	Replicate 3
HKC	1.43	0.15	1.3	1.6	1.4
CAR+ACT	9.6	1.1	8.5	10.6	9.8
CAR	1.3	0.9	0.7	0.9	2.3
Unconverted Carbazole					
HKC	98.8%	3.4%	95.2%	101.8%	99.2%
CAR+ACT	6.7 %	3.8%	2.7%	7.4%	10.2%
CAR	86.0%	24.4%	98.3%	101.8%	57.9%

Examination of the CO_2 fraction from each test condition showed that, despite the difference in the total supplies of carbon, live cultures of CP19 produced essentially the same amount of $^{14}CO_2$. Given $^{14}CO_2$ releases of 48.0 ± 1.1 % from the carbazole plus acetate culture and 46.7 ± 2.0 % from the carbazole only culture, it was evident that the same amount of carbazole carbon mineralization occurred regardless of the presence of an additional soluble carbon source. As expected, the heat-killed controls showed essentially no release of $^{14}CO_2$.

The extractable compounds in the carbazole cultures made up 17.9 ± 2.4% of the total radiolabel, in comparison to 10.8 ± 2.2 % in the carbazole and acetate cultures. This trend was consistent with a higher carbazole conversion in the culture with acetate, as observed in Table 4-8.

The amount of radiolabel collected in the cell pellet represented the fraction of the total carbazole carbon incorporated into macromolecules. At $p= 0.05$, the fraction of the total radiolabel used by the cell was statistically greater in the carbazole cultures than in the carbazole plus acetate cultures. With average values of 23.5 ± 1.3 % and 20.8 ± 1.2 % respectively, 2.8 ± 1.8 % more of the total radiolabel accumulated in the biomass of the carbazole cultures than in the carbazole plus acetate cultures. This difference is marginal as there is no statistical difference at a significance level of $p= 0.025$. Radiolabel was also present in the biomass fraction of heat-killed controls. This value may represent the equilibrium amount of carbazole present by passive diffusion through the cell wall.

Combining the values of ^{14}C accumulated in the pellet and $^{14}CO_2$ gave an indication of the ratios in which the cell uses the carbazole carbon. A ratio of $^{14}C_{biomass}/^{14}C_{CO2}$ gave values of 0.35 ± 0.03 and 0.39 ± 0.05 in the supplemented and non-supplemented conditions, respectively. A non-pooled t-test at 95 % confidence indicates that these two numbers are not statistically different. The marginal difference seen between each condition in the incorporation of the radiolabel into biomass was minimized when $^{14}CO_2$ release was included in the comparison. Overall, the extra carbon source did not influence the cells' tendency to incorporate the carbazole carbon.

The aqueous supernatant contained polar metabolites that were not extracted by the neutral extraction. As can be seen in Table 4-9, the carbazole plus acetate cultures accumulated more of these types of compounds than did the carbazole only cultures. In fact the acetate cultures accumulated just less than twice the amount of water soluble carbazole metabolites.

Table 4-9 Summary of normalized data collected by extracting and counting the amount of radiolabel in each fraction.

	% Recovery of Radiolabel		
Fraction	*HKC*	*CAR + ACT*	*CAR*
Extract	95.0 ± 0.7	10.8 ± 2.2	17.9 ± 2.4
CO_2	0.06 ± 0.02	48.0 ± 1.1	46.7 ± 2.0
Supernatant	3.2 ± 0.9	20.5 ± 0.3	11.9 ± 0.8
Pellet	1.8 ± 0.7	20.8 ± 1.2	23.5 ± 1.3

4.6 Selectivity of strain CP19 for carbazole relative to other PACs.

An important characteristic of a suitable biocatalyst is the ability to selectively consume the target substrate without affecting any of the surrounding compounds. The selectivity of CP19 was evaluated starting with three and four ring compounds, including the oxygen, sulphur and carbon analogues of carbazole.

To minimize the effects of possible substrate or metabolite toxicity on bacterial growth, the cultures were grown with a concentrated cell inoculum for a short time period. The short time period minimized the amount of bacterial growth that could accumulate and it minimized the amount of contact time between the cells and any potentially toxic substances. Substrate solubility and mass transfer differences were not controlled in this experimental design; therefore, the bacterium can only be deemed "selective" if it shows significant carbazole conversion and minimal conversion of other PACs.

Cultures containing a mixture of fluorene, DBT, pyrene, fluoranthene, dibenzofuran and carbazole were prepared as outlined in section 3.2.2. Shake flasks containing only carbazole were used as positive controls. Heat-killed control cultures containing the substrate mixture were used to quantify abiotic substrate losses. These cultures were inoculated with washed cell suspensions grown on TSB and harvested in the mid-exponential phase. The initial OD_{600} of each flask was 5. The cultures were incubated for 50 h at which time they were acidified and extracted with ethyl acetate. An internal standard of thianthrene was used for quantification using GC-FID.

Figure 4-26 illustrates the results of substrate conversion in both sets of cultures. In the carbazole only condition, the growth conditions and incubation time allowed for extensive conversion of carbazole at 102 ± 9.7 %. This value has been corrected using the results of the heat-killed control. Much less carbazole was converted in the mixed conditions, with a conversion of 20.8 ± 1.3 %.

In the presence of carbazole, there was significant transformation of the other PACs. The sulphur and oxygen analogues of carbazole, benzothiophene and dibenzofuran, showed 5.4 % and 8.7 % transformation, respectively. The four ring compound fluoranthene showed 8.3 % transformation. There was little transformation of fluorene and essentially no transformation of pyrene. The low level of pyrene conversion, relative to carbazole, was consistent with its lower aqueous solubility. As seen in Table 4-10, the solubility of fluorene is close to that of carbazole, so it is possible that the low fluorene conversion is a result of selectivity for the other substrates or the need for alternate enzymes for degradation.

Figure 4-26 Removal of PACs by strain CP19. A high cell inoculum was used with an incubation time of 50 h. Each marker represents the average of three replicates and the error bars are the corresponding standard deviations.

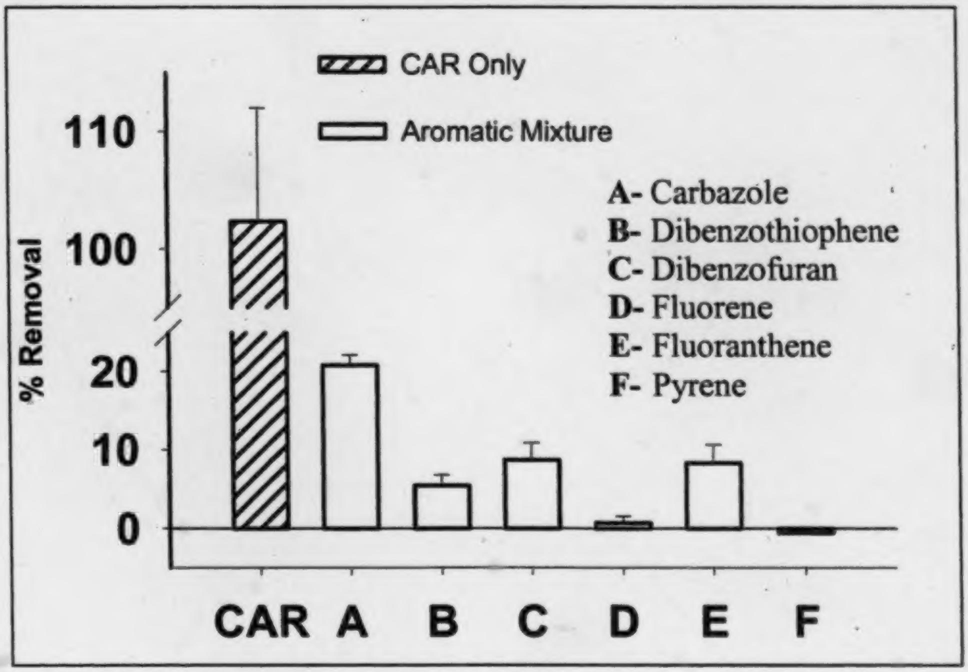

Table 4-10 Aqueous solubilities of polycyclic aromatic compounds used in selectivity experiment. [6]

Compound	Aqueous Solubility (mg L^{-1})
Dibenzofuran	3.112-10.025
Fluorene	1.687-1.978
Carbazole	0.907-1.670
DBT	0.531-1.472
Fluoranthene	0.129-0.165
Pyrene	0.122-0.273

---

[6] Aqueous solubilities from Pearlman *et al* 1984.

4.7 Formation of carbazole metabolites by CP19[7]

Incubation of CP19 with carbazole as sole nitrogen source produced four metabolites. These were extracted using ethyl acetate and identified by GC-MS. The first product (A) (Figure 4-27) was found in the neutral extract from CP19. High resolution, GC-MS analysis gave a molecular formula of $C_{12}H_8N_2O_2$ (M^+= 212.06). The compound was found at a retention time of 29.3 min The spectrum from GC-MS showed m/z 212 (47.36 %, M^+), 185 (36.8 %, M-HCN) and 84 (100 %) which matches that the spectrum given in literature for 2-amino-3H-phenoxazin-3-one (Bolognese and Scherillo, 1985).

The structure of this product suggests that it is a condensation product of biological products, where the biological products resulted from carbazole metabolism. To prove this point, 2- aminophenol was added to sterile culture medium and allowed to stand for 72 h. The product was extracted at neutral pH and analyzed using GC-MS. The resulting extract contained no 2-aminophenol and the product gave the same mass spectrum as metabolite (A): m/z 212 (100 %, M^+), 185 (71.6 %, M-HCN). Thus it was confirmed that 2-amino-3H-phenoxazin-3-one is an abiotic condensation product of 2-aminophenol.

Three other metabolites were extracted from the aqueous fraction from the first neutral extraction. The concentrations of these compounds were quite low consequently the extracts were concentrated significantly in order to produce GC-MS peaks large enough to be identified. These products were tentatively identified by comparing their mass spectra with those reported in literature (Gieg *et al.*, 1996). The products and their corresponding mass spectra are outlined in Table 4-11.

---

[7] All the information outlined in this section is the result of work completed by Dr. D.C. Bressler.

Table 4-11 Mass spectrum of CP19 metabolites

Compound	Major Peaks
A. 2-Amino-3H-phenoxazin-3-one	m/z 212 (47.36 %, M^+), 185 (36.8 %, M-HCN), 84 (100 %)
B. Indole-3-acetic acid	m/z 189 (15.7%, M^+), 130 (100%)
C. 2-(2,3-Dihydro-4-oxo-1H-quinoline-2-yl) acetic acid methyl ester	m/z 219 (12.9%, M^+), 146 (100%).
D. 3a,4-Dihydro-2-methoxy-pyrrolo[1,2-*a*]quinoline-1,5-dione	m/z 229 (68.4%, M^+), 186 (31.6%), 158 (100%), 130 (68.4%), 120 (31.5%), 90 (57.9%).

Figure 4-27 Structures of identified carbazole metabolites produced by strain CP19

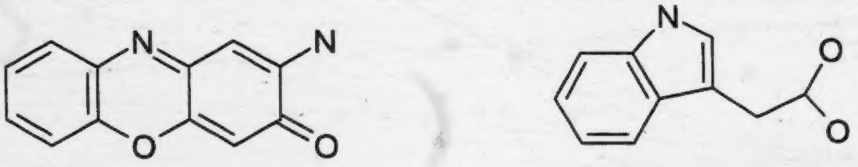
A. 2-Amino-3H-phenoxazin-3-one

B. Indole-3-acetic acid

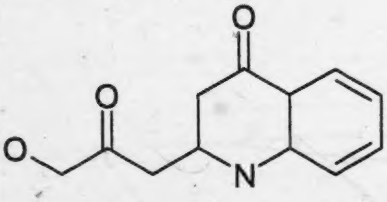
C. 2-(2,3-Dihydro-4-oxo-1H-quinoline-2-yl) acetic acid

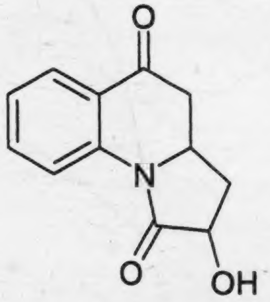
D. 6-(2-Aminophenyl)-2-hydroxy-6-oxohexa-2,4-dienoic acid

5.0 DISCUSSION

5.1 Isolation of bacteria growing on carbazole as a nitrogen source

Evidence resulting from hydrotreatment work completed by Bressler and Gray (2002) suggests that biochemical conversion of carbazole must give complete denitrogenation of the structure in order to be a suitable pretreatment to conventional hydrotreating processing. The objective of facilitating oil processing also necessitates minimal degradation to the carbon skeleton. Together, these two considerations resulted in stringent criteria for selection of a suitable carbazole isolate.

This specific activity was not identified in any of the carbazole degraders described previously (Fedorak and Westlake 1984; Finnerty *et al.*, 1983; Gieg *et al.*, 1996; Habe *et al.*, 2002; Kilbane *et al.*, 2002; Kirimura *et al.*, 1999; Kobayashi *et al.*, 1995; Nakagawa *et al.*, 2002; Ouchiyama *et al.*, 1993; Ouchiyama *et al.*, 1998; Schneider *et al.*, 2000; Shotbolt-Brown *et al.*, 1996) and therefore a search for new carbazole-targeted, biochemical pathways was started. Creosote-contaminated soil and selective enrichment conditions were used to isolate and screen for bacterial denitrogenation of carbazole with minimal degradation to the carbon backbone.

Despite the use of inoculum and screening conditions that would be most likely to isolate and identify this activity, the search for more useful carbazole transforming activity did not produce isolates that fit the characteristics of the ideal organism.

The contaminated site from which the soil inoculum originated was carefully selected based on the type of oil that had been spilt there, the length of time the site had rested in the contaminated state and the lack of soil remediation that had been performed. Creosote is a type of oil rich in carbazoles and carbazole analogs (Mueller *et al.*, 1989). This oil contains an abundance of the carbon-nitrogen bonds that are the target of the desired activity. The site had lain contaminated for several decades without any active soil remediation. Bacteria require various elements for growth and energy. In the nitrogen-limited environment of a hydrocarbon spill, the bacteria would likely be growth limited by the availability of nitrogen. Without the addition of any other nitrogen sources (like those found in fertilizers), the main source of available nitrogen would be that found in creosote, of which the majority is in the form of carbazoles. Bacterial survival and growth would depend on the existence of biochemical pathways able to use the carbazole nitrogen. The age of the contaminated site increased the likelihood that remediation by natural biological systems had started. This very specific inoculum, coupled with the selective pressures applied in enrichment conditions were the prime techniques for finding the unusual activity targeted in this research. Although the existence of such specific activity cannot be dismissed just because it was not detected with these methods, its probability is low based on the detailed approach that was taken here.

The data presented in Figure 4-5 and Figure 4-6 illustrate that the bacteria that grew on carbazole as a nitrogen source were also able to grow on it as a carbon and energy source. In other words, all the bacteria capable of breaking the target carbon-nitrogen bond also tended to use carbazole as a carbon and energy source. Figure 4-9 illustrate that the carbon was not only transformed into metabolites, potentially with intact carbon structures, but it was also mineralized to CO_2. Without knowing the actual degradation pathway, this type of ability to use the carbon ring structure resembles that illustrated in the carbon-destructive pathways of naphthalene degradation, a representative PAH, (Denome *et al.*, 1993; Eaton and Chapman, 1992), and dibenzothiophene degradation (Kodama *et al.*, 1973; van Afferden *et al.*, 1992). Considering the desired application for the biological activity, converting oil components into CO_2 is not attractive.

Figure 4-7 illustrated that the enzymes represented in the carbazole isolates did not show regulation of carbazole transformation by the nitrogen sources potassium nitrate or ammonium chloride. This lack of regulation suggested that the activity is not nitrogen specific. The bacteria used carbazole as a source of nutrients, not specifically as a nitrogen source as would be preferred for this application. In order to be a useful candidate, nitrogen specific activity is required of an isolate able to use the carbazole carbon. Nitrogen specific activity implies that the nitrogen atom is removed from the structure before degradation of the carbon backbone proceeds. A mutation to block degradation of the carbon backbone after the ring is opened, such as with *Pseudomonas fluoresens* LP6a (Foght *et al.,* 1997) could then be possible. The lack of nitrogen regulation suggested that the strains isolated in this study were similar to previously reported carbazole degraders, with nitrogen removed only late in the pathway.

One isolate exhibited the formation of a unique metabolite, bright yellow in colour. Isolate CP19 was selected for its unique metabolic characteristics and its production of this distinct, yellow metabolite. As observed by Foght *et al.* (1997) with *Pseudomonas fluoresens* LP6a, colour formation can be an indicator of metabolites. These metabolites, of strain CP19 were potentially more suitable for the targeted technology. This isolate also showed unique growth characteristics compared to the other isolates, as the magnitude of difference in the amount of growth due to the additional carbon source was much greater for CP19 than for the other isolates (Figure 4-6). The combination of these metabolic traits and the formation of an unique metabolite suggested that CP19 merited further characterization.

5.2 Conversion of carbazole by *Sphingomonas sp.* CP19

CP19 was identified by 16S rDNA analysis as a member of the genus *Sphingomonas.* Genus *Sphingomonas* is not unique to the group of carbazole degraders. Four other *Sphingomonas* sp. isolates have been reported with carbazole transforming activity including: *Sphingomonas* sp. KA1 (Habe *et al.*, 2002), *Sphingomonas* sp. GTIN11 (Kilbane *et al.*, 2002), *Sphingomonas sp.* CDH-7 (Kirimura *et al.*, 1999) and *Sphingomonas* sp. CB3 (Shepherd and Lloyd-Jones, 1998).

Like the other bacteria, *Sphingomonas* sp. CP19 was able to grow on carbazole as a sole nitrogen and carbon source. Despite the difference in biomass accumulation, neither carbon nor nitrogen regulation was obvious based on carbazole conversion. Higher conversions were achieved when additional soluble carbon and nitrogen sources were supplied; however, the mean specific activities were not statistically different between the different growing conditions. With carbazole as sole nitrogen source, CP19 gave a specific activity of carbazole conversion of 1.8 μmol CAR (mg DCW-min)$^{-1}$.

Compared to other carbazole isolates, CP19 showed slow activity. For example, the specific activity of *Sphingomonas* sp. GTIN11 (Kilbane *et al.*, 2002) was determined to be 8 μmol CAR (mg DCW- min)$^{-1}$, far exceeding that of CP19. In terms of overall conversion, CP19 transformed 77 % of 1.5 mmol L^{-1} carbazole within 7 days, when supplementary carbon and nitrogen sources were provided. With a supplementary carbon source, 65 % conversion was possible in the same time period. *Sphingomonas sp.* GTIN11 was also evaluated for its activity on carbazole as a sole nitrogen source; it was able to remove 82 % of 1.7 mmol L^{-1} carbazole in 8 h (Kilbane *et al.*, 2002).

A more consistent comparison of culture performance was that between CP19 and *Pseudomonas sp.* LD2 (Gieg *et al.*, 1996). The experimental conditions of the experiments on these two isolates were similar in that carbazole was dispensed in crystalline form at a concentration of 0.25 mg mL^{-1}. The culture volumes were also equivalent. As sole carbon and nitrogen source, 44 % of carbazole was converted by CP19 within 7 d whereas LD2 transformed 87 % of carbazole within 24 h and removed essentially 100 % within 3 d.

5.2.1 Reasons for slow growth

5.2.1.1 Induction

One possible explanation for this slow activity was the absence of an inducer in the inoculum preparation. A 2-d lag period occurred when CP19 was grown on carbazole as sole carbon and nitrogen source (see Figure 4-18). Even at a cell inoculum density 50 times higher than that used in the transformation experiment (Section 4.4), visible loss of carbazole crystals was not apparent until at least 24 h of incubation. These observations came from preliminary experiments designed to determine an appropriate incubation time for the selectivity experiment (Section 4.6) where minimal incubation time and maximum conversion were desired. At least 48 h was necessary to achieve substantial conversion.

Typically, enzymes involved in the catabolism of carbon and energy sources are inducible (Madigan *et al.* 1997) and the process of induction can be completed within a few h or minutes (Alexander, 1994). The 48-hour period before growth may be the induction period, where carbazole or a carbazole metabolite was required to start the process of synthesizing carbazole degradation enzymes. The dioxygenase of *Sphingomonas* sp. CB3 was induced with carbazole and biphenyl (Shepherd *et al.* 1998). Within the time of the first time point of 20 h, a lag period was not displayed by LD2 growing under similar conditions, but the mode of inoculum preparation was different. CP19 cultures were pre-grown on TSB and then exposed to carbazole, whereas LD2 was maintained on selective medium with carbazole as sole carbon and nitrogen source. The carbazole pre-growth could induce the enzymes responsible for carbazole degradation, making them fully active when they are exposed to new substrate, whereas growth on the nutrient rich medium of TSB would not likely provide induction.

Unlike the growth pattern of CP19 growing on carbazole as sole carbon and nitrogen source (Figure 4-18), growth on carbazole with supplementary carbon and nitrogen did not show a lag period within the first sampling point of 2 d. Because the first sample point did not occur until 2 d of exposure, the existence of a lag period can not be evaluated; however, comparison between the two growth conditions indicates that the lag period is longer without supplementary carbon and nitrogen. The cultures with supplementary carbon and nitrogen were able to form biomass much more quickly. By itself, carbazole presented a lean diet for the cells, thus growth was slow. A higher density of represents a higher concentration of enzymes (assuming that the cells have the same concentration of enzyme). Consequently, in the initial growth stages before the mass transfer effects of cells agglomerating with the carbazole were obvious, more carbazole transformation was possible. If the inducer was a product of carbazole degradation, then the higher initial transformation rate increased the production of the metabolites responsible for induction. On the contrary, without the additional nutrients, the only cells able to catalyse transformation were those supplied in the inoculum. This reaction potential was limited until more cells formed by carbazole consumption.

5.2.1.2 Solid substrate mass transfer limitations

One of the areas of interest when studying microbial activity on poorly soluble substrates is the effect of mass transfer and its relationship to bacterial growth. There are three main mechanisms involved in the transfer of these substrates from the environment to the cell surface where it then enters the cell: passive uptake of soluble substrate that has entered the aqueous phase through dissolution, production of surface active agents that increase solubility and direct uptake through contact with substrate surface.

The linear growth curve of *Sphingomonas* sp. CP19 on carbazole as sole nitrogen and carbon source was characteristic of mass transfer limited growth conditions (Volkering *et al.*, 1992). This trend, combined with the fact that the aqueous phase concentration of carbazole was essentially zero in live cultures, implied that the rate of carbazole dissolution was limiting carbazole uptake.

As outlined in equation (3-3), the rate of mass transfer would be directly related to the surface area of substrate, exposed to the medium. Increased surface area not only increases the rate of substrate dissolution, it also provides a greater area for cell attachment. A common method used to increase the surface area of a poorly soluble substrate is the use of a dispersion agent that facilitates dispensing the compound into the aqueous phase resulting in a suspension of fine particles.

In the case of *Sphingomonas* sp. CP19, a dispersion chemical was not used. Conversely the majority of studies involving carbazole did make use of dispersion agents including dimethyl sulfoxide (Kilbane *et al.*, 2002; Ouchiyama *et al.*, 1993 and 1998; Shotbolt-Brown *et al.*, 1996), *n*-hexadecane (Kirimura *et al.*, 1999) and acetone (Finnerty *et al.*, 1983). Significantly different results can be obtained using the same organism exposed to carbazole with and without the use of a dispersion agent. Both *Pseudomonas* spp. CA06 and CA10 showed 100 % removal of 5.7 mmol L^{-1} carbazole within 18 h; however, in the absence of dimethyl sulfoxide, growth was poor (Ouchiyama *et al.*, 1993). The contributions of dispersion agents to rate of carbazole degradation, via the exposed surface area, must be considered when comparing the performance of CP19 to other carbazole isolates.

Surfactants are often used to improve the degradation rates of solid, poorly soluble substrates. Volkering *et al.* (1995) used non-ionic surfactants to improve the biodegradation of naphthalene and phenanthrene by two *Pseudomonas* strains. An increase in degradation was seen in the dissolution-limited growth phase; however, because the aqueous concentration of the hydrocarbons was still essentially zero, the increased growth was attributed to the increased dissolution rate versus the increased solubility.

Live cells of *Sphingomonas sp.* CP19 were shown to increase the aqueous solubility of carbazole by over 6 times compared to that measured in medium alone (Figure 4-16). The production of biosurfactants is often found to be the reason behind biologically increased solubility levels. A known biosurfactant producer is the strain of *Pseudomonas aeruginosa* studied by Guerra-Santos (1984). Cell-free filtrate of this organism resulted in a surface tension value as low as 40 mN m^{-1}. When compared to the surface tension of distilled water, measured at 73 mN m^{-1}, this represented a 45 % reduction. Surface tension measurements of cell-free, CP19 filtrate gave values of approximately 60 mN m^{-1}. The magnitude of surface tension reduction was not sufficient to suggest that CP19 produces biosurfactant; however the increased solubility of substrate indicates the presence of some type of cellular material.

Further investigation into the surface properties of CP19 cells resulted in the identification of a capsule layer coating the cell exterior. This observation, combined with the surface tension measurements, suggests that the solubilization effects were a result of surface components, possibly similar to emulsan, the surface agent produced by *Acinetobacter caloaceticus* RAG-1(Rosenberg and Rosenberg, 1985). Emulsan is a material that sheds from cells in the stationary growth phase and has been tied to the hydrophobic characteristics of that culture.

The presence of capsule layer also provides insight into the tendency of CP19 to form clumps of cells when grown on carbazole. The clumping behaviour was the reason behind the various difficulties experienced when working with this organism. Such behaviour was not mentioned in the work involving the other carbazole degraders of the genus *Sphingomonas*. The same aggregation tendency was not evident when the cells were grown on complex medium (TSB), which suggests that hydrophobic characteristics are potentially repressed in the presence of extra nutrients. Such repression was shown with *Mycobacterium* sp. LB501T that formed a biofilm when grown on anthracene but not in the presence of glucose as an additional carbon source (Wick *et al.*, 2002).

The "clumping" growth behaviour also suggests that the mass transfer of carbazole could involve direct uptake mechanisms in conjunction with the two more traditional mechanisms previously discussed. There are various observations available on the influence of cell attachment on the uptake of poorly-soluble substrates. Cell agglomeration to the substrate surfaces does not imply direct uptake. This was shown by Mukherji and Weber (1998) who used a mathematical model based on the mass transfer coefficients of a system of naphthalene in a nonaqueous phase liquid exposed to both pure and mixed cultures. Despite the formation of a biofilm at the interface, the rate of naphthalene removal was never higher than that predicted by the model, indicating that the biofilm did not affect naphthalene uptake. As well, Efroymson and Alexander (1991) worked with an *Arthrobacter* sp. that showed strong evidence for direct uptake of the alkane hexadecane but not for the polycyclic aromatic hydrocarbon, naphthalene. Without having completed appropriate experiments, linking the aggregation tendencies of CP19 cells to direct uptake mechanisms of mass transfer is only speculative.

In addition to contributing to possible mechanisms for direct uptake of carbazole, the agglomeration tendencies of CP19 likely adversely affected the mass transfer of carbazole. Without a dispersant to counteract the affinity of CP19 for clumping with carbazole crystals, the total surface area of carbazole is effectively decreased. This reduction would slow the overall rate of carbazole dissolution thus reducing bioavailability.

Considering the contributions that induction and mass transfer conceivably have on the biodegradation of carbazole by CP19, it can be concluded that the actual metabolic capabilities of CP19 growing on carbazole have not been accurately evaluated by the experimental design represented in this work. It is quite possible that CP19 is able to convert carbazole more quickly; however, its properties of induction and an optimal method of carbazole distribution would have to be studied more closely.

5.2.1.3 Formation of condensation product

The main culture medium used in this study contained carbazole as sole nitrogen source with acetate as a soluble carbon source. As mentioned previously the conversion of carbazole by *Sphingomonas* sp. CP19 was very limited and slow compared to that of previously isolated carbazole degraders. In addition to the conversion limitations presented by induction and mass transfer, the formation of a highly cyclized condensation product containing the nitrogen atom potentially limits carbazole conversion. As outlined in section 4.7 and discussed in more detail in section 5.3, the conversion of carbazole by CP19 is characterized by the formation of 2-amino-3H-phenoxazin-3-one which is the abiotic condensation product of 2-aminophenol. This product contains three, six-membered rings where one nitrogen atom remains within the ring structure and another is a free amino group attached to the ring. Accumulation of carbazole carbon and nitrogen in the form of this complex metabolite likely contributes to the low conversion of carbazole characterized by CP19.

5.2.2 Regulation of carbazole degradation

As previously mentioned, none of the carbazole-degrading isolates showed evidence for carbon regulation of carbazole conversion. In fact, similar conversions were measured regardless of the available carbon sources (Figure 4-7), even though very different amounts of biomass were measured. A proper evaluation of cell activity in each condition required both biomass and conversion measurements to be used in combination and then compared.

Regulation was evaluated using normalized conversion, i.e. conversion per unit biomass. When this measurement is broken into its two components, absolute conversion and biomass accumulation, it was obvious that the contribution of biomass in the non-supplemented condition was the basis of perceived regulation. Regulation of carbazole conversion was not apparent until the seventh day of incubation. There were no statistical differences in the data points preceding the last set. At the end of 7 d, the actual magnitude of carbazole conversion in the carbazole only condition was only 5/8 of that of the nitrogen supplemented condition and ¾ of that of the acetate supplemented conditions. The proportions of biomass accumulation in the carbazole only condition were even less. The amount of biomass accumulated in the carbazole only condition was a mere 1/8 of that accumulated in the nitrogen supplemented conditions and ¼ of that accumulated in the acetate supplemented conditions. Because the biomass yield was so low, when it was used to normalize conversion, a high value was obtained. The fact that this carbon regulation is only apparent at one time point suggests that a measurement may be inconsistent. The measurements of biomass appear to be the cause of the apparent regulation so biomass is likely to be the inconsistent measurement.

The apparent carbon regulation found with the data from the transformation experiment, was not consistent with the conclusions from the radiolabeled experiment. At values of 47 ± 1 % and 48 ± 1 % the degree of mineralization of the carbon backbone remained consistent regardless of the carbon source(s).

The conclusions regarding carbon regulation are conflicting between data points of the transformation experiment and also conflicting between the two separate experiments. These inconsistencies appear to be related to the measurements of biomass in the transformation experiment. The following section investigates how well the measured values of biomass correlated to predicted values calculated based on the combination of all the other measured properties.

5.2.2.1 Reconciliation of dry cell weight measurement

In an attempt to reconcile the inconsistent results of regulation, the consistency of the unusually low biomass yields obtained with carbazole as sole nitrogen and carbon source was investigated. Biomass was chosen as the parameter to reconcile because it was the measurement containing the most uncertainty, due to the physical characteristics of both the bacterium and the substrate. Carbazole conversion measurements, from Figure 4-17, the corresponding biomass measurements summarized in Figure 4-18 and the results from elemental analysis (Figure 4-22) of the accumulated biomass were combined to determine mean yield coefficients.

The reconciliation procedure used several of assumptions. The formation of intermediate products was assumed to be minimal, so that any consumed carbon formed carbon dioxide and biomass. This assumption can be justified based on the difficulty of actually finding carbazole metabolites from CP19 and the very low concentrations of those that were identified. Second, biomass composition was determined from data collected at the final time point. Cellular composition was assumed to remain constant over time, regardless of growth stage. The fraction of carbazole carbon that contributed to biomass was assumed to remain constant, regardless of the addition of a soluble carbon source. This assumption was validated in section 4.5, where the mineralization data showed that the ratio of ${}^{14}C_{biomass}/{}^{14}C_{CO2}$ remained constant regardless of the presence of acetate carbon. Using these assumptions, yield coefficients were calculated for the set of data collected at each time point. Any outliers from the resulting data set were excluded from the final, overall, mean yield coefficients: consequently any gross inconsistencies within the data would be eliminated from the dry weight predictions. An outlier was defined as any data point that was order of magnitudes different from the same trend of the majority of data. One outlier was omitted from the calculation of yield coefficient of CO_2 from acetate carbon.

On a mass basis, the yield coefficients of carbazole utilization were defined as:

$$Y_{X/CAR} = \frac{X_{CAR}}{\Delta CAR} * \frac{1}{MW_{CAR}} \tag{5-1}$$

$$Y_{CO2/CAR} = \frac{b_{CAR}}{\Delta CAR} * \frac{MW_{CO_2}}{MW_{CAR}} \tag{5-2}$$

Where X_{CAR} represents the mass of biomass from carbazole-carbon; ΔCAR is the moles of carbazole consumed and b_{CAR} is the moles of CO_2 that formed from carbazole-carbon.

Similarly, the yield coefficients of acetate utilization were calculated using the following equations:

$$Y_{x/ACT} = \frac{X_{ACT}}{\Delta ACT} * \frac{1}{MW_{ACT}} \tag{5-3}$$

$$Y_{CO2/ACT} = \frac{b_{ACT}}{\Delta ACT} * \frac{MW_{CO_2}}{MW_{CAR}} \tag{5-4}$$

Where X_{ACT} is the mass of biomass from acetate-carbon; ΔACT is the moles of acetate consumed and b_{CAR} is the moles of CO_2 that formed from carbazole-carbon.

A mole balance on the carbazole carbon gives:

$$\Delta CAR * \frac{12 \mu moles C}{\mu mol CAR} = f_{CAR} * X_{CAR} + b_{CAR} \tag{5-5}$$

$$f_{CAR} = \frac{C_{CAR}}{X_{CAR}} \tag{5-6}$$

Where C_{CAR} is the moles of carbazole-carbon that accumulate in biomass and ΔCAR is the moles of carbazole consumed.

The fraction of carbazole mineralized is defined as:

$$R_{CAR} = \frac{b_{CAR}}{f_{CAR} X_{CAR}} \tag{5-7}$$

A mass balance on the biomass accumulation where two substrates, acetate and carbazole, are supplied as carbon sources, gives:

$$X_{TOTAL} = X_{ACT} - X_{CAR} \tag{5-8}$$

Re-arranging Equation (5-1) to solve for X_{CAR} and substituting the resulting equation into Equation (5-8) gives:

$$X_{ACT} = X_{TOTAL} - X_{CAR} = X_{TOTAL} - Y_{X/CAR} * \Delta CAR * MW_{CAR} \tag{5-9}$$

A mole balance on acetate carbon gives:

$$\Delta ACT * \frac{2\mu molC}{\mu mol\ acetate} = f_{ACT} * X_{ACT} + b_{ACT} \tag{5-10}$$

Where f_{ACT} is defined as:

$$f_{CAR} = \frac{C_{ACT}}{X_{ACT}} = \frac{C_{TOTAL} - C_{CAR}}{X_{ACT}} \tag{5-11}$$

Where total moles of carbon in biomass is represented with C_{TOTAL} and moles of carbon in biomass due to acetate carbon is C_{ACT}.

The fraction of acetate mineralized is defined as:

$$R_{ACT} = \frac{b_{ACT}}{f_{ACT} X_{ACT}} \tag{5-12}$$

Biomass accumulation, based on substrate conversion is defined with the following equation:

$$X_{Total} = \left(Y_{x/CAR} * \Delta CAR * MW_{CAR}\right) + \left(Y_{X/ACT} * \Delta ACT * MW_{ACT}\right) \tag{5-13}$$

With carbazole as sole substrate, the following data were collected after 7 d of incubation: C_{CAR}, $X_{TOTAL}=X_{CAR}$, and ΔCAR. With this information $Y_{X/CAR}$ was calculated using equation 5-1. Equation 5-5 was then rearranged to solve for b_{CAR} and substituted into equation 5-2 to solve for $Y_{CO2/CAR}$. The fraction of carbazole-carbon mineralized, R_{CAR}, was then determined using equation 5-7.

The acetate yield coefficients were calculated using the carbazole yield coefficients along with the measurements of X_{TOTAL}, ΔACT, ΔCAR and C_{TOTAL} (total moles of carbon in biomass) obtained from the condition where both carbazole and acetate were substrates.

With Equation 5-9, X_{ACT} was determined: $Y_{X/ACT}$ was calculated with equation 5-3. Equation 5-10 was rearranged to solve for b_{ACT} where f_{ACT} was calculated with equation 5-11. The final yield coefficient, $Y_{CO2/ACT}$, was calculated with equation 5-4 and R_{ACT} was determined from equation 5-12.

Yield coefficients were calculated at each time point and overall, mean yield coefficients were found. The mean yield coefficients were then used with the loss data at each time point to calculate the predicted biomass accumulation with equation 5-13.

Using information from the transformation experiment (Section 4.4) the biomass yield coefficients ($Y_{X/CAR}$ and $Y_{X/ACT}$) were calculated to be 0.25 ± 0.19 mg biomass (mg carbazole converted)$^{-1}$ and 0.29 ± 0.22 mg biomass (mg acetate converted)$^{-1}$. These coefficients suggest that the consumption of carbazole and acetate produced the same amount of biomass on a mass basis. When the carbon content of each substrate was considered the coefficients are 0.29 ± 0.22 mg biomass (mg carbazole-carbon converted)$^{-1}$ and 0.68 mg biomass (mg acetate-carbon converted)$^{-1}$. From these values, it is evident that acetate carbon produced over twice the amount of biomass than did carbazole carbon. Acetate was clearly a more efficient substrate than carbazole for CP19.

The data from the transformation experiment (Section 4.4) was used to calculate carbon dioxide yield coefficients ($Y_{CO2/CAR}$ and $Y_{CO2/ACT}$). They were found to be 2.7 ± 0.3 carbon dioxide (mg carbazole converted)$^{-1}$ and 1.1 ± 0.1 mg carbon dioxide (mg acetate converted)$^{-1}$. Combining this data with that of biomass formation represents the fraction of substrate mineralization (R_{CAR} and R_{ACT}): 8.0 ± 0.6 μmol CO_2 (μmol carbazole-carbon to biomass)$^{-1}$ and 3.2 μmol CO_2 (μmol acetate-carbon to biomass)$^{-1}$.

The coefficients of biomass composition (f_{CAR} and f_{ACT}) were calculated to be 36.2 ± 0.3 μmol carbon (mg biomass_{CAR})$^{-1}$ and 36 ± 9 μmol carbon (mg biomass_{ACT})$^{-1}$. These coefficients were derived from the carbon and nitrogen analysis completed on cells incubated for 7 d. Aside from the fact that growth on acetate carbon accumulates less biomass, the carbon content of the cells remained essentially constant. There was no evidence for a change in cell composition due to different growth substrates.

Figure 5-1 illustrates the prediction of dry cell weight based on the mean biomass yield coefficients ($Y_{X/CAR}$ and $Y_{X/ACT}$) and the data of substrate consumption. The substrate conversion data indicate that metabolism continued between 5 and days of incubation, therefore, the biomass formation in Figure 5-1 demonstrate the true activity of the cultures during this period. The substrate-based growth curves for carbazole suggest linear growth, consistent with mass transfer limitations and the negligible carbazole concentration in the supernatant.

Figure 5-1 Consistency check on formation of biomass using the yield coefficients calculated from all the measured data of the transformation experiment. The lines represent the biomass profile as predicted by the model using $Y_{X/CAR}$ = 0.25 ± 0.19 mg biomass (mg carbazole converted)$^{-1}$, $Y_{X/ACT}$ = 0.29 ± 0.22 mg biomass (mg acetate converted)$^{-1}$, f_{CAR} = 36.2 ± 0.3 µmol carbon (mg biomass$_{CAR}$)$^{-1}$ and f_{ACT} = 36 ± 9 µmol carbon (mg biomass$_{ACT}$)$^{-1}$.

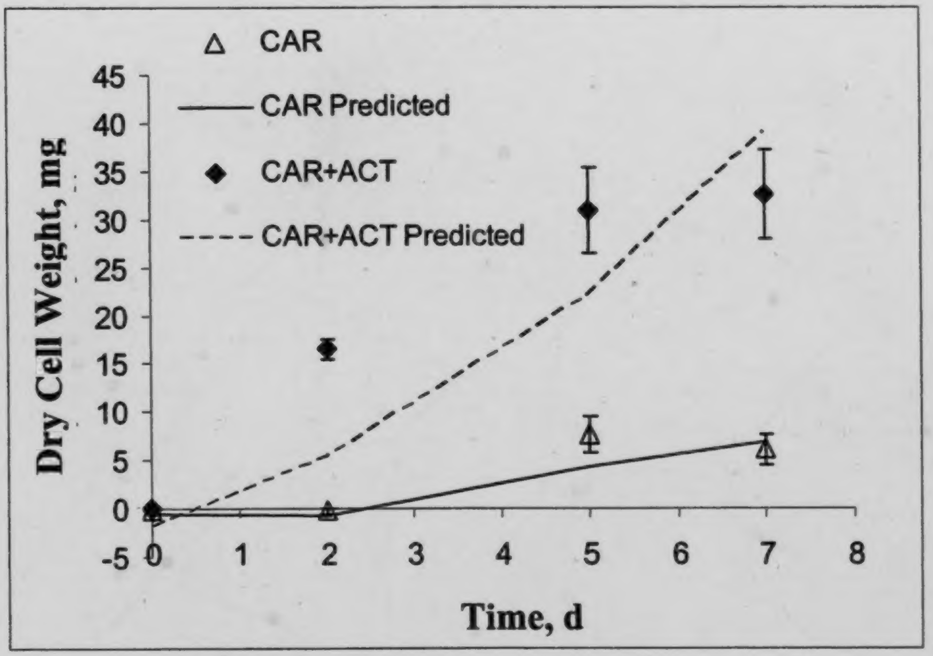

5.2.2.2 Validation of assumptions

Two of the three assumptions made in the reconciliation procedure were evaluated in further detail by using data from the mineralization experiment. Uniformly labeled carbazole was used and the radiolabel concentration was counted in each fraction. These counts provide a direct measurement of the distribution of carbazole carbon without knowing anything about the formation of intermediates or using material balances.

One major assumption used in the reconciliation calculation was that carbazole mineralization (R_{CAR}) remained constant regardless of the presence of acetate. In section 4.5, this assumption was validated because the ratio of $^{14}C_{CO2}$ /$^{14}C_{biomass}$ was essentially constant at 2.6 ± 0.3 regardless of the presence of acetate. Comparing this ratio to that calculated in the transformation experiment 8.0 ± 0.6 μmol CO_2 (μmol carbazole-carbon to biomass)$^{-1}$ shows a reduction in carbazole mineralization of a factor of approximately 3. Investigation of this inconsistency showed that the analysis of the carbon content of biomass was the most likely problem.

The data collected from quantifying the composition of cells growing with different carbon sources showed 440 ± 28 μmol of carbon in the carbazole grown cells, 218 ± 25 μmol of carbon in the heat-killed controls and 1384 ± 110 μmol of carbon in the cultures grown with acetate. This data suggests a mere doubling of carbon content between the initial inoculum, as reflected in the heat-killed controls and the carbazole-grown cells. This implies that after 7 d of incubation and growth on carbazole, the cells in the initial inoculum only divided once. One of the characteristics of CP19 that distinguished it from the other carbazole degraders was its growth on carbazole as a sole carbon and nitrogen source versus growth on carbazole solely as a nitrogen source. The ability to grow better on carbazole as a nitrogen source than as a carbon and nitrogen source implied that the bacterium cannot use the carbazole carbon effectively which was one of the criteria for an ideal isolate. The low accumulation of dry weight is plausible but considering the carbazole conversion (~50 %) in this time period, one would expect higher biomass accumulation.

In light of these observations, the reconciliation calculation was repeated using the fraction of carbazole mineralization as determined from the mineralization experiment. The carbon content of biomass (f_{CAR}= 36.2 ± 0.3 μmol carbon (mg biomass$_{CAR}$)$^{-1}$) as determined from the transformation experiment was assumed to constant and was used again. Also it was assumed that the radiolabel counted in the extract portion was essentially unconverted carbazole. Yield coefficients were calculated using the following equations.

$$Y_{x/CAR} = \frac{{}^{14}X}{{}^{14}\Delta CAR} * \frac{12\mu molC}{\mu molCAR} * \frac{1}{MW_{CAR} * f_{CAR}} \tag{5-14}$$

$$Y_{COa/CAR} = \frac{{}^{14}CO_2}{{}^{14}\Delta CAR} * \frac{12\mu molC}{\mu molCAR} * \frac{MW_{CO_2}1}{MW_{CAR}} \tag{5-15}$$

Where $^{14}CO_2$ is the molar fraction of radiolabel released as CO_2, ^{14}X is the molar fraction of radiolabel accumulated in biomass and the molar fraction of converted carbazole carbon is represented with $^{14}\Delta CAR$.

A range of values for $^{14}\Delta CAR$ was used when performing these calculations for the carbazole and acetate cultures. As outlined in Table 4-7, the neutral extract also contained extractable, non-polar metabolites. Three of the four identified metabolites were acidic and thus remained in the aqueous phase, but the condensation product, 2-amino-3H-phenoxazin-3-one, would be extracted at neutral pH. The contribution of products extracted at neutral pH was not directly quantified; however, the difference between the carbazole conversion measured directly from HPLC data and that obtained from counting ^{14}C was 4.1 ± 4.4 %. This difference provides an indirect quantification of the condensation. The minimum value of carbazole conversion was 89.2 ± 2.2 % and the maximum conversion, including metabolite formation, was 93.3 ± 5.0 %.

A carbazole yield coefficient was calculated for both the carbazole only and the carbazole and acetate conditions. As outlined in Table 5-1, the results of both biomass and CO_2

coefficients did not show any statistical differences between the two conditions. Including the possibility of neutral metabolites reduced the biomass yield coefficient by 0.02 ± 0.009 mg of biomass (mg of carbazole consumed)$^{-1}$. Despite the slight reduction with 95 % confidence, the values are not statistically different.

When the coefficients are compared to those calculated with the data from the transformation experiment, it is evident that the distribution of carbazole is different. At a value of 0.25 mg biomass (mg carbazole consumed)$^{-1}$, the biomass yield in the transformation experiment was almost ½ of that determined from the mineralization experiment, 0.46-0.53 mg biomass (mg carbazole)$^{-1}$. This reinforces the notion that the dry cell weight measurements in the transformation experiment were underestimated. The underestimation carries over to the CO_2 yield coefficients where 2.76 mg CO_2 (mg carbazole consumed)$^{-1}$ was calculated from the transformation, data whereas 1.7-1.8 mg CO_2 (mg carbazole)$^{-1}$ was determined from the mineralization experiment. Fewer assumptions were made to determine the second set of values, and thus are most likely more accurate.

As illustrated in Figure 5-2, the higher yield coefficients shifted the biomass profile of the carbazole and acetate conditions closer to that of measured results. The curve from the carbazole only conditions was also shifted higher, decreasing the difference between the two biomass curves. Overall, an increased in biomass formation was obvious. At the final time point of the carbazole only condition, the biomass prediction is more than double the experimental value. Using these biomass measurements coupled with the carbazole conversion data gives normalized conversions of 9.2 ± 1.3 µmol CAR (mg DCW)$^{-1}$ and 7.1 ± 0.96 µmol CAR (mg DCW)$^{-1}$ for the carbazole only and the carbazole and acetate cultures, respectively. At 95 % confidence, the first value was not statistically greater than the second, therefore, the apparent carbon regulation was not evident using the reconciled data.

Table 5-1 Summary of yield coefficients calculated for carbazole and acetate using the data from ^{14}C- carbazole.

	CAR	CAR+ACT
	(mg of end product (mg of carbazole consumed)$^{-1}$)	
$Y_{x/CAR}^{Max}$	0.58 ± 0.17	0.46 ± 0.15
$Y_{CO2/CAR}^{Max}$	1.8 ± 0.1	1.70 ± 0.06
$Y_{x/CAR}^{Min}$	--	0.44 ± 0.14
$Y_{CO2/CAR}^{Min}$	--	1.6 ± 0.1

Figure 5-2 Consistency check on dry cell weight data, using the carbazole yield coefficients as calculated from the mineralization experiment (Table 5-1). Acetate yield coefficients calculated with data from the transformation experiment were used.

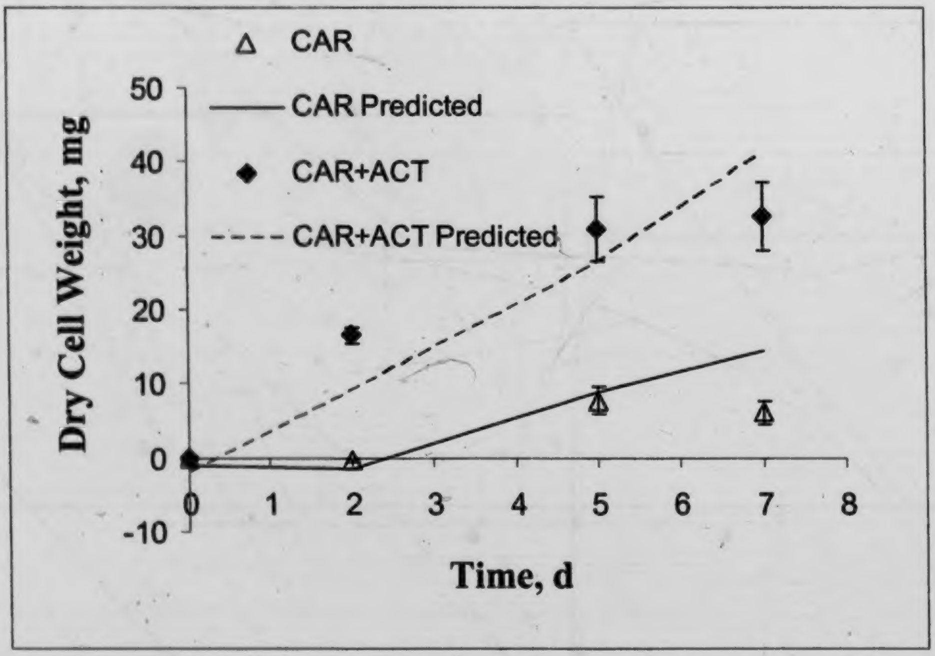

5.2.2.3 Inconsistencies between mineralization and transformation experiments: sources of discrepancies

Transformation experiments with strain CP19 were conducted in 500-mL shake flasks with 200 mL of mineral salts medium. Mineralization experiments were completed in 250-mL shake flasks with 50 mL of mineral salts medium. A comparison between the results of both experiments shows some inconsistencies in the behaviour of CP19 or perhaps variations in the method of scale-down. Apart from the volume differences, there are two main factors that may be contributors to the variations: method of carbazole distribution and actual concentration of carbazole used.

In the larger cultures, carbazole was added in the crystalline form and was autoclaved with the medium. Because radiolabelled carbazole was used in the mineralization experiments the same procedure was not possible; carbazole was dispensed into sterile flasks as a solution in ether. The resulting carbazole crystals in the aqueous medium were finer using the ether recrystallization method, consequently more surface area was exposed to the medium and the cells.

The amount of carbazole used in the larger flasks was 50 mg L^{-1} whereas that used in the 250-mL flasks was 25 mg L^{-1}. In contrast to the effects of ether dispersion, this reduction in carbazole crystals would tend to reduce the surface area of carbazole per unit volume of culture. The rate of dissolution is directly proportional to the surface area of a solid substrate. As previously discussed in section 5.2.1.2 , a major factor affecting growth of CP19 is the rate of carbazole dissolution, thus a reduction in carbazole dissolution would imply a reduction in conversion.

The influence of these factors is most accurately quantified by comparing the transformation results of the 200-mL cultures to the transformation results of the non-radiolabelled, 50-mL cultures. As outlined in Figure 4-17, CP19 showed 43.9 ± 10.5 % and 64.9 ± 9.1 % conversions in the 200-mL cultures without and with acetate respectively. The conversions of the 50-mL cultures were 40.9 ± 3.4 % and 92.0 ± 5.1 %

without and with acetate respectively (Table 4-8). Scale down did not cause any statistical differences in the conversion of carbazole in the carbazole only cultures. However in the acetate supplemented cultures, statistically higher conversions were obvious in the 50-mL cultures than in the 200-mL cultures. The increased conversion may be the result of the cells growing more easily on the acetate carbon achieving a high biomass. The increased surface area of the carbazole, as a result of ether dispersion, would then increase the availability of carbazole for consumption.

Another comparison that must be included is the performance of the non-radiolabelled cultures in the 250-mL shake flasks, to the radiolabelled cultures in the 250-mL biometers. The amount of carbazole converted was measured using HPLC for the non-radiolabelled cultures, and it was inferred in the hot cultures, by counting the ^{14}C collected in the solvent extract collected at neutral pH. Using this method, the amount of carbazole transformed is an indirect measurement as the solvent extract contains both unconverted carbazole and any converted carbazole that is extractable at neutral pH. The conversion factor obtained from this measurement is a conservative value because it does not include the amount of carbazole that was transformed but remained in the neutral extract. With that considered, if the cultures did indeed behave as parallel cultures, the conversion values determined from the non-radiolabelled cultures should be either equivalent or slightly higher than those obtained from the radiolabelled cultures. The difference is attributed to the transformed metabolites. This trend was present in the acetate-supplemented cultures however it was not evident in the carbazole only cultures.

As outlined in Section 4.5, in the carbazole only conditions, 41 % conversion was obtained in the non-radiolabelled flasks (Table 4-8) whereas 82 % conversion was obtained in the radiolabelled flasks (Figure 4-25). Even though it is a conservative estimate of total conversion, overall more carbazole was converted in the radiolabelled flask than in the non-radiolabelled flask. These results suggest that the non-radiolabelled flasks did not succeed in replicating the activity of the radiolabelled flasks.

Despite the inconsistencies evident in the carbazole-only cultures, the data from the radiolabelled and non-radiolabelled cultures with carbazole and acetate did provide comparable results. The conservative estimate of conversion in the radiolabelled flask was 84 % (Figure 4-25) and the data of the non-radiolabelled flasks quantified 92 % conversion of carbazole (Table 4-8). The difference, 4.1 ± 4.4 %, may be the result of accumulated extractable metabolites. Considering the nature of the metabolites that have been identified, the likely contributor to this difference is the 2-aminophenol condensation product, 2-amino-3H-phenoxazin-3-one.

5.3 Metabolite formation from carbazole degradation

Three of the carbazole degradation products produced by isolate CP19 were identified as indole-3-acetic acid, 2-(2,3-dihydro-4-oxo-1H-quinoline-2-yl) acetic acid, 6-(2-aminophenyl)-2-hydroxy-6-oxohexa-2,4-dienoic acid as illustrated in Figure 4-27. These closed-ring structures have been previously identified by Gieg (1996) using *Pseudomonas* sp. LD2. Schneider *et al.* (2000) found products similar to the indole structures using *Ralstonia* sp. RJGII.123.

The indole-type structure represented with indole-3-acetic acid is analogous to those found in the Kodama pathway of DBT degradation where the one of the aromatic rings is cleaved (Kodama *et al.* 1973). The formation of the latter two compounds was extensively discussed by Gieg (1996) and she suggested they formed through non-enzymatic reactions with 2-aminophenyl derivatives. The formation of these open-ring structures show similarities with the DBT degradation pathway proposed by van Afferden *et al.* (1993), whereby the compound is attacked at the heteroatom with an angular dioxygenase followed by ring opening with substantial carbon loss. These pathways do not illustrate the denitrogenation activity, analogous to the desulphurization activity described in the 4S DBT pathway (Omori *et al.* 1992) that was the objective of this research.

Despite the absence of any new carbazole metabolites more suitable for hydrotreating, the investigation of transformation products did result in the identification of one unique compound. 2-Amino-3H-phenoxazin-3-one, hereafter referred to as compound A, was determined to be the compound responsible for the yellow colour that distinguished CP19 from the other carbazole degraders. Further experimental analysis indicated that the presence of compound A, infers an alternate sequence to the final steps of the known carbazole pathways.

Compound A was also detected in the extract of sterile culture medium, incubated with 2-aminophenol. This result provided confirmation that compound A was indeed an abiotic condensation product of 2-aminophenol. Neither compound has been reported in the work done on other carbazole degraders, nor are they mentioned in the either of the two pathways suggested by Ouchiyama *et al.* (1993) and Gieg (1996). Although 2-aminophenol was not found directly in culture extract, the presence of the condensation product infers that 2-aminophenol was a product of carbazole degradation. They both concluded that the step after anthranilic acid was deamination of the aromatic ring, leaving catechol. The indirect identification of 2-aminophenol suggests that CP19 follows an alternate sequence whereby anthranilic acid undergoes decarboxylation to 2-aminophenol. Further investigation showed that strain CP19 was able to use 2-aminobenzoate as a carbon and nitrogen source and accumulate compound A. These results provided further evidence that 2-aminobenzoate undergoes decarboxylation reactions to form 2-aminophenol. Conceivably, decarboxylation simply precedes deamination of the single aromatic ring. It is also possible that this sequence is not unique to CP19 and that these products were simply overlooked in the other studies. However this is the first report of this type for alternate carbazole degradation pathways.

The formation of the condensation product in CP19 cultures further highlights the tendency of biological oxidation products to undergo ring closure reactions. As shown by Bressler and Gray (2002), when the functional groups are in close proximity to each other hydrotreating conditions tend to provoke the closure of open-ringed compounds. The formation of compound A in CP19 cultures suggests that some of the same reactions can occur at culture conditions.

5.4 Substrate specificity

5.4.1 Conversion of carbazole within substrate mixture

As shown in Figure 4-26, significant differences in carbazole conversion were measured with and without the presence of the aromatic test compounds. The flask containing only carbazole tested the effectiveness of the experimental conditions. At a carbazole conversion of a 102 ± 9.66 %, the experimental set-up was successful in achieving high conversion. In contrast, only 20 % of the carbazole was converted in the presence of a mixture of polyaromatic compounds. This reduction could be due to inhibition by the other compounds or due to changes in mass transfer from a mixture of solid substrate.

The reduction in conversion suggested that the additional PACs could have interfered with the carbazole-degrading enzymes. The extra compounds could provide competition for the enzyme binding site (competitive inhibition), or interact with the enzyme-substrate complex, preventing the chemical reactions of carbazole degradation to occur (non-competitive inhibition), or possibly both mechanisms.

Further consideration of the growth characteristics of CP19 with carbazole suggests that the change in carbazole conversions could simply be related to its mass transfer. The growth characteristics of CP19 on carbazole show degradation to be limited by the rate of carbazole dissolution into the aqueous phase, which implies that the capability of the carbazole enzymes were not fully utilized and they should be able to convert more substrate if it is available. Carbazole had one of the highest aqueous solubility values out of the set of compounds tested therefore, it should be one of the most readily available. Consequently inhibition of enzyme activity was unlikely.

As outlined in Equation (3-3), dissolution rate is directly related to surface area of the solid exposed to the bulk liquid. All the substrates were added to the culture flasks in a solution of dimethylformamide. When the solution came into contact with culture medium all the compounds came out of solution and formed a suspension of fine particles. The presence of additional compounds increase the concentration of solid particles, which were composed of a number of compounds agglomerated together. Although equivalent masses of carbazole were used in each flask, the amount of exposed surface area would be reduced in the mixture. A fraction of the carbazole surface area would be covered by the other compounds that solidified. The reduction in carbazole transformation was, therefore, most likely related to the decrease in carbazole dissolution rather than inhibition of enzyme activity.

5.4.2 Selectivity of strain CP19 for carbazole

The substrates used to test the selectivity of CP19 towards carbazole were selected based on the notion that bacteria degrade smaller ringed compounds more easily than multi-ringed compounds (Grosser, 1995). If the larger compounds can be transformed then it is probable that the one- and two-ringed compounds can be transformed as well. The oxygen, sulphur and carbon analogues to carbazole were all included because they are similar in structure to carbazole. This similarity reduces the likelihood that carbazole-specific activity would occur in their presence. Compounds with substrate-similar structures frequently have an inhibitory affect on the enzyme responsible for substrate degradation (Madigan *et al.* 1997). Therefore if substrate specificity is evident in the presence of the carbazole analogues than it is most likely to occur in the presence of other compounds.

CP19 grown in mineral medium, with carbazole as sole nitrogen source and acetate added as an additional soluble carbon source provided no evidence for selectivity to carbazole. Despite higher conversions of carbazole (20.8 %) in the presence of the other compounds (see Figure 4-26), there was still significant conversion of dibenzofuran (8.7 %), DBT (5.4 %) and fluoranthene (8.3 %).

The absolute differences cannot be used to quantify selectivity because the aqueous solubility of each substrate is different from each other and from carbazole. At a value ranging from 3-10 mg L^{-1} the aqueous solubility of dibenzofuran is larger than that of carbazole (0.91-1.67 mg L^{-1}) whereas the aqueous solubilities of DBT and fluoranthene are lower that that of carbazole, with values ranging from 0.53-1.5 mg L^{-1} and 0.12-0.273 mg L^{-1} respectively[8]. The aqueous solubility of carbazole is one of the higher values in this group of compounds, thus a higher conversion of carbazole could simply be the result of solubility differences that affect the bioavailability of the compound.

When the magnitudes of aqueous solubility are compared to the conversion of test compounds, it is evident that degradation of the PACs was not proportional to aqueous solubility. Pyrene and fluoranthene had similar solubilities; however, significant conversion of fluoranthene occurred but no conversion of pyrene. Minimal fluorene conversion occurred therefore CP19 may be selective for carbazole over fluorene. A similar argument could suggest that CP19 was selective for carbazole over dibenzofuran, considering that over twice the amount of carbazole was converted over dibenzofuran and carbazole was the less soluble of the two. Regardless of the solubility differences, significant conversion of other test substrates was evident with CP19 grown on carbazole as a nitrogen source, thus substrate selectivity was low.

The only carbazole degrader reported to have selective activity towards carbazole in the presence of its analogues was *Sphingomonas* sp. CDH-7 (Kirimura *et al.*, 1999). This culture was cultivated on carbazole and exposed to the test compounds in a resting cell suspension. Kilbane *et al.* (2002) found the degradation activity of *Sphingomonas* sp. GTIN11 to be non-selective in the presence of other substrates. Similarly *Pseudomonas* sp. LD2 (Gieg *et al.* 1996) was able to transform all the carbazole analogues in the presence of carbazole. However further investigation by Gieg *et al.* (1996) showed that despite the activity in the presence of carbazole, none of the analogues supported growth as carbon sources. This type of substrate-specific growth is common to the group of carbazole degraders including *Sphingomonas* sp. KA1 (Habe *et al.*, 2002) and the carbazole degrader described by Grosser *et al.* (1991).

---

[8] All the solubility values quoted in the text have been taken from Pearlman *et al.* 1984. These were reported as molar concentrations but converted to mass concentrations using the molecular weight.

The actual mode of substrate transformation is not known for the test compounds exposed to CP19. Conversion was simply a measure of loss of compound. It is quite possible that the alteration of the test compounds was merely an oxidation reaction, quite similar to the activity shown by the CARDO enzymes from *Pseudomonas* sp. CA10 which were found to have a broad substrate range in terms of initial oxidation (Sato *et al.*, 1997a). Nevertheless, the lack of selectivity toward carbazole in the presence of other polyaromatic compounds is highly undesirable for a biocatalyst.

6.0 CONCLUSIONS

Using creosote-contaminated soil enriched on carbazole as sole nitrogen and acetate as a soluble carbon source, several bacteria capable of using carbazole were isolated. None of these isolates showed nitrogen specific removal from carbazole and their degradation of carbazole resulted in substantial loss of organic carbon. From the group, one isolate was chosen to be studied in detail based on its metabolic activities and the formation of a unique, bright-yellow coloured metabolite when grown on carbazole. 16S rDNA sequencing identified CP19 as a member of the *Sphingomonas* genus and thus it was designated *Sphingomonas* sp. CP19.

CP19 grew on carbazole as a nitrogen and carbon source and it agglomerated with the carbazole crystals during growth. The "clumpy" biomass prevented the use of OD_{600} as a method for monitoring growth. Consequently dry cell weight of the biomass collected from an entire culture was used. The crystalline carbazole was removed by first adding ethanol to the culture to solubilize the substrate. This method was also used in parallel with HPLC analysis to measure carbazole loss.

Carbazole solubility was over 6 times greater in spent medium than in distilled water. Surface tension measurements of filtered, sterile medium and filtered spent culture medium showed that the change in solubility was not attributed to the production of conventional biosurfactants. The increased aqueous solubility of carbazole evident in cell-free filtrate likely resulted from the release of cell-associated material.

Measurements of biocatalytic activity were completed on cultures grown in 200 mL mineral medium in 500-mL shake flasks with 50 mg of carbazole added in crystalline form. As the sole source of nitrogen and carbon, 44 % conversion of carbazole was achieved; as sole nitrogen source with acetate as soluble carbon source, 65 % conversion was achieved; and with both supplementary carbon and nitrogen sources 77 % conversion was achieved. The quantity of biomass accumulation was very different in each condition. When biomass was factored into carbazole conversion, the differences attributed to nutrient supplies were lessened. With additional carbon added in the form of sodium acetate, the specific activity of CP19 was determined to be 1.8 μmol CAR (mg DCW- day)$^{-1}$. There was no statistical difference in specific activity of strain CP19 towards carbazole with and without supplementary carbon and nitrogen source. Regulation of carbazole transformation was not evident with acetate, nitrate or ammonium. Carbazole mineralization was not regulated by acetate either. Seven days of incubation with uniformly radiolabelled carbazole resulted in 46 % and 48 % carbazole mineralization with and without acetate, respectively.

Substrate yield coefficients were determined using data from the radiolabelled experiment and data from the non-radiolabelled. The coefficients calculated with the data from the non-radiolabelled experiment showed that acetate is a more efficient substrate for CP19 with $Y_{X/CAR}$ = 0.29 mg biomass (mg carbazole-carbon converted)$^{-1}$ and $Y_{X/ACT}$= 0.68 mg biomass (mg acetate-carbon converted)$^{-1}$. The yield coefficients for CO_2 were $Y_{CO2/CAR}$ = 2.76 mg CO_2 (mg carbazole converted)$^{-1}$ and $Y_{CO2/ACT}$= 1.05 mg CO_2 (mg acetate converted)$^{-1}$. The yield coefficients for carbazole were also determined using the radiolabelled data and gave values of $Y_{X/CAR}$ = 0.53 mg biomass (mg carbazole-carbon converted)$^{-1}$ $Y_{CO2/CAR}$ = 1.80 mg CO_2 (mg carbazole-carbon converted)$^{-1}$. An in depth analysis of the consistency of biomass measurements as related to measurements of the other parameters showed that the carbazole yield coefficients as calculated with the data from the radiolabelled experiment gave the most plausible prediction of biomass. The carbazole yield coefficients calculated with the data from the radiolabelled experiment.

The final distribution of carbazole-carbon was not consistent between experiments. The variations in methods of adding carbazole to the culture flasks increased the exposed surface area of carbazole in the radiolabelled experiment. This variable was attributed to the inconsistent conclusions of carbon regulation. Also the low values of biomass accumulation as measured in the non-radiolabelled experiment were attributed to this difference.

In the presence of live cultures, the aqueous concentration of carbazole was essentially zero. This observation supports the conclusion that growth of strain CP19 on carbazole was mass transfer limited. Also, the growth patterns of CP19 growing on carbazole somewhat followed a zero-order growth curve. These two factors supported the conclusion that carbazole conversion by strain CP19 was limited by the bioavailability of carbazole.

As a carbazole degrader, CP19 showed slow conversion rates. This trend was attributed to three main factors: mass transfer limitations, lack of induction and formation of a dead-end metabolite. The rate of carbazole dissolution limited the amount of carbazole in the aqueous phase and thus limited the amount of carbazole available to the cells. Dissolution limitations resulted from restricted exposure of carbazole surface area. Surface area was reduced by the cells' tendencies to agglomerate with the crystals; as well, the surface area of the solid substrate was limited as a dispersant was not used. Growth on carbazole as sole nitrogen and carbon source was not evident until 48 h of incubation: this lag period was somewhat less defined on carbon supplemented cultures but still present. Preparation of inoculum cells on nutrient-rich medium, lacking inducers, is a plausible cause of this delay in growth. Extracts removed at neutral pH from the filtrate of CP19 contained 2-amino-3H-pheanoxazin-3-one. Accumulation of this abiotic condensation product of 2-aminophenol suggests that some of the converted carbazole carbon remains in a complex structure, not easily metabolized by the cell for growth.

Other carbazole metabolites identified in the filtrate of CP19 link its biochemical pathway to those previously published by Ouchiyama *et al.* (1992) and Gieg (1996). The metabolites 2-(2,3-dihydro-4-oxo-1H-quinoline-2-yl) acetic acid and 6-(2-aminophenyl)-2-hydroxy-6-oxohexa-2,4-dienoic acid indicate that strain CP19 follows the angular attack pathway proposed by Ouchiyama *et al.* (1992) and Gieg (1996). The indole derivative of indole-3-acetic acid was also found, linking the biochemical pathway of CP19 to the second carbazole pathway postulated by Gieg (1996). The presence of both types of compounds indicated that the activity of CP19 was similar to that of *Pseudomonas* sp. LD2. The identification of the condensation product of 2-aminophenol suggested either a possible alternative lower-pathway of carbazole degradation or an addition to those previously published. Until this study, degradation of anthranilic acid has been postulated to go directly to catechol. The indirect identification of 2-aminophenol suggests that anthranilic acid was decarboxylated first and then deaminated to catechol.

The accumulation of the abiotic condensation product of 2-aminophenol and the absence of 2-aminophenol in culture filtrate illustrated the tendency of functional groups of biochemical oxidation products to undergo ring-closure reactions. The fact that it occurred under culture conditions solidifies the necessity for a carbazole isolate to completely denitrogenate carbazole to be a useful addition to hydrotreatment.

Strain CP19 was shown to have little to no selectivity towards carbazole in the presence of the carbazole analogues dibenzofuran, DBT and fluorene, and the hydrocarbons fluoranthene and pyrene. Transformation of fluorene and pyrene was not detected; however, significant conversion of the other compounds was evident. The aqueous solubility of each compound was different and this factor was not controlled in the experimental design. Nevertheless, conversion was not proportional to the aqueous solubilities. Carbazole degradation activity by CP19 was not substrate specific and thus highly undesirable as a biocatalyst.

Overall, a carbazole-degrading bacterium with metabolic characteristics unique from those of previously published isolates has been identified. The biochemical activity of this new isolate is also not suitable for the application of pre-treating gas oil before hydrotreatment. The biocatalyst could remove carbazoles, however, it converts the majority of the carbon backbone to carbon dioxide, it is capable of transforming other polyaromatic compounds and hydrocarbon structures possibly using some of the carbon, and the only metabolite that accumulates significantly is a ring-closure product with the nitrogen atom still intact. In the process of characterizing this isolate a new step in the carbazole degradation pathway has been identified.

7.0 REFERENCES

Adams A.H., C.M. Huang, F.K. Higson, V. Brenner, and D.D. Focht. 1992. Construction of a 3-chlorobiphenyl-utilizing recombinant from an intergeneric mating. Applied and Environmental Microbiology **58**: 647-654.

Alexander, M., 1994. *Biodegradation & Bioremediation*. Academic Press, Inc.: San Diego.

American Society of Microbiology, 1974. *Bergey's Manual for Determinative Bacteriology*. 8th Edition. Williams & Wilkins Co.: Baltimore.

Atlas, R.M., and R. Bartha, 1997. *Microbial Ecology Fundamentals and Applications*. 4th Edition. Benjamin/Cummings Science Publishing: Toronto.

Balashova, N.V., A. Stolz, H.J. Knackmuss, I.A. Kosheleva, A.V. Naumov and A.M. Boronim. 2001. Purification and characterization of a salicylate hydroxylase involved in 1-hydroxy-2-naphthoic acid hydroxylation from the naphthalene and phenanthrene-degrading bacterial strain *Pseudomonas putida* BS202-P1. Biodegradation **12**: 179-188.

Balkwill, D.L., G.R. Drake, R.H. Reeves, J.K. Frederickson, D.C. White, D.B. Ringelberg, D.P. Chandler, M.F. Romine, D.W. Kennedy, and C.M. Spadoni. 1997. Taxonomic study of aromatic-degrading bacteria from deep-terrestrial-subsurface sediments and description of *Sphingomonas aromaticivorans* sp nov, *Sphingomonas subterranea* sp nov, and *Sphingomonas stygia* sp nov. International Journal of Systematic Bacteriology **47**: 191-201.

Bartha, R., and D. Pramer. 1965. Features of a flask and method for measuring the persistence and biological effects of pesticides in soil. Soil Science **100**: 68-70.

Benedik, M.J., P.R. Gibbs, R.R. Riddle and R.C. Wilson. 1998. Microbial denitrogenation of fossil fuels. Trends in Biotechnology **16**: 390-395.

Bolognese, A., and G. Scherillo. 1986. Reaction of *o*-aminophenol and *p*-benzoquinone in acetic acid. Journal of Heterocyclic Chemistry **23**: 1003-1006.

Bressler, D.C., and P.M. Fedorak. 2000. Bacterial metabolism of fluorene, dibenzofuran, dibenzothiophene, and carbazole. Canadian Journal of Microbiology **46**: 397-409.

Bressler, D.C., and P.M. Fedorak. 2001. Identification of disulfides from the biodegradation of dibenzothiophene. Applied and Environmental Microbiology **67**: 5084-5093.

Bressler, D.C., and M.R. Gray. 2002. Hydrotreating reactions of model products from bioprocessing of carbazoles. Energy and Fuels **16**: 1076-1086.

Bressler, D.C., P.M. Fedorak, and M.A. Pickard. 2000. Oxidation of carbazole, N-ethylcarbazole, fluorene, and dibenzothiophene by the laccase of *Coriolopsis gallica*. Biotechnology Letters **22**: 1119-1125.

Dagley, S., and D.E. Nicholson. 1970. *An Introduction to Metabolic Pathways*. John Wiley and Sons Inc.: New York.

Denome, S.A., D.C. Stanley, E.S. Olson, and K.D. Young. 1993. Metabolism of dibenzothiophene and naphthalene in *Pseudomonas* strains: Complete DNA sequence of an upper naphthalene catabolic pathway. Journal of Bacteriology **175**: 6890-6901.

Desai, J.D. and I.M. Banat. 1997. Microbial production of surfactants and their commercial potential. Microbiology, Molecular and Biological Reviews **61**: 47-60.

Dorbon, M. and C. Bernasconi. 1989. Nitrogen-compounds in light cycle oils- identification and consequences of aging. Fuel **68**: 1067-1074.

Dorbon, M., I. Ignatiadis, J.M. Schmitter, P. Arpino, G. Guiochon, H. Toulhoat, and A. Huc. 1984. Identification of carbazole and benzocarbazoles in a coker gas oil influence of catalytic hydrotreatment on their distribution. Fuel **63**: 565.

Dua, M., A. Singh, N. Sethunathan, and A.K. Johri. 2002. Biotechnology and bioremediation: successes and limitations. Applied Microbiology and Biotechnology **59**: 143-152.

Eaton, R.W., and P. J. Chapman. 1992. Bacterial metabolism of naphthalene-construction and use of recombinant bacteria to study ring cleavage of 1,2-dihydroxynaphthalene and subsequent reactions. Journal of Bacteriology **174**: 7542-7554.

Efroymson, R.A., and M. Alexander. 1991. Biodegradation by an *Arthrobacter* species of hydrocarbons partitioned into an organic-solvent. Applied and Environmental Microbiology **57**: 1441-1447.

Ensley, B.D., D.T. Gibson, and A.L. Laborde. 1982. Oxidation of naphthalene by a multicomponent enzyme system from *Pseudomonas* sp. strain NCIB 9816. Journal of Bacteriology **149**: 948-954.

Fedorak, P.M. and D. Grbic'-Galic'. 1991. Aerobic microbial cometabolism of benzothiophene and 3-methylbenzothiophene. Applied and Environmental Microbiology **57**: 932-940.

Fedorak, P.M. and D.W.S. Westlake. 1984. Microbial degradation of alkyl carbazoles in Norman Wells crude oil. Applied and Environmental Microbiology **47**: 858-862.

Finnerty, W.R., K. Shockley, and H. Attaway. 1983. Microbial desulphurization and denitrogenation of hydrocarbons. In: Microbial Enhanced Oil Recovery. J.E. Zajic, D.C. Cooper, T.R. Jack and N. Kosaric. Eds. PennWell Publishing: Tulsa, pp. 83-91.

Foght, J.M., Q. Wu, P.M. Fedorak, M.A. Pickard, and M.R. Gray. 1997. Biocatalytic upgrading of petroleum distillates: ring cleavage of aromatic hydrocarbons and heterocycles commonly present in petroleum distillates. Paper 97-13. Pre-print from 48th Annual Technical Meeting of the Petroleum Society.

Frakman, Z., T.M. Ignasiak, D.S. Montgomery, and O.P. Strausz. 1987. Nitrogen compounds in Athabasca asphaltene: the carbazoles. AOSTRA Journal of Research **3**: 131-138.

Furimsky, E., R. Ranganathan, and B. I. Parsons. 1977. Catalytic hydrodenitrogenation of basic and non-basic nitrogen compounds in Athabasca bitumen distillates. Fuel **57**: 427-430.

Gieg L.M. 1996. Microbial metabolism of carbazole and other components of coal tar creosote. Ph. D. thesis, University of Alberta, Edmonton, Alberta.

Gieg, L.M., A.Otter, and P.M. Fedorak. 1996. Carbazole degradation by *Pseudomonas* sp. LD2: metabolic characteristics and the identification of some metabolites. Environmental Science and Technology **30**: 575-585.

Gray, M.R. 1990. Composition and hydrotreating of bitumen and heavy oil-derived distillates. AOSTRA Journal of Research **6**: 185-198.

Grosser, R.J., D. Warshawsky, and J.R. Vestal. 1991. Indigenous and enhanced mineralization of pyrene, benzo[a]pyrene, and carbazole in soils. Applied and Environmental Microbiology **57**: 3462-3469.

Grosser, R.J., D. Warshawsky, and J.R. Vestal. 1995. Mineralization of polycyclic and N-heterocyclic aromatic compounds in hydrocarbon-contaminated soils. Environmental Toxicology and Chemistry **14**: 375-382.

Guerra-Santos, L., O. Kappeli, and A. Fiechter. 1984. *Pseudomonas aeruginosa* biosurfactant production in continuous culture with glucose as carbon source. Applied and Environmental Microbiology **48**: 301-305.

Habe, H., K. Ide, M. Yotsumoto, H. Tsuji, H. Hirano, J. Widada, T. Yoshida, H. Nojiri, and T. Omori. 2001. Preliminary examinations for applying a carbazole-degrader, *Pseudomonas* sp. strain CA10, to dioxin-contaminated soil remediation. Applied Microbiology and Biotechnology **56**: 788-795.

Habe, H., Y. Ashikawa, Y. Saiki, T. Yoshida, H. Nojiri, and T. Omori. 2002. *Sphingomonas* sp. strain KA1, carrying a carbazole dioxygenase gene homologue, degrades chlorinated dibenzo-*p*-dioxins in soil. FEMS Microbiology Letters **211**: 43-49.

Hayat, M.A., 2000. *Principles and Techniques of Electron Microscopy Biological Applications 4th Edition*. Cambridge University Press.: Cambridge.

Held, M., A. Schmid, H.P.E. Kohler, W. Suske, B. Witholt, and M.G. Wubbolts. 1999. An integrated process for the production of toxic catechols from toxic phenols based on a designer biocatalyst. Biotechnology and Bioengineering **62**: 641-648.

Hyndman, A.W. and R.W. Luhning. 1991. Recovery and upgrading of bitumen and heavy oil in Canada. The Journal of Canadian Petroleum Technology **30**: 61-71.

Izac, V. and J.L. Tholozan. 1998. Comparison of different methods of cell lysis and protein measurements in *Clostridium perfringens*: Application to the cell volume determination. Current Microbiology **36**: 131-135.

Kappeli O., P. Walther, M. Mueller, and A. Fiechter. 1984. Structure of the cell surface of the yeast *Candida tropicalis* and its relation to hydrocarbon transport. Archives of Microbiology **138**: 279-282.

Kayser, K.J., B.A. Bielaga-Jones, K. Jackowski, O. Odusan, and J.J. Kilbane. 1993. Utilization of organosulphur compounds by axenic and mixed cultures of *Rhodococcus-rhodochrous* IGTS8. Journal of General Microbiology **139**: 3123-3129.

Kilbane, J.J., R. Ranganathan, L. Cleveland, K.J. Kayser, C. Ribiero, and M.M. Linhares. 2000. Selective removal of nitrogen from quinoline and petroleum by *Pseudomonas ayucida* IGTN9m. Applied and Environmental Microbiology **66**: 688-693.

Kilbane, J.J., A. Daram, J. Abbasian, and K.J. Kayser. 2002. Isolation and characterization of *Sphingomonas* sp. GTIN11 capable of carbazole metabolism in petroleum. Biochemical and Biophysical Research Communications **297**: 242-248.

Kimura, T., Y. Zhang, T. Kodama, and T. Omori. 1996. Isolation and characterization of *Tn 5*-induced mutants deficient in carbazole catabolism. FEMS Microbiology Letters **135**: 65-70.

Kirimura, K., H. Nakagawa, K. Tsuji, K. Matsuda, R. Kurane, and S. Usami. 1999. Selective and continuous degradation of carbazole contained in petroleum oil by resting cells of *Sphingomonas* sp. CDH-7. Bioscience Biotechnology and Biochemistry **63**: 1563-1568.

Kobayashi, T., R. Kurane, K. Nakajima, Y. Nakamura, K. Kirimura, and S. Usami. 1995. Isolation of bacteria degrading carbazole under microaerobic conditions, i.e. nitrogen gas substituted conditions. Bioscience Biotechnology and Biochemistry **59**: 932-933.

Kodama, K., K. Umehara, K. Shimizu, S. Nakatani, Y. Minoda, and K. Yamada. 1973. Identification of microbial products from dibenzothiophene and its proposed oxidation pathway. Agricultural and Biological Chemistry **37**: 45-50.

Maeda K., H. Nojiri, M. Shintani, T. Yoshida, H. Habe, and T. Omori. 2003. Complete nucleotide sequence of carbazole/dioxin-degrading plasmid pCAR1 in *Pseudomonas resinovorans* strain CA10 indicates its mosaicity and the presence of large catabolic transposon *Tn4676*. Journal of Molecular Biology **326**: 21-33.

Madigan, M.T., J.M. Martinko, and J. Parker, 1997. *Brock Biology of Microorganisms.* 8th Edition. Prentice-Hall: New Jersey.

Mueller, J.G., P.J. Chapman, and P.H. Pritchard, 1989. Creosote-contaminated sites. Environmental Science and Technology **23**: 1197-1201.

Mukherji, S., and W.J. Weber Jr. 1998. Mass transfer effects on microbial uptake of naphthalene from complex NAPLs. Biotechnology and Bioengineering **60**: 750-760.

Nakagawa, H., K. Kirimura, T. Nitta, K. Kino, R. Kurane, and S. Usami. 2002. Recycle use of *Sphingomonas* sp. CDH-7 cells for continuous degradation of carbazole in the presence of $MgCl_2$. Current Microbiology **44**: 251-256.

Nojiri, H., H. Sekiguchi, K. Maeda, M. Urata, S. Nakai, T. Yoshida, H. Habe, and T. Omori. 2001. Genetic characterization and evolutionary implication of a *car* gene cluster in the carbazole degrader *Pseudomonas* sp. strain CA10. Journal of Bacteriology **183**: 3663-3679.

Omori, T., L. Monnas, Y. Saiki, and T. Kodama. 1992. Desulphurization of dibenzothiophene by *Corynebacterium* sp. strain SY1. Applied and Environmental Microbiology **58**: 911-915.

Ouchiyama, N., Y. Zhang, T. Omori, and T. Kodama. 1993. Biodegradation of carbazole by *Pseudomonas* spp. CA06 and CA10. Bioscience Biotechnology and Biochemistry **57**: 455-460.

Ouchiyama, N., S. Miyachi, and T. Omori. 1998. Cloning and nucleotide sequence of carbazole catabolic genes from *Pseudomonas stutzeri* strain OM1, isolated from activated sludge. Journal of General and Applied Microbiology **44**: 57-63.

Pearlman, R.S., S.H. Yalkowsky, and S. Banerjee. 1984. Water solubilities of polynuclear aromatic and heteroaromatic compounds. Journal of Physical and Chemical Reference Data **13**: 555-562.

Perry, R.H. and D.W., Green. 1984. *Perry's Chemical Engineering Handbook.* 6th Edition. McGraw-Hill Inc.: Toronto.

Pieper, D.H., and W. Reineke. 2000. Engineering bacteria for bioremediation. Current Opinion in Biotechnology **11**: 262-270.

Reisfeld, A., E. Rosenberg, and D. Gutnick. 1972. Microbial degradation of crude oil: factors affecting the dispersion in sea water by mixed and pure cultures. Applied Microbiology **24**: 363-368.

Riddle R.R., P.R. Gibbs, R.C. Willson, and M.J. Benedik. 2003. Recombinant carbazole-degrading strains for enhanced petroleum processing. Journal of Industrial Microbiology and Biotechnology **30**: 6-12.

Rosenberg, M., and E. Rosenberg. 1985. Bacterial adherence at the hydrocarbon-water interface. Oil and Petrochemical Pollution **2**: 155-162.

Sáchez-Cortés, S., O. Francioso, J.V. García-Ramos, C. Ciavatta, and C. Gessa. 2001. Catechol polymerization in the presence of silver surface. Colloids and Surfaces A: Physicochemical and Engineering Aspects **176**: 177-184.

Sato, S., N. Ouchiyama, T. Kimura, H. Nojiri, H. Yamane, and T. Omori. 1997a. Cloning of genes involved in carbazole degradation of *Pseudomonas* sp. strain CA10: Nucleotide sequences of genes and characterization of meta-cleavage enzymes and hydrolase. Journal of Bacteriology **179:** 4841-4849.

Sato, S., J. Nam, K. Kasuga, H. Nojiri, H. Yamane, and T. Omori. 1997b. Identification and characterization of genes encoding carbazole 1,9a-dioxygenase in *Pseudomonas* sp. strain CA10. Journal of Bacteriology **179**: 4850-4858.

Schneider, J., R.J. Grosser, K. Jayasimhulu, W. Xue, B. Kinkle, and D. Warchawsky. 2000. Biodegradation of carbazole by *Ralstonia* sp. RJGII.123 isolated from a hydrocarbon contaminated soil. Canadian Journal of Microbiology **46**: 269-277.

Shennan, J.L. 1996. Microbial attack on sulphur-containing hydrocarbons: Implications for the biodesulphurisation of oils and coals. Journal of Chemical Technology and Biotechnology **67**: 109-123.

Shepherd, J.M., and G. Lloyd-Jones. 1998. Novel carbazole degradation genes of *Sphingomonas* CB3: Sequence analysis, transcription, and molecular ecology. Biochemical and Biophysical Research Communications **247**: 129-135.

Shotbolt-Brown, J., D.W.F. Hunter, and J. Aislabie. 1996. Isolation and description of carbazole-degrading bacteria. Canadian Journal of Microbiology **42**: 79-82.

Strubel, V., K.H. Engesser, P. Fischer, and H.J. Knackmuss. 1991. 3-(2-Hydroxyphenyl) catechol as substrate for proximal *meta* ring cleavage in dibenzofuran degradation by *Brevibacterium* sp. strain DPO-1361. Journal of Bacteriology **173**: 1932-1937.

Stucki, G., and M. Alexander. 1987. Role of dissolution rate and solubility in biodegradation of aromatic compounds. Applied and Environmental Microbiology **53**: 292-297.

Van Afferden, M., D. Tappe, M. Beyer, H.G. Trüper, and J. Klein. 1993. Biochemical mechanisms for the desulphurization of coal-relevant organic sulfur compounds. Fuel **72**: 1635:1643.

Voet, D., and J.G. Voet. 1995. *Biochemistry*. 2nd Edition. John Wiley and Sons, Inc. Toronto

Volkering, F., A.M. Breure, A. Sterkenburg, and J.G. van Andel. 1992. Microbial degradation of polycyclic aromatic hydrocarbons: effect of substrate availability on bacterial growth kinetics. Applied Microbiology Biotechnology **36**: 548-552.

Volkering, F., A.M. Breure, J.G. Van Andel, and W.H. Rulkens. 1995. Influence of nonionic surfactants on bioavailability and biodegradation of polycyclic aromatic hydrocarbons. Applied and Environmental Microbiology **61**: 1699-1705.

Von Graevenitz, A., and C. Bucher. 1983. Accuracy of the KOH and vanomycin tests in determining the Gram reaction of non-enterobacterial rods. Journal of Clinical Microbiology **18**: 983-985.

Wick, L.Y., A.R. de Munain, D. Springael, and H. Harms. 2002. Responses of *Mycobacterium* sp. LB501T to the low bioavailability of solid anthracene. Applied Microbiology and Biotechnology **58**: 378-385.

Wodzinski, R.S., and J.E. Coyle. 1974. Physical state of phenanthrene for utilization by bacteria. Applied Microbiology **27**: 1081-1084.

8.0 APPENDIX A

Medium Formulations

Mineral Salts Medium (B+N8P)	
NH_4Cl	1 g
Na_2SO_4	2 g
KNO_3	2 g
$FeSO_4 \bullet 7H_2O$	Trace
Trace metals	1 mL
Purified water	900 mL
Phosphate buffer	100 mL
0.04 g $MgSO_4 \bullet 7H_2O$ mL^{-1} (aqueous solution)	1 mL

Mineral Salts Medium (B+8P)	
KCl	1.5 g
Na_2SO_4	2 g
$FeSO_4 \bullet 7H_2O$	Trace
Trace metals	1 mL
Purified water	900 mL
Phosphate buffer	100 mL
0.04 g $MgSO_4 \bullet 7H_2O$ mL^{-1} (aqueous solution)	1 mL

Add the first two components to the water and buffer solution and mix until all crystals are dissolved. The third component is added and mixed until it dissolves. Finally, the trace metals solution (Fedorak and Grbic'-Galic', 1991) is added. Distribute and autoclave medium. After cooling, aseptically add sterile $MgSO_4 \bullet 7H_2O$ solution to each culture at a concentration of 0.005 mL mL^{-1} of medium to each culture.

Phosphate Buffer Solution	
KH_2PO_4	16 g
K_2HPO_4	24 g
Purified water	1000 mL

Trace Metals Solution (Fedorak and Grbic'-Galic', 1991)	
$CaCl_2 \bullet 2H_2O$	3.7 g
H_3BO_3	2.5 g
$MnCl_2$	0.87 g
$FeCl_3$	0.65 g
$ZnCl_2$	0.44 g
$Na_2MoO_2 \bullet 2H_2O$	0.29 g
$CoCl_2$	0.01 g
$CuCl_2$	0.0001 g
H_2O	1.0 L

Mineral Salts Medium Plates (B+8P+ ACT)	
KCl	1.5 g
Na_2SO_4	2 g
$FeSO_4 \bullet 7H_2O$	Trace
Trace metals	1 mL
Purified water	900 mL
Phosphate buffer	100 mL
0.04g $MgSO_4 \bullet 7H_2O$ mL^{-1} (aqueous solution)	1 mL
$CH_3COONa \bullet 3H_2O$	2 g
Noble Agar, Difco	15 g

Add the first two components to the water and buffer solution and mix until all crystals are dissolved. The third component and acetate are then added and mixed again. Finally, the trace metals solution is added. Once the medium was removed from the autoclave and cooled to approximately 50 °C, the $MgSO_4 \bullet 7H_2O$ solution was added at a concentration of 0.005 mL mL^{-1} of medium. The plates were then poured and let to solidify overnight.

½ Plate Count Agar Plates (1/2 PCA)	
PCA powder, Difco	7.5 g
Bacto Agar, Difco	7.5 g
Purified water	1000 mL

Sources of Chemicals Used

Compound	*Manufacturer*
Inorganic Salts	
Ferrous sulphate	Fisher Scientific Co. (Fair Lawn, NJ)
Magnesium sulphate	EM Science (Hawthorn, NY)
Potassium chloride	BDH (Poole, England)
Potassium phosphate dibasic	Fisher Scientific Co.
Potassium phosphate monobasic	Fisher Scientific Co.
Sodium acetate trihydrate	Fisher Scientific Co.
Sodium sulphate, anhydrous	BDH
8.1 Hydrocarbons	
Anthracene	Aldrich Chemical Co.
2-Aminobiphenyl	Aldrich Chemical Co.
Carbazole, 99% Purity	Aldrich Chemical Co.
Dibenzofuran	Aldrich Chemical Co.
Dibenzothiophene	Aldrich Chemical Co.
9- Ethyl carbazole	Aldrich Chemical Co.
Fluoranthene	Aldrich Chemical Co.
Fluorene	Aldrich Chemical Co.
Naphthalene	Aldrich Chemical Co.
Phenanthrene	Aldrich Chemical Co.
Pyrene	Aldrich Chemical Co.
Thianaphthene (benzothiophene)	Aldrich Chemical Co.
Thianthrene, 97% Purity	Aldrich Chemical Co.
8.2 Miscellaneous Products	
Bacto™ Agar	Difco Laboratories
Plate Count Agar (PCA)	Difco Laboratories
Tryptic Soy Broth (TSB)	Difco Laboratories
Noble Agar	Difco Laboratories

8.3 Solvents and Acids

HCl, Technical Grade	Fisher Scientific
Ethyl acetate, HPLC Grade	Fisher Scientific
Dichloromethane, HPLC-GC/MS Grade	Fisher Scientific
Diethyl ether anhydrous (99% Purity)	EM Science (Darmstadt, Germany)
Acetonitrile, HPLC Grade	Fisher Scientific
N,N-dimethylformamide	Sigma Chemical Co.

9.0 APPENDIX B

Figure 9-1 A typical calibration curve used to determine aqueous acetate concentrations using GC-FID.

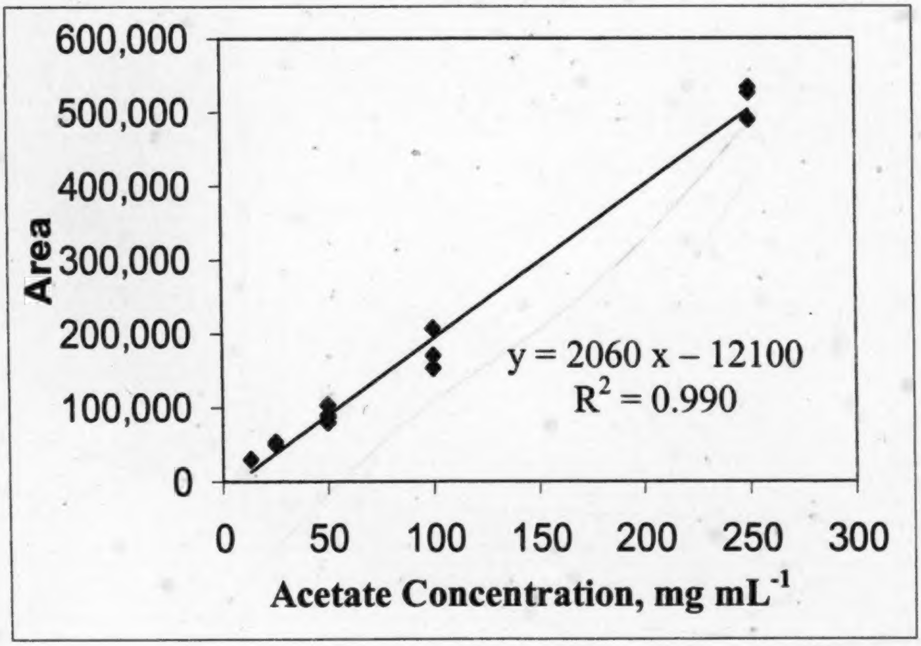

10.0 APPENDIX C

10.1 Sample calculation for error analysis

10.1.1 Error analysis for numbers undergoing addition or subtraction.

The following sample calculation was performed using the data from Figure 4-18 (A). The values were taken from cultures grown for 2 days in mineral medium with carbazole and acetate (CAR+ACT).

$$Z = (X - Y) \pm \sqrt{x^2 + y^2}$$

$$31.27 \pm 2.81 = (34.89 - 3.63) \pm \sqrt{1.25^2 + 2.52^2}$$

Z= Corrected value of carbazole removal at T=2 days in condition, CAR+ACT
X= Average value of carbazole removal at T=2 days (CAR+ACT), % Removal
Y= Average value of carbazole removal at T=2 days (HKC), % Removal
x= Standard deviation of culture value
y= Standard deviation of heat-killed control value

10.1.2 Error analysis for numbers undergoing multiplication or division.

The following sample calculation was performed using the dry weight measurements outlined in Figure 4-19 and the amount of carbazole transformed as outlined in Figure 4-21. Data from cultures grown for 2 days in mineral medium with carbazole and acetate (CAR+ACT) were used to complete the sample calculation.

$$Z = \frac{X}{Y} \pm \left(\sqrt{\left(\frac{x}{X}\right)^2 + \left(\frac{y}{Y}\right)^2} \right) * Z$$

$$4.307 \pm 0.095 = \frac{101.73}{23.63} \pm \left(\sqrt{\left(\frac{3.167}{101.73}\right)^2 + \left(\frac{1.05}{23.63}\right)^2} \right) * 4.307$$

Z= Transformation of carbazole per gram of dry cell weight (μmol (mg DCW)$^{-1}$)
X= Mean amount of carbazole transformed (μmol)
Y= Mean amount of dry cell weight (mg)

x= Standard deviation of X
y=Standard deviation of Y

10.2 Sample calculation for carbazole conversion rate

The following sample calculation was performed using the data in the carbazole and acetate condition between 2 and 5 days. (Table 12-17)

Measured:

$\Delta CAR_{t=2}$= 101.73 ±3.17 μmol
$\Delta CAR_{t=5}$= 156.90 ± 14.89 μmol
$\Delta CAR^{HKC}{}_{t=2}$= 11.57 ± 7.95 μmol
$\Delta CAR^{HKC}{}_{t=5}$= -24.34 ±13.26 μmol

$M_{t=2}$= 23.63 ± 1.05 mg
$M_{t=5}$= 37.7 ± 4.13 mg
$M^{HKC}{}_{t=2}$= 7.13 ± 0.15 mg
$M^{HKC}{}_{t=2}$ = 6.82 ± 1.57 mg

Calculated:

$$\Delta \mathrm{CAR}^{\mathrm{corr}}_{t=2} = \Delta \mathrm{CAR}_{t=2} - \Delta \mathrm{CAR}^{\mathrm{HKC}}_{t=2} = 101.73 - 11.57 = 90.16 \pm 8.56 \mu mol\ CAR$$

$$\Delta \mathrm{CAR}^{\mathrm{corr}}_{t=5} = \Delta \mathrm{CAR}_{t=5} - \Delta \mathrm{CAR}^{\mathrm{HKC}}_{t=5} = 156.90 - -24.34 = 181.24 \pm 19.94 \mu mol\ CAR$$

$$M^{Corr}_{t=2} = M_{t=2} - M^{HKC}_{t=2} = 23.63 - 7.13 = 16.5 \pm 1.06\ mg\ biomass$$

$$M^{Corr}_{t=5} = M_{t=5} - M^{HKC}_{t=5} = 37.7 - 6.82 = 30.88 \pm 4.42\ mg\ biomass$$

Rate of carbazole transformation.

$$R_{mean} = \frac{\Delta CAR_t - \Delta CAR_{t-1}}{\Delta T\left(\frac{M_i + M_{i+1}}{2}\right)} = \frac{\Delta CAR^{corr}_{t=5} - \Delta CAR^{corr}_{t=2}}{3days\left(\frac{M^{corr}_{t=2} + M^{corr}_{t=5}}{2}\right)} = \frac{181.24 - 90.16}{3 * \left(\frac{16.5 + 30.88}{2}\right)} = 1.28 \qquad (12\text{-}3)$$

10.3 Sample calculation for $^{14}CO_2$ release

Calculation completed on carbazole and acetate growing condition, replicate 1.

Given:

V_{sample}= 0.5 ml
$(V_{total})_{initial}$ = 10 ml (KOH)
Sampling No.= 3
Total Counts Removed ($TCR|_{24hrs}$)= 143.50 DPM (Table 12-21)
Accumulative Counts Removed ($ACR|_{24hrs}$)= 2420.50 DPM (Table 12-22)

Measured at that time point:

Counts 0%= 23 DPM (Table 12-22)
Counts ACT1= 2464.50 DPM (Table 12-20)

Calculations:

1. Correct for Background (CB)

$$(CB\,|_{48hrs}) = C\,|_{24hrs} - C\,|_{0\%} = 2464.50 - 23\ DPM = 2441.50\ DPM$$

2. Total Counts Removed

$$(TCR\,|_{48hrs}) = TCR\,|_{24hrs} + CB\,|_{48hrs} = 143.50 + 2441.50\ DPM$$

3. Fraction of Total Counted

$$f = \frac{V_{sample}}{(V_{total})_i - V_{sample}(SN-1)} = \frac{0.5}{10-(0.5)(3-1)} = 0.055555$$

4. Accumulative Removal

$$AR\,|_{48hrs} = \frac{CB\,|_{48hrs}}{f} + TCR\,|_{24hrs} = \frac{2441.50}{0.0555} + 143.50 = 44134.49$$

10.4 Sample calculation for ^{14}C in biomass

Sample calculation was completed using data from heat-killed control culture, replicate 1.

Measured for each sample:

Volume of aqueous used to collect pellet ($V_{\text{to pellet}}$)= 6 ml (Table 12-24)
Volume of total aqueous fraction (V_{total})= 50 ml (Table 12-23)
Count 0%= 24 DPM (Table 12-19)
1 ml pellet suspension HKC1= 201.5 DPM (Table 12-24)

Calculations

1. Count corrected for background (CB)

$$CB = C\,|_{HKC1} - C\,|_{0\%} = 201.5 - 24\ DPM = 177.5\ DPM$$

2. Fraction of total pellet counted

$$f = \frac{V_{to\ pellet}}{V_{total}} = \frac{6\,ml}{50\,ml} = 0.12$$

3. Total counts in pellet

$$TC\,|_{HKC1} = \frac{CB\,|_{HKC1}}{f} = \frac{177.5}{0.12} = 1479$$

10.5 Sample calculation for protein content.

Sample calculation with sample 4 at Day 5 from dry weight/protein content correlation.(Table 12-7)

Measured for each sample

Volume of cell suspension in buffer after sonication V_{tot}= 30 ml
Adsorbance of buffer A_{blank} = 0.0891
Adsorbance of sample A_{sample} = 0.1986
Dilution of sample (Df) = 1
Equation of calibration curve (adsorbance vs protein concentration) (Figure 12-3)
Y=0.0016x –0.0013 (Y= adsorbance, x= protein concentration)

Calculations

1. Correct adsorbance for background (AB)

$$AB|_{S4} = A|_{S4} - A|_{blank} = 0.1986 - 0.0891 = 0.1104$$

2. Correct adsorbance for dilution (AD)

$$AD|_{S4} = \frac{AB|_{S4}}{Df} = \frac{0.1104}{1} = 0.1104$$

3. Correlate adsorbance to protein concentration (P)

$$P = \frac{AD|_{S4} + 0.0013}{0.0016} = \frac{0.1104 + 0.0013}{0.0016} = 69.81\mu g/ml$$

4. Total Protein Content (TP)

$$TP = P * V_{Total} = 69.81\mu g/ml * 30ml = 2094.3\mu g/ml$$

11.0 APPENDIX D

Carbazole Overlay Plates

At the end of screening these isolates, the ideal bacterium had not been found, so we went back to initial dilution plates from the enrichment cultures. Also new dilution plates were made from an additional set of enrichment cultures that were started with the original soil samples but with glycerol as an additional carbon source. All the colonies from these two sets of dilution plates were re-streaked onto carbazole-overlay plates. These plates essentially mimicked the liquid culture conditions whereby one plate contained mineral salts medium and acetate and the other contained only mineral salts medium. Both types of plates contained an agarous overlay of carbazole. A positive control plate, made from ½ PCA was used for each group of isolates. From this screening procedure hundreds of isolated colonies were screened, monitoring solely the presence of growth. In the end the ideal candidate was not found here either.

12.0 APPENDIX E

12.1 Validation Experiment for HPLC versus GC

Table 12-1 Raw data from ethyl acetate extraction of carbazole flasks. Cultures were grown on carbazole and acetate medium for 7 d.

	Mass (mg)			Area			$Mass_{ini}$	Loss	Extract	
	CAR	Thia	Ratio	CAR	Thia	Ratio	(mg)	%	Eff.	m
Extraction Controls										
EC1	51.2	25	2.05	100,197	44,197	2.27				1.11
2	54.34			105,278	43,756	2.41	55.3	1.74	99.00	
NC	48.80			66,160	30,618	2.16	50.1	2.59	69.28	
8	39.94			63,673	36,000	1.77	57.5	30.53	81.45	
7	35.83			60,580	38,181	1.59	52.8	32.13	86.39	
10	37.02			70,627	43,091	1.64	53.3	30.55	97.50	
9	39.69			71,290	40,566	1.76	55.1	27.97	91.78	

Calculations:

Carbazole Removal and Extraction Efficiency:

The equation of the calibration curve is $y=mx+y_0$, where $y=A_{CAR}/A_{Thian}$, $x=M_{CAR}/M_{Thia}$ and $y_o=0$. Each set of samples is completed with a calibration sample which provides as estimate of m, in the equation of the calibration curve, at the time of analysis.

Assume: Thianthrene and carbazole are extracted with the same efficiency.

$$m|_{EC}=\frac{A_{CAR}/A_{Thia}}{M_{CAR}/M_{Thia}}=\frac{100197/44197}{51.2/25}=1.11$$

Measured for each sample (sample 2 for illustration):

Area of Carbazole (A_{CAR})= 105278
Area of Thianthrene (A_{Thia})= 43756

Mass of thianthrene added just before extraction (M_{Thia})= 25 mg

1. Final mass of carbazole

$$M_{CAR} = M_{Thia} * \frac{A_{CAR}/A_{Thia}}{m} = 25mg * \frac{105278/43756}{1.11} = 54\,mg$$

2. Removal of Carbazole

$$\text{Re}\,moval\ of\ Carbazole = \frac{M_{CAR}^{Initial} - M_{CAR}^{Final}}{M_{CAR}^{Initial}} * 100\% = \frac{55.3mg - 54.19mg}{55.3mg} * 100\% = 1.74\%$$

3. Extraction Efficiency

All samples were suspended in equivalent volumes and each sample received the same amount of thianthrene. Therefore the concentration of thianthrene (and thus area) in each sample should be equivalent if extraction efficiency is 100 %.

$$Extraction\ Efficiency = \frac{M_{Thia}^{Sample}}{M_{Thian}^{EC}} * 100\% = \frac{43756}{44197} * 100\% = 99\%$$

Table 12-2 Raw Data from HPLC analysis of ethanol/water solubilization of carbazole. Cultures were grown in parallel with those analyzed in the preceeding table.

Sample	Total	Carbazole Initial mg	HPLC Analysis Retention Time (min)	Area	CAR Conc. mg/ml	CAR Final mg
1	452	50.00	3.08	15,132,128	0.076459	34.57
3	455	48.60	3.086	16,204,832	0.081912	37.25
4	444	49.80	3.092	17,927,200	0.090666	40.23
5	445	53.80	3.1	18,483,472	0.093493	41.57
6	442	51.10	3.108	15,708,192	0.079387	35.10
NC	450	52.80	3.11	18,214,096	0.092124	41.46

Figure 12-1 Calibration curve for HPLC used in quantifying carbazole loss in the validation experiment.

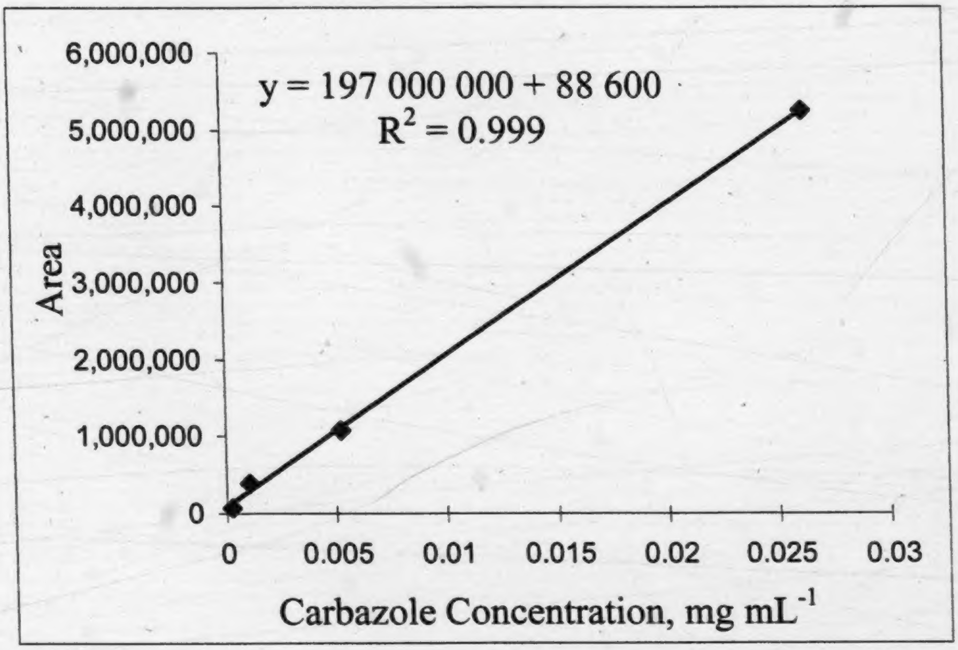

Figure 12-2 Statistical analysis of HPLC and GC results using the un-pooled t-test, assuming unequal variances.

t-Test: Two-Sample Assuming Unequal Variances		
Alpha= 0.05		
	HPLC	*GC*
Mean	25.495	30.296
Variance	28.629	2.971
Observations	5	4
Hypothesized Mean Diff.	0	
df	5	
t Stat	-1.8875	
P(T<=t) one-tail	0.0589	
t Critical one-tail	2.0150	
P(T<=t) two-tail	0.1177	
t Critical two-tail	2.5706	

12.2 Raw data for validating the recovery of ethanol-treated cells.

Table 12-3 Raw data for determining effectiveness of dry cell weight collection with vacuum filtering.

Sample	Mass (mg)			Total Volume	Mass of Cells			
	Filter Paper	Filter+Cells	Cells	ml	mg/5ml	mg	Average	Stdev
TSB								
6	76	83.22	7.22	200	7.21	288.4		
7	75.98	86.23	10.25	200	10.24	409.6		
8	76.77	85.36	8.59	200	8.58	343.2		
9	75.59	87.29	11.7	200	11.69	467.6		
10	76.37	86.34	9.97	200	9.96	398.4	381.44	68.2329
TSB + Ethanol								
1	73.64	83	9.36	380	9.35	710.6		
2	76.66	87.02	10.36	360	10.35	745.2		
3	74.77	85.23	10.46	358	10.45	748.22		
4	76.59	86.55	9.96	350	9.95	696.5		
5	76.55	85.59	9.04	370	9.03	668.22	713.748	33.75555
B+8P + Car + Acetate								
1	25	34.98	9.98			12.57		
3	77.3	93.1	15.8			15.79		
4	76.1	90.41	14.31			14.3		
5	77.2	90.42	13.22			13.21		
6	78.6	88.8	10.2			10.19	13.212	2.084135
NC	77.3	77.3	0			-0.01		

Table 12-4 Statistical analysis of dry cell weight data where one sample set contained untreated cells and the other contained cells treated with ethanol prior to filtering.

t-Test: Two-Sample Assuming Unequal

	TSB	*TSB+Ethan*
Mea	381.4	713.74
Varianc	4655.72	1139.437
Observatio	5	5
Hypothesized Mean	0	
df	6	
t Stat	-	
P(T<=t) one-	3.32E-	
t Critical one-	1.43975	
P(T<=t) two-	6.65E-	
t Critical two-	1.94318	

Table 12-5 Raw data of optical density readings completed on samples before and after filtering. Sample 9 was a culture without any ethanol treatment whereas E2 is a culture that had undergone ethanol pretreatment.

Sample	Dilution	OD600				Removed by Filter (%)
		Measured	Actual	Average	St. Dev	
Initial 9	10	0.985	9.85			
Initial 9	100	0.129	12.9	11.38	2.16	
Filtrate 9	10	0.332	3.32			
Filtrate 9	10	0.297	2.97			
Filtrate 9	10	0.418	4.18	3.49	0.62	
						69.32
Initial E2	10	0.6	6			
Initial E2	100	0.084	8.4	7.20	1.70	
Filtrate E2	1	0.25	0.25			
Filtrate E2	1	0.19	0.19			
Filtrate E2	1	0.19	0.19	0.21	0.03	
						97.08

Table 12-6 Descriptive Statistics on biomass collection of carbazole grown cultures.

B+8P +ACT Cells	
Mean	13.212
Standard Error	0.932054
Median	13.21
Mode	#N/A
Standard Deviation	2.084135
Sample Variance	4.34362
Kurtosis	0.556182
Skewness	-0.43456
Range	5.6
Minimum	10.19
Maximum	15.79
Sum	66.06
Count	5
Confidence Level(95.0%)	2.587801

12.3 Data for calculating the ratio of dry cell weight to protein content

Table 12-7 Dry cell weight of biomass collection for the experiment to correlate dry cell weight to protein content.

Sample	Filter No.	Mass (mg)						
		Filter						
T=5dys		Before	After	Total Dry Cells	Sample	Total Sample	Avg	Std. Dev.
Samples	K	75.8	88.6	12.8	1			
	B	75.5	88.6	13.1	1			
	D	75.4	82.2	6.8	1	32.7		
	R	74	86.8	12.8	2			
	P	76.7	92.6	15.9	2			
	O	74.6	77.3	2.7	2	31.4		
	S	74.6	78.8	4.2	3			
	Q	74.9	87.2	12.3	3			
	H	74.8	81.3	6.5	3			
	I	74.6	82.5	7.9	3			
	F	75.7	79.1	3.4	3	34.3	32.8	1.45
HKC	J	74.6	79.7	5.1	4	5.1		
	N	74.9	80.3	5.4	5			
	M	75.8	76.8	1	5	6.4		
	L	76.3	82	5.7	6	5.7	5.73	0.65
t=7DAYS								
HKC	C	75.5	80.4	4.9	1			
	ALPHA	73.9	74.9	1	1	5.9		
	4	75.8	80.7	4.9	3			
	3	72.9	74.1	1.2	3	6.1		
	BETA	75.3	78.6	3.3	4			
	5	74.4	76.8	2.4	4	5.7	5.9	0.2
Samples	E	75.7	78.7	3	23			
	8	74.9	86.5	11.6	23			
	2	75.5	93.2	17.7	23	32.3		
	7	75.6	95	19.4	24			
	10	74.6	77.7	3.1	24			
	9	75.4	86.6	11.2	24	33.7		
	D	74.7	95.5	20.8	25			
	6	75.1	81.5	6.4	25			
	1	73.4	82.4	9	25	36.2	34.06	1.98

Figure 12-3 Calibration curve of protein assay completed for biomass correlated measurements. The lower curve was constructed for the day 7 samples while the upper curve was constructed for the day 5 samples.

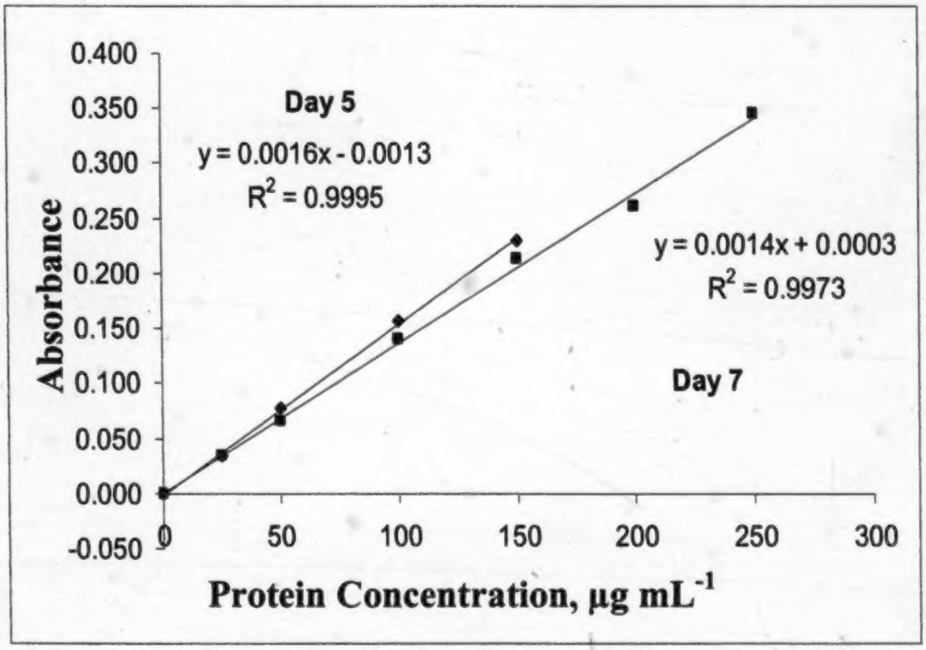

Table 12-8 Raw data for protein analysis. All OD_{600} readings were taken without the need for any dilution.

	Absorbance	Conc.	Volume	Total Protein		
T= 5 days		µg/ml	mL	µg	Average	Std. Dev
NC1	0.0034	2.92	25	73		
NC2	0.0046	3.67	22.5	82		
NC3	0.0050	3.92	35	137	97	34.61
S4	0.1104	69.79	30	2094		
S5	0.1032	65.29	37.5	2448		
S6	0.0907	57.48	37.5	2155	2233	189.49
Blank	0.0891					
T= 7 days						
NC2	0.00455	3.04	37.5	114		
NC5	0.00485	3.25	31	101		
NC6	0.00315	2.04	41	83	99	15.23574
S20	0.10455	74.46	42	3128	0	0
S21	0.13885	98.96	32.5	3216	0	0
S22	0.21345	152.25	24	3654	3333	281.8515
Blank	0.00065					

Table 12-9 Data used to correlate dry cell weight to protein content.

	Dry Weight (mg)			Protein (µg)			Conversion Factor	
	Avg	St. Dev	Error	Avg	St. Dev	Error	(µg protein / mg dry cell weight)	
							Value	Error
Day 5	5.73	0.65	0.11	97	34.61	0.36	17.01	7.97
Day 7	5.90	0.20	0.03	99	15.24	0.15	16.84	3.15
Day 5	32.80	1.45	0.04	2233	189.49	0.08	68.07	8.79
Day 7	34.07	1.98	0.06	3333	281.85	0.08	97.83	13.95

Table 12-10 Statistical analysis of the correlation relating dry weight to protein content and how it behaves over time in CP19 cells.

t-Test: Two-Sample Assuming Unequal Variances		
10% significance		
	T=5 days	*T= 7days*
Mean	68.28214	97.7354
Variance	70.82653	8.17885
Observations	3	3
Hypothesized Mean Difference	0	
df	2	
t Stat	-5.73939	
P(T<=t) one-tail	0.014521	
t Critical one-tail	1.885619	
P(T<=t) two-tail	0.029042	
t Critical two-tail	2.919987	

12.4 Data from measurements of the aqueous solubility of carbazole incubated with CP19 filtrate

Figure 12-4 HPLC calibration curve for measuring the aqueous solubility of carbazole and for quantifying the effects of the presence of cells.

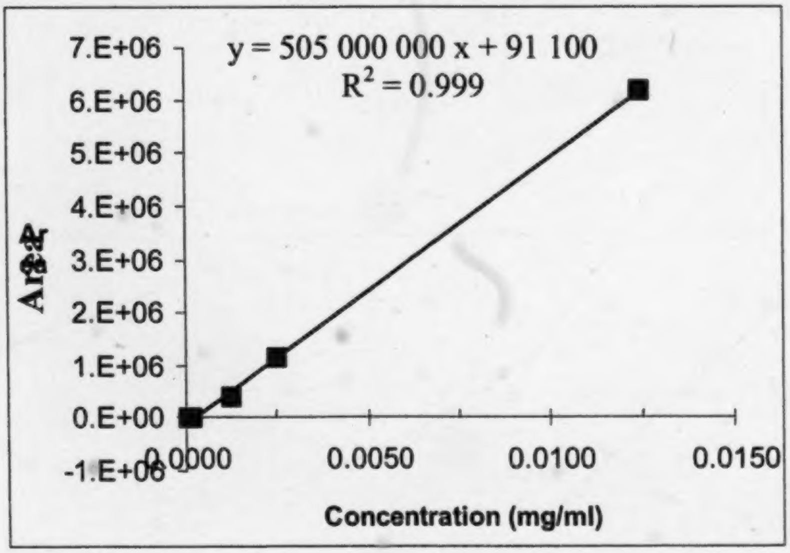

Table 12-11 HPLC data for HKC samples of solubilization experiment.

				Concentration	
Sample	**Method**	**Area**		**(mg/mL**	**(µg/mL)**
HKC #1	Filtered	0		0.00E+00	0.0000
HKC #2	Filtered	0		0.00E+00	0.0000
HKC #3	Filtered	480,219		1.13E-03	1.1322
HKC #3	Filtered	27,033		2.34E-04	0.2341
			average	6.83E-04	0.6832
			Total		
			average	2.28E-04	0.2277
			std dev	3.94E-04	0.3944
HKC #1	F+ CAR	208,706	242468	6.28E-04	0.6276
HKC #2	F+ CAR	0	239003	0.00E+00	0.0000
HKC #3	F+ CAR	366,291	330276	8.71E-04	0.8708
			Average	4.99E-04	0.4995
			Std. Dev	4.49E-04	0.4493
Water +CAR	Filtered	22,715		2.26E-04	0.2256
Medium	Filtered	37,090		2.54E-04	0.2541
Medium	Filtered+CAR	283,112		7.42E-04	0.7416
water+ car 1	straight	978,415		2.12E-03	2.12
water + car 2	straight	998,472		2.16E-03	2.16
				Average	2.14
				Std Dev.	0.03

Table 12-12 HPLC data of CP19 culture filtrate exposed to carbazole.

			Retention	Concentration	
Sample	Method	Area	Time (min)	(mg/mL)	(µg/mL)
CP19 #1	Filtered	0		0.00E+00	0.00
CP19 #2	Filtered	0		0.00E+00	0.00
CP19 #3	Filtered	0		0.00E+00	0.00
			Average	0.00E+00	0.00
			Std. Dev	0.00E+00	0.00
CP19 #1	F+CAR	6,832,000		1.37E-02	13.72
CP19 #1	F+CAR	5,190,256		1.05E-02	10.47
CP19 #1	F+CAR	6,414,714		1.29E-02	12.89
			Average	1.24E-02	12.36
CP19 #2	F+CAR	7,178,877		1.44E-02	14.41
CP19 #3	F+ CAR	977,894			
			Average	1.34E-02	13.38
			Std. Dev	1.45E-03	1.45

12.5 Data from experiments measuring carbon regulation of carbazole transformation.

Table 12-13 Dry cell weight data from regulation experiment.

			Mass of Filter (mg)			Mass (mg)				Fraction
Sample	Replicate	Time (days)	Filter No.	Initial	With Cells	Cells	Total	Average	StDev.	Error
B+N8P	1	0	M	75	82.6	7.6	7.6			
	2	0	W	75.9	83.9	8	8			
	3	0	Y	76.8	83.9	7.1	7.1	7.57	0.45	0.059594
B+N8P	1	2	N	75.8	96.3	20.5				
			O	75.6	93.4	17.8	38.3			
	2		S	75.5	89.4	13.9				
			A	77.4	94.1	16.7	30.6			
	3		32	74.9	97.2	22.3				
		2	25	73.3	89.3	16	38.3	35.73	4.45	0.12441
B+N8P	1	5	18	75.1	98.1	23				
			12	74.9	94.2	19.3				
			5	75	90.2	15.2	57.5			
	2		1	74.8	90.9	16.1				
			9	73.7	92.7	19				
			vii	75.5	84.4	8.9				
			13	74.6	89.2	14.6	58.6			
	3		3	76.3	88.2	11.9				
			2	75.4	83.2	7.8				
			17	75.7	84.4	8.7				
			vi	76	77	1				
		5	21	76.6	77.3	0.7	30.1	48.73	16.15	0.33132
B+N8P	1	7	A	74.85	90.99	16.14				
			L	73.21	81.54	8.33				
			M	73.93	84.55	10.62				
			I	73.63	89.24	15.61				
			N-10	24.06	27.14	3.08				
			J	74.5	86.37	11.87	65.65			
	2		2	75.3	89.29	13.99				
			G	74.37	97.38	23.01				
			F	74.48	86.44	11.96				
			viii	75.2	81.4	6.2				
			N-8	24.23	28.03	3.8				
			C	75.67	84.77	9.1	68.06			
	3		E	74.72	92,24	17.52				
			D	76.27	92.46	16.19				
			xi	75.2	85.8	10.6				
			N-9	24.19	28.24	4.05				
		7	B	74.93	91.13	16.2	64.56	66.09	1.79	0.027099
CAR	1	0	X	75.3	82.2	6.9	6.9			
	2		Z	74.4	81.5	7.1	7.1			
	3	0	U	77.8	84.8	7	7	7.00	0.10	0.014286
						0				
CAR	1	2	I	75.7	82.8	7.1	7.1			
	2		H	76.2	82.9	6.7	6.7			
	3	2	E	74.7	81.6	6.9	6.9	6.90	0.20	0.028986

Continued on the next page.

CAR	1	5	16	75.2	88.9	13.7	13.7			
	2		15	76.3	90.6	14.3	14.3			
	3	5	19	74.5	90	15.5	15.5	14.50	0.92	0.063208
CAR	1	7	9	78.8	88.82	10.02				
			N-3	24.58	28.94	4.36	14.38			
	2		5	76.13	87.4	11.27				
			N-1	24.38	26.1	1.72	12.99			
	3		6	75.4	87.36	11.96				
		7	N-5	24.5	28.59	4.09	16.05	14.47	1.53	0.105859
CAR+ACT	1	0	IV	75.9	83.1	7.2	7.2			
	2		T	74.6	81.6	7	7			
	3	0	V	76.3	83.4	7.1	7.1	7.10	0.10	0.014085
CAR+ACT	1	2	P	74.8	86.9	12.1				
			Q	75.9	77.1	1.2				
			J	75.8	87.2	11.4	24.7			
	2		R	76.9	87.3	10.4				
			K	75.4	77.9	2.5				
			F	73.8	84.5	10.7	23.6			
	3		B	75.5	82.9	7.4				
			L	74	80.1	6.1				
		2	30	75.6	84.7	9.1	22.6	23.63	1.05	0.044446
CAR+ACT	1	5	36	75.2	81.1	5.9				
			35	73.7	94.1	20.4				
			31	74.9	90.9	16	42.3			
	2	5	10	75.3	83	7.7				
			11	76.1	84.2	8.1				
			14	76.3	82.6	6.3				
			20	73.6	74.3	0.7				
			200	75.9	87.4	11.5	34.3			
	3	5	6	76.1	81.1	5				
			8	74.8	81.9	7.1				
			7	76.2	83.8	7.6				
			32	74.3	82.7	8.4				
			33	74.3	78.9	4.6				
		5	37	74.3	78.1	3.8	36.5	37.70	4.13	0.109623
CAR+ACT	1	7	Q	73.45	81.4	7.95				
			7	76.55	83.8	7.25				
			4	75	82.9	7.9				
			P	74.19	87.9	13.71				
			N-6	23.7	26.5	2.8				
			3	74.6	81	6.4	46.01			
	2		X	73.9	78.8	4.9				
			IV	74.4	82.4	8				
			III	74.7	93.5	18.8				
			N-7	24.24	29.4		31.7			
	3	7	K	74.87	83.36	8.49				
			N	73.7	88.85	15.15				

Continued on the next page.

CAR+ACT	1	7	Q	73.45	81.4	7.95				
			7	76.55	83.8	7.25				
			4	75	82.9	7.9				
			P	74.19	87.9	13.71				
			N-6	23.7	26.5	2.8				
			3	74.6	81	6.4	46.01			
	2		X	73.9	78.8	4.9				
			IV	74.4	82.4	8				
			III	74.7	93.5	18.8				
			N-7	24.24	29.4		31.7			
	3	7	K	74.87	83.36	8.49				
			N	73.7	88.85	15.15				
			I	75.3	85.2	9.9				
			N-2	23.91	28.9	4.99				
		7	O	73.81	75.21	1.4	39.93	39.21	7.18	0.183149
NC	1	2	G	75.4	82.5	7.1	7.1			
	2		D	74.7	82	7.3	7.3			
	3	2	C	75.2	82.2	7	7	7.13	0.15	0.021414
NC	1	5	1	75.7	82.49	6.79	6.79			
	2		4	74.7	83.1	8.4	8.4			
	3	5	8	76.1	81.37	5.27	5.27	6.82	1.57	0.229504
NC	1	7	V	76.6	83.6	7				
			N-11	24.3	25.6	1.3	8.3			
	2		IX	75	81.6	6.6				
			N-21	23.3	24.7	1.4	8			
	3		II	75.4	82.6	7.2				
		7	N-22	24.1	25.6	1.5	8.7	8.33	0.35	0.042143

Table 12-14 HPLC data for measuring residual carbazole remaining after exposure to CP19 growing in the presence of various carbon and nitrogen sources.

Sample	Rep	Time	Area	Conc.	Vtot	Carbazole (mg)		% Removal		
		(days)		(mg/mL)	(mL)	Remain	Initial	Value	Avg	Stdev
CAR+ ACT+N	1	0	22,707,328	0.1180	430	50.74	52.5	3.35		
	2		20,786,912	0.1079	420	45.33	48.5	6.54		
	3	0	22,847,360	0.1187	415	49.28	52.3	5.78	5.22	1.67
	1	2	17,042,192	0.0925	370	34.22	54.4	37.10		
	2		16,230,600	0.0880	375	33.01	50.7	34.90		
	3	2	18,179,248	0.0987	375	37.03	50.9	27.26	33.09	5.17
	1	5	14,366,984	0.0845	380	32.11	48.9	34.33		
	2		13,126,112	0.0746	375	27.97	47.7	41.37		
	3	5	15,994,552	0.0975	360	35.11	52.2	32.73	36.14	4.59
	1	7	8,691,603	0.0356	390	13.88	47.9	71.03		
	2		5,662,394	0.0183	385	7.05	52.6	86.60		
	3	7	8,390,662	0.0339	360	12.19	47.1	74.12	77.25	8.24
CAR	1	0	22,713,824	0.1180	420	49.58	52.2	5.03		
	2		25,074,400	0.1304	430	56.08	55.2	-1.60		
	3	0	22,400,624	0.1164	442	51.45	49.7	-3.51	-0.03	4.48
	1	2	24,670,096	0.1344	370	49.75	51.8	3.96		
	2		26,199,664	0.1429	390	55.72	52.8	-5.53		
	3	2	28,823,664	0.1573	370	58.20	55.7	-4.49	-2.02	5.21
	1	5	16,523,952	0.1040	385	40.06	52.8	24.14		
	2		16,437,760	0.1011	385	38.92	51.9	25.02		
	3	5	17,031,792	0.1058	400	42.33	55.2	23.31	24.15	0.85
	1	7	19,893,744	0.0994	370	36.79	57.6	36.12		
	2		17,725,072	0.0871	365	31.78	52.9	39.92		
	3	7	12,552,568	0.0576	380	21.88	49.2	55.52	43.85	10.28
CAR+ACT	1	0	23,269,248	0.1210	410	49.59	50.5	1.80		
	2		23,004,832	0.1196	440	52.61	53.2	1.11		
	3	0	24,126,896	0.1254	455	57.08	55.6	-2.66	0.09	2.40
	1	2	13,976,352	0.0756	410	31.00	48.6	36.21		
	2		15,249,680	0.0826	380	31.39	48.1	34.73		
	3	2	16,761,920	0.0909	360	32.74	49.4	33.73	34.89	1.25
	1	5	9,802,022	0.0480	400	19.19	48.2	60.18		
	2		12,991,872	0.0735	380	27.93	52.2	46.49		
	3	5	12,872,288	0.0726	380	27.57	52.9	47.88	51.52	7.54
	1	7	8,006,099	0.0365	350	12.78	51.5	75.18		
	2		11,545,016	0.0558	350	19.51	50.9	61.66		
	3	7	12,086,144	0.0587	380	22.30	52.8	57.76	64.87	9.14
HKC	1	2	25,427,360	0.1386	370	51.29	51.8	0.99		
	2		24,107,360	0.1314	375	49.26	52.4	6.00		
	3	2	24,296,256	0.1324	400	52.96	55.1	3.89	3.63	2.51
	1	5	28,558,464	0.1482	385	57.07	50.6	-12.78		
	2		26,224,256	0.1355	380	51.51	49.4	-4.26		
	3	5	27,666,576	0.1434	390	55.92	52.3	-6.92	-7.99	4.36
	1	7	29,744,800	0.1547	375	58.00	52.5	-10.49		
	2		27,725,472	0.1437	380	54.61	51.4	-6.24		
	3	7	28,432,045	0.1481	380	56.29	52.4	-7.42	-8.05	2.19

Table 12-15 Normalized carbazole conversions for CP19 exposed to carbazole in the presence of various combinations of carbon and nitrogen sources. Data taken from Figure 4-19.

	Carbazole Conversion (μmol CAR (mg DCW)$^{-1}$)	
Condition	**T= 5 d**	**T=7 d**
CAR	9.1 ± 2.15	12.6 ± 1.2
CAR+ACT	7.9 ± 2.1	7.9 ± 0.9
CAR+ACT+N	5.4 ± 2.3	6.5 ± 1.0

Table 12-16 Statistical analysis of the normalized carbazole conversion for each growing condition. The data used in each calculation are outlined in Table 12-15. Completed using equations 12-1 and 12-2. Significance level of 0.05 was used.

	T= 5 d			T=7 d		
	N/ACT	N/CAR	ACT/CAR	N/ACT	N/CAR	ACT/CAR
t-value	-1.4065	-2.0388	-0.6658	-3.454	-11.378	-7.442
df	4	4	4	4	4	4
$t_{\alpha/2}$	2.776	2.776	2.776	2.776	2.776	2.776
t_{α}	2.132	2.132	2.132	2.132	2.132	2.132

Calculation of t-statistic for non-pooled t-test assuming unequal variances.

$$t = \frac{x_1 - x_2}{\sqrt{\left(\frac{s_1{}^2}{n_1}\right) + \left(\frac{s_2{}^2}{n_2}\right)}} \tag{12-1}$$

Calculation of degrees of freedom required for the non-pooled t-test with unequal variances.

$$df = \frac{\left[\left(\frac{s_1{}^2}{n_1}\right) + \left(\frac{s_2{}^2}{n_2}\right)\right]^2}{\left[\frac{\left(\frac{s_1{}^2}{n_1}\right)^2}{(n_1 - 1)} + \frac{\left(\frac{s_2{}^2}{n_2}\right)^2}{(n_2 - 1)}\right]} \tag{12-2}$$

Calculation of mean rate of carbazole transformation.

$$R_{mean} = \frac{C_i - C_{i-1}}{\Delta T\left(\frac{M_i + M_{i+1}}{2}\right)} \tag{12-3}$$

Ci= carbazole concentration corrected with the heat-killed control

Mi= DCW of culture corrected with the heat-killed control.

I= indicator of time interval

ΔT= time interval

Table 12-17 Data and calculations of the mean rate of carbazole conversion within all growing conditions.

	Time (d)	µmol removed						Biomass (mg)				Mass Btw. Time Pts. (mg)		Rate of Removal		Mean Rate	
														umol CAR removed/mg DCW/day			
		Value	STD	Value-HKC	Error	C(t)-C(t-1)	Error	Avg	STD	AVG-HKC	Error	Value	Error	Value	Error	Value	Error
B+N8P	0	15.88	4.65	15.88	4.65			7.57	0.45	7.57	0.45						
	2	103.29	19.03	91.72	20.62	75.85	21.14	35.73	4.45	28.60	4.45	18.08	4.47	2.10	0.78	1.110	1.023
	5	106.99	9.71	131.33	16.44	39.61	26.37	48.73	16.15	41.91	16.22	35.26	16.82	0.37	0.31		
	7	228.51	38.41	253.66	39.06	122.32	42.37	66.09	1.79	57.76	1.83	49.84	16.32	1.23	0.59		
CAR	0	0.00	13.86	0.00	13.86			7.00	0.10	7.00	0.10						
	2	-6.72	16.51	-18.29	18.33	-18.29	22.98	6.90	0.20	-0.23	0.25	3.38	0.27	-2.70	-3.40	5.100	7.042
	5	77.03	0.71	101.37	13.28	119.66	22.64	14.50	0.92	7.68	1.81	3.72	1.83	10.71	5.64		
	7	138.20	21.99	163.34	23.10	61.97	26.64	14.47	1.53	6.14	1.57	6.91	2.40	4.48	2.48		
CAR+ ACT	0	0.05	7.77	0.05	7.77			7.10	0.10	7.10	0.10						
	2	101.73	3.17	90.16	8.56	90.11	11.56	23.63	1.05	16.50	1.06	11.80	1.07	3.82	0.60	1.847	0.919
	5	156.90	14.89	181.24	19.94	91.08	21.70	37.70	4.13	30.88	4.42	23.69	4.54	1.28	0.39		
	7	200.80	27.02	225.95	27.93	44.71	34.32	39.21	4.66	30.88	4.67	30.88	6.43	0.72	0.58		
HKC	2	11.57	7.95					7.13	0.15								
	5	-24.34	13.26					6.82	1.57								
	7	-25.15	7.07					8.33	0.35								

Table 12-18 Final composition of biomass from CN analysis.

			Results of CHN Analysis Completed at T= 7days						
			ug of element		Mass of sample (mg)		Fraction	Total Element (umol/ mg DCW)	
Condition	Replicate	Filter	N	C	Filter	Total	Analyzed	N	C
CAR+ACT	1	6	153.75	1102.54	2.8	46.01	0.0609	3.92	32.81
CAR+ACT	2	7	324.25	2189.39	5.16	36.86	0.1400	4.49	35.36
CAR+ACT	3	2	332.51	2008.96	4.99	39.93	0.1250	4.76	33.55
CAR	1	1	214.75	713	1.72	12.99	0.1324	8.92	34.54
CAR	3	3	475.04	1486.52	4.36	14.38	0.3032	7.78	28.41
CAR	3	5	446.49	1411.58	4.09	16.05	0.2548	7.80	28.76
CAR+ACT+N	1	10	353.11	1101.85	3.08	65.65	0.0469	8.19	29.81
CAR+ACT+N	2	8	419.47	1287.95	3.8	68.06	0.0558	7.88	28.24
CAR+ACT+N	3	9	455.69	1382.69	4.05	64.56	0.0627	8.04	28.45
HKC	1	11	109.75	450.68	1.3	8.3	0.1566	6.03	28.89
HKC	2	21	97.77	399.67	1.4	8	0.1750	4.99	23.79
HKC	3	22	113.4	460.68	1.5	8.7	0.1724	5.40	25.59

Figure 12-5 Data from monitoring acetate concentrations over incubation time of CP19 with carbazole.

Sample	Time	Replicate	Dilution	Area	ACT Conc (mg/L)		Volume	Acetate Consumed				
	(d)				Injection	Total Sample	(mL)	Mass (mg)	mmol	Remove	AVG	STDEV
CAR+ACT+N	0	3	0.3	4,383,526	259.26	864.20	186	0.68818	0.01	0.43		
	0	2	0.3	4,739,309	281.73	939.10	193	-13.7702	-0.23	-8.20		
	0	1	0.3	3,942,048	231.38	771.26	190	18.355	0.31	11.13	1.12	9.69
											1.47	
	2	1	0.3	1,471,522	75.35	251.17	186	114.53	1.94	71.06	41.10	
	2	2	0.3	1,039,973	48.10	160.32	184	129.98	2.20	81.53	76.29	
	2	3	0.3	889,296	38.58	128.60	198	146.45	2.48	85.2	79.26	
	2	3	0.3	1,082,394	50.78	169.25	198	138.40	2.34	80.5	82.40	6.02
											82.84	
	5	1	1	4,641	below range	0.00	192	166.72	2.82	100	90.25	
	5	2	1	0	0.00	0.00	186	161.08	2.73	100	100	
	5	3	1	0	0.00	0.00	195	169.07	2.86	100	100	0.00
											100	
	7	1	1	0	0.00	0.00	204	176.96	3.00	100	100	
	7	2	1	0	0.00	0.00	200	173.41	2.94	100	100	
	7	3	1	0	0.00	0.00	196	169.85	2.88	100	100	0.00

Continued on the next page.

CAR+ACT	0	3	0.3	1,939,704	104.92	349.73	160	0.46	0.01	0.8		
	0	2	0.3	2,043,652	111.48	371.61	149	-2.83	-0.05	-5.40	-2.29	4.39
	2	1	0.3	4,187,557	246.88	822.94	163	7.32	0.12	5.18		
	2	2	0.3	3,958,165	232.40	774.65	149	13.92	0.24	10.74		
	2	3	0.3	4,192,424	247.19	823.97	158	6.95	0.12	5.06	6.99	3.25
	5	1	0.3	3,287,929	190.07	633.56	156	36.61	0.62	27.001		
	5	2	0.3	2,882,427	164.46	548.19	155	49.42	0.84	36.84		
	5	3	0.3	2,596,824	146.42	488.07	149	56.54	0.96	43.76	35.87	8.42
	7	1	1	169,030	87.70	87.70	162	126.70	2.15	89.90		
	7	2	1	122,350	65.09	65.09	155	124.17	2.10	92.50		
	7	3	1	167,250	86.84	86.84	147	114.90	1.95	89.99	90.80	1.48
NC	2	1	0.300	4,300,783	254.03	846.78	185	3.90	0.07	2.43		
	2	2	0.300	4,546,233	269.54	898.45	172	-5.24	-0.09	-3.52		
	2	3	0.300	4,094,859	241.03	803.43	190	12.22	0.21	7.43	2.11	5.48
	5	1	0.300	5,621,551	337.45	1124.83	190	-48.69	-0.82	-29.60		
	5	2	0.3		234.03	780.11	144	12.61	0.21	10.12		
	5	3	0.3		225.10	750.32	197	23.14	0.39	13.55	-1.98	23.98
	7	1	0.3	446470	222.07	740.22	190	24.22	0.41	14.71		
	7	2	0.3	504860	250.34	834.48	200	6.69	0.11	3.85		
	7	3	0.3	467190	232.10	773.67	176	16.57	0.28	10.86	9.81	5.51

Table 12-19 Data collected by measuring $^{14}CO_2$ release from CP19 cultures with ^{14}C-carbazole.

		Actual Counts (DPM) of 0.5ml sample.								
		Monday 11am	Tuesday 1pm	Wed 11am	Thurs 11:30am	Friday 9am	Sat 11:15am	Sun 1:30pm	Mon 10:30am	Mon 3pm,
	Time (hrs)	0	26	49	73	95	121	147	168	173
	100%	239570	243240	243690	244970	245295	244525	246535	242395	244610
	100%			248160	256065	256225	257325	257610	258845	257635
100%	Avg	239570	243240	245925	250518	250760	250925	252073	250620	251123
0%	0%	25	22	23	22	26	21	23	25	24
	HKC1	31	38	31	58	23	37	80	30	31
	HKC2	33	34	28	34	25	32	30	38	39
	HKC3	39	30	21	37	41	29	29	30	28
HKC	**AVG**	34	34	26	43	30	33	46	33	33
	Std Dev	4	4	5	13	10	4	29	5	6
	ACT1	42	149	2465	4976	6364	7400	8097	8958	8251
	ACT2	41	73	2060	4162	5442	7058	7602	7990	8559
	ACT3	31	184	2599	4893	6125	7297	7645	8749	8821
B+8P+ ACT	**AVG**	38	135	2375	4677	5977	7252	7781	8565	8544
	Std Dev	6	57	281	448	478	176	274	509	285
	CAR1	39	43	87	676	811	7117	8792	10125	9807
	CAR2	30	39	63	290	2178	5896	8119	8606	8682
B+8P	CAR3	26	38	70	409	942	5838	7924	8585	9083
	AVG	31	40	73	458	1310	6283	8278	9105	9190
	Std Dev	6	3	13	198	754	722	455	883	570

Table 12-20 ^{14}Carbon dioxide release data corrected for background ^{14}C.

		Counts (DPM) Corrected for background								
		Mon 11am	Tues 1pm	Wed 11am	Thurs 11:30am	Friday 9am	Sat 11:15am	Sun 1:30pm	Mon 10:30am	Mon 3pm
	Time (hr)	0	26	48.5	72.5	94.5	120.75	147	168	172.5
	100%	239570	243240	243690	244970	245295	244525	246535	242395	244610
	100%			248160	256065	256225	257325	257610	258845	257635
100%	Average	239570	243240	245925	250518	250760	250925	252073	250620	251123
0%	0%	25	22	23	22	26	21	23	25	24
	HKC1	7	16	8	36	-3	17	58	5	7
	HKC2	8	12	5	12	-2	12	8	13	15
	HKC3	14	8	-3	15	15	8	6	5	4
HKC	**Avg**	10	12	3	21	4	12	24	8	9
	Std Dev	4	4	5	13	10	4	29	5	6
	ACT1	17	127	2442	4954	6338	7380	8074	8933	8227
	ACT2	16	51	2037	4140	5416	7037	7579	7965	8535
	ACT3	6	162	2576	4871	6099	7277	7623	8724	8797
B+8P+ ACT	**Avg**	13	113	2352	4655	5951	7231	7759	8540	8520
	Std Dev	6	57	281	448	478	176	274	509	285
	CAR1	14	21	64	654	785	7096	8769	10100	9783
	CAR2	5	17	40	268	2152	5876	8097	8581	8658
B+8P	CAR3	2	16	47	387	916	5817	7902	8560	9059
	Avg	7	18	50	436	1284	6263	8256	9080	9166
	Std Dev	6	3	13	198	754	722	455	883	570

Table 12-21 Calculated data for the amount of radiolabel removed from each culture from daily sampling of KOH.

		Total Counts Removed (DPM)								
		Monday 11am	**Tuesday 1pm**	**Wed 11am**	**Thurs 11:30am**	**Friday 9am**	**Sat 11:15am**	**Sun 1:30pm**	**Mon 10:30am**	**Mon 3pm**
	Time (hr)	0	26	48.5	72.5	94.5	120.75	147	168	172.5
	100%	239570	243240	243690	244970	245295	244525	246535	242395	244610
	100%			248160	256065	256225	257325	257610	258845	257635
100 %	Average	239,570.0	243,240.0	245,925.0	250,517.5	250,760.0	250,925.0	252,072.5	250,620	251,122
0%	0%	24.50	22.00	23.00	22.00	26.00	20.50	22.50	25.00	24.00
	HKC1	6.50	22.50	30.00	66.00	63.00	79.50	137.00	142.00	149.00
	HKC2	8.00	19.50	24.00	35.50	34.00	45.50	53.00	66.00	81.00
	HKC3	14.00	21.50	19.00	33.50	48.50	56.50	62.50	67.50	71.50
HKC	**Average**	9.50	21.17	24.33	45.00	48.50	60.50	84.17	91.83	100.50
	Std Dev	3.97	1.53	5.51	18.21	14.50	17.35	46.00	43.45	42.27
	ACT1	17.00	143.50	2,585.00	7,539.00	13,877.00	21,256.50	29,330.5	38,263.0	46,490
	ACT2	16.00	66.50	2,103.50	6,243.00	11,659.00	18,696.00	26,275.0	34,240.0	42,774.5
	ACT3	6.00	167.50	2,743.50	7,614.00	13,713.00	20,989.50	28,612.0	37,335.5	46,132.5
B+8P + ACT	**Average**	13.00	125.83	2,477.33	7,132.00	13,083.00	20,314.00	28,072.5	36,612.8	45,132.3
	Std Dev	6.08	52.77	333.31	770.81	1,235.94	1,407.57	1,597.60	2,106.61	2,049.75
	CAR1	14.00	35.00	99.00	753.00	1,538.00	8,634.00	17,403.0	27,502.5	37,285.5
	CAR2	5.00	21.50	61.00	328.50	2,480.00	8,355.50	16,452.0	25,032.5	33,690
B+8P	CAR3	1.50	17.50	64.50	451.00	1,366.50	7,183.50	15,085.0	23,645.0	32,703.5
	Average	6.83	24.67	74.83	510.83	1,794.83	8,057.67	16,313.33	25,393.33	34,559.67
	Std Dev	6.45	9.17	21.00	218.48	599.54	769.75	1,165.20	1,953.90	2,411.62

Table 12-22 Calculated values of cumulative $^{14}CO_2$ release from CP19 cultures with ^{14}C-carbazole.

		Correction factors for removing 0.5mL of KOH every day.								
		10.00	9.50	9.00	8.50	8.00	7.50	7.00	6.50	6.00
		20.00	19.00	18.00	17.00	16.00	15.00	14.00	13.00	12.00
		Accumulative C14 Released (DPM)								
		Monday 11am	**Tuesday 1pm**	**Wed 11am**	**Thurs 11:30am**	**Friday 9am**	**Sat 11:15am**	**Sun 1:30pm**	**Mon 10:30am**	**Mon 3pm**
	Time (hr)	0	26	48.5	72.5	94.5	120.75	147	168	172.5
	100%	239570	243240	243690	244970	245295	244525	246535	242395	244610
	100%			248160	256065	256225	257325	257610	258845	257635
100%	Avg	239570	243240	245925	250518	250760	250925	252073	250620	251123
0%	0%	25	22	23	22	26	21	23	25	24
	HKC1	130	311	158	642	18	311	885	202	226
	HKC2	160	227	101	220	12	207	151	222	246
	HKC3	280	157	-24	266	274	169	141	128	116
HKC	**Avg**	190	231	78	376	101	229	392	184	196
	Std	79	77	93	232	149	74	427	50	70
	ACT1	340	2421	44091	86803	108947	124570	134293	145453	136987
	ACT2	320	976	36733	72475	92899	117214	124802	129820	136654
	ACT3	120	3075	46536	85542	105198	122861	127705	142018	142900
B+8P+ ACT	**Avg**	260	2157	42453	81607	102348	121548	128933	139097	138847
	Std	122	1074	5103	7933	8395	3849	4863	8216	3514
	CAR1	280	413	1187	11217	13313	107978	131400	148697	144899
	CAR2	100	319	733	4609	34753	90613	121707	127999	128923
B+8P	CAR3	30	306	864	6635	15099	88622	117805	126365	132347
	Avg	137	346	928	7487	21055	95737	123637	134353	135389
	Std	129	59	234	3386	11896	10647	7000	12448	8411

Table 12-23 Distribution of radiolabel throughout culture fractions.

	Removed as CO2 DCM	Extract				Aqueous Fraction				Total
		Count (in 1mL)	Less bkgrd	Vol (mL)	Total (DPM)	Count (in 1mL)	Less bkgrd	Vol (mL	Total (DPM)	
HKC1	226	22,427	22,407	15	336,108	359	335	50	16,725	352,833
HKC2	246	20,374	20,354	16	325,656	325	300.5	50	15,025	340,681
HKC3	116	16,038	16,018	17	272,298	359	334.5	50	16,725	289,023
Average	**196**	**19,613**	**19,593**		**311,354**	**347**				**327,512**
Std Dev	**70**	**3,262**	**3,262**		**34,225**	**20**				**33,882**
ACT1	136,987	1,442	1,422	19	27,018	2,389	2365	50	118,250	145,268
ACT2	136,654	2,325	2,305	17	39,177	2,358	2334	50	116,700	155,877
ACT3	142,900	1,648	1,628	17	27,676	2,475	2451	50	122,550	150,226
Average	**138,847**					**2,407**				
Std Dev	**3,514**					**61**				
CAR1	144,899	2,257	2,237	20	44,730	2,163	2139	50	106,950	151,680
CAR2	128,923	2,688	2,668	21	56,018	2,063	2039	50	101,950	157,968
CAR3	132,347	2,958	2,938	18.5	54,344	1,995	1971	50	98,550	152,894
Average	**135,389**					**2,074**				
Std Dev	**8,411**					**85**				

Table 12-24 Distribution of radiolabel throughout culture fractions, continued from Table 12-23.

	Removed as CO2 DCM	Supernatant				Pellet				
		Cnt (in 0.5ml)	Corr. Bk.	Mult.	Total (DPM)	Count	Corr. Bk	Aq. Col. (mL)	Mult.	Total (DPM)
HKC1	226	79	55	100	5,500	201.5	177.5	6	8.33	1,479
HKC2	246	75	51	100	5,100	713.5	689.5	7	7.14	4,925
HKC3	116	71	47	100	4,700	339.5	315.5	6	8.33	2,629
Average	**196**	**75**			**5,100**	**418**				**3,011**
Std Dev	**70**	**4**			**400**	**265**				**1,754**
ACT1	136,987	549	525	100	52,500	1098	1074	1	50.00	53,700
ACT2	136,654	549.5	525.5	100	52,550	1023.5	999.5	1	50.00	49,975
ACT3	142,900	561.5	537.5	100	53,750	1174	1150	1	50.00	57,500
Average	**138,847**	**553**			**52,933**	**1,099**				**53,725**
Std Dev	**3,514**	**7**			**708**	**75**				**3,763**
CAR1	144,899	317.5	293.5	100	29,350	3546.5	3522.5	3	16.67	58,708
CAR2	128,923	295.5	271.5	100	27,150	3634	3610	3	16.67	60,167
CAR3	132,347	296	272	100	27,200	2883.5	2859.5	3	16.67	47,658
Average	**135,389**	**303**			**27,900**	**3,355**				**55,511**
Std Dev	**8,411**	**13**			**1,256**	**410**				**6,840**